Optimization of 2,3-Dihydroquinazolinone-3-carboxamides as Antimalarials Targeting PfATP4

Trent D. Ashton,[⊠] Madeline G. Dans,[⊠] Paola Favuzza, Anna Ngo, Adele M. Lehane, Xinxin Zhang, Deyun Qiu, Bikash Chandra Maity, Nirupam De, Kyra A. Schindler, Tomas Yeo, Heekuk Park, Anne-Catrin Uhlemann, Alisje Churchyard, Jake Baum, David A. Fidock, Kate E. Jarman, Kym N. Lowes, Delphine Baud, Stephen Brand, Paul F. Jackson, Alan F. Cowman, and Brad E. Sleebs*

Read Online

ACCESS | Metrics & More | Article Recommendations | Supporting Information

ABSTRACT: There is an urgent need to populate the antimalarial clinical portfolio with new candidates because of resistance against frontline antimalarials. To discover new antimalarial chemotypes, we performed a high-throughput screen of the Janssen Jumpstarter library against the *Plasmodium falciparum* asexual blood-stage parasite and identified the 2,3-dihydroquinazolinone-3-carboxamide scaffold. We defined the SAR and found that 8-substitution on the tricyclic ring system and 3-substitution of the exocyclic arene produced analogues with potent activity against asexual parasites equivalent to clinically used antimalarials. Resistance selection and profiling against drug-resistant parasite strains revealed that this antimalarial chemotype targets PfATP4. Dihydroquinazolinone analogues were shown to disrupt parasite Na^+ homeostasis and affect parasite pH, exhibited a fast-to-moderate rate of asexual kill, and blocked gametogenesis, consistent with the phenotype of clinically used PfATP4 inhibitors. Finally, we observed that optimized frontrunner analogue WJM-921 demonstrates oral efficacy in a mouse model of malaria.
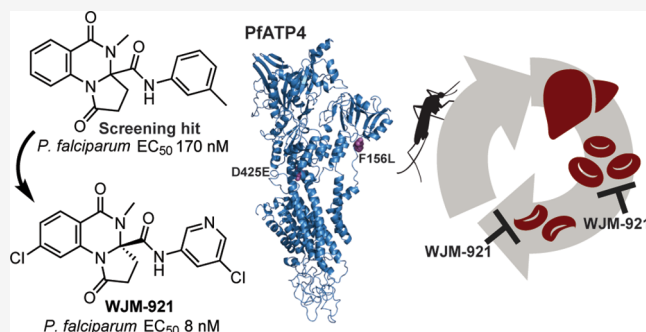
INTRODUCTION

Malaria is a devastating disease that caused approximately 619,00 deaths in 2021.[1] This was a significant increase in cases compared to recent years, primarily due to disruptions in access to diagnosis and treatment resources because of the COVID-19 global pandemic. Malaria is caused by an intracellular obligate parasite from the genus *Plasmodium*. In humans, five species of *Plasmodium* are known to cause the disease. *Plasmodium falciparum* is the most lethal and accounts for 93% of cases in sub-Saharan Africa.[2] *P. vivax* is prevalent in South East Asia and the Americas and is responsible for post-treatment disease relapse because of a latent hepatocyte form of the parasite called the hypnozoite.[3] *P. ovale* and *P. malariae* are known to cause human disease, but they do not cause mortality.[4] *P. knowlesi* is commonly the causative parasite of malaria in South East Asia and is the most common cause of malaria in Malaysia.[5,6]

Artemisinin combination therapies (ACTs) are the mainstay frontline strategy for the treatment of malaria. Curtailing the potential effectiveness of ACTs is the emergence of resistance in South East Asia[7,8] and recently in Sub-Saharan Africa,[9] highlighting the need for the development of new therapies with novel mechanisms of action. Recently, several novel antimalarial candidates have advanced to clinical trials,[10] including the DHODH inhibitor DSM265[11−13] and the

PfATP4 inhibitor KAE609 (cipargamin)[14−16] (Figure 1). While the clinical efficacy of these candidates has been promising, both DSM265 and cipargamin displayed a low barrier to resistance.[12,14,17] These results emphasize the need for the continual population of the antimalarial pipeline with new structural chemotypes that have a high barrier to resistance.[18]

To identify new antimalarial chemotypes, we performed a high-throughput screen of the Janssen Jumpstarter library comprising 80,000 drug-like compounds against the *P. falciparum* asexual blood-stage 3D7 parasite using the previously described lactate dehydrogenase (LDH) assay format.[19] The screen identified the 1,5-dioxo-2,3-dihydropyrrolo[1,2-a]quinazoline-3a-carboxamide chemotype (Figure 1), referred to herein as the dihydroquinazolinone class. Representative hits from this class, **5** and **6** (both racemates), exhibited EC_{50} values of 0.17 and 0.94 μM against

R = Me **5** Pf 3D7 EC$_{50}$ 0.17 μM

HepG2 EC$_{50}$ >40 μM

R = OMe **6** Pf 3D7 EC$_{50}$ 0.94 μM

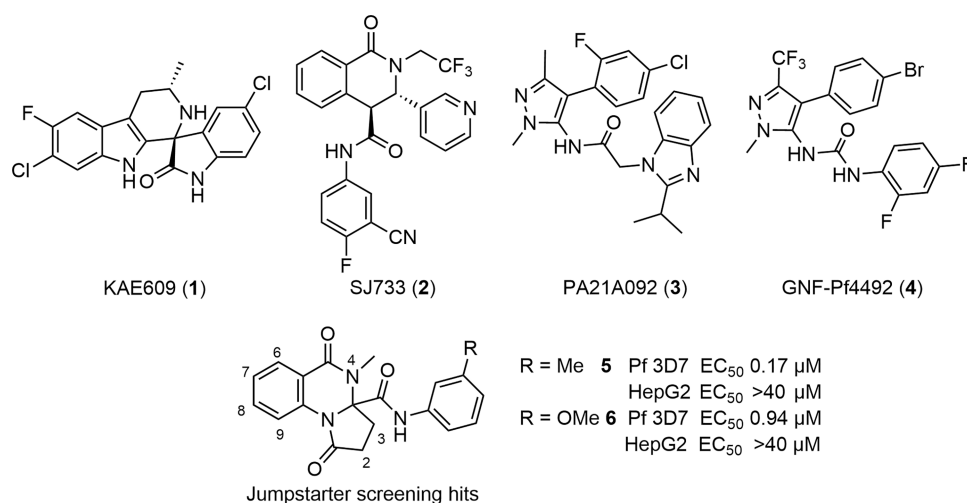HepG2 EC$_{50}$ >40 μM

Jumpstarter screening hits

Figure 1. Known PfATP4 inhibitors and the hit compound class, which is the focus of this research. The biological activity of the two hit compounds is shown.

asexual blood-stage *P. falciparum* (Figure 1). Notably, the hit compounds did not inhibit the LDH enzyme nor interfere with the LDH signal demonstrating that they were not interfering with the assay technology. Additionally, the hit compounds **5** and **6** were not cytotoxic against the human HepG2 cell line at the highest concentration tested (EC$_{50}$ > 40 μM).

A literature search revealed that the hit chemotype structure had not been previously reported as a hit identified from antimalarial screening campaigns or under development. The structure of the dihydroquinazolinone class, however, shared similarities with the structure of PfATP4 inhibitors, such as SJ733[20] (Figure 1) and other compounds identified in the Medicines for Malaria Venture (MMV) Malaria Box[21] and MMV Pathogen Box.[22] PfATP4 is an essential plasma membrane P-type ATPase that regulates the parasite's intracellular Na$^+$ concentration and is believed to import H$^+$ while exporting Na$^+$.[23] Compounds that inhibit PfATP4 are characterized by a fast-to-moderate onset of asexual parasite arrest and also inhibit early- and late-stage gametocytogenesis,[24] suggesting that PfATP4 inhibitors have target product profiles suitable for a treatment and a transmission-blocking therapy (TCP-1 and TCP-5).[25] Accordingly, several PfATP4 inhibitors have been identified as preclinical candidates, cipargamin (KAE609) (**1**),[14] SJ733 (**2**),[20] PA21A092 (**3**),[26] and GNF-Pf4492 (**4**)[17] (Figure 1), and both **1** and **2** are in human clinical trials assessing their curative and transmission-blocking efficacy. Concerningly, a G358S mutation in PfATP4 has been shown to confer a clinically relevant level of resistance to KAE609 and SJ733,[27] which necessitates the need to uncover novel PfATP4 inhibitor chemotypes that have a high barrier to resistance and are active against drug-resistant clinical isolates.

Herein, we investigate the structure–activity relationship (SAR) and optimize the asexual parasite activity of the dihydroquinazolinone class while monitoring human HepG2 cytotoxicity, ADME, and physicochemical properties. To identify the mechanism of action, we selected resistance against an analogue of the dihydroquinazolinone class and performed whole-genome sequencing (WGS) to reveal genetic alterations in the *Pfatp4* gene. To confirm PfATP4 was the molecular target, we benchmarked the activity of dihydroquinazolinone analogues against known PfATP4 inhibitors in

asexual phenotypic and rate of kill assays, in parasite Na$^+$ and pH assays and against parasite strains resistant to other PfATP4 inhibitors. Finally, we examined the efficacy of frontrunner compounds against gametes *in vitro* and in a malaria asexual mouse model to show their potential as transmission-blocking and curative antimalarial agents.

■ RESULTS AND DISCUSSION

Synthesis. The synthesis of the 1,5-dioxo-dihydropyrrolo-[1,2-*a*]quinazoline-3a-carboxylic acid scaffold began with the preparation of substituted N-alkyl 2-aminobenzamides **8** from the corresponding 2-aminobenzoic acids **7** using one of two methods. The first method began with the reaction of 2-aminobenzoic acid with CDI in THF, leading to the *in situ* formation of the isatoic anhydride, which was then converted to benzamide **8** using 8 M MeNH$_2$ in EtOH (Scheme 1).

Scheme 1. Synthesis of the Benzamide Intermediate[a]
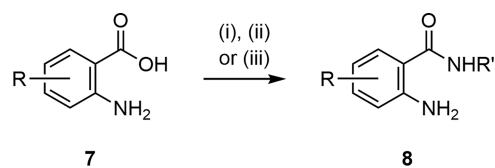
[a]*Reagents and Conditions:* (i) CDI, THF, 0 °C, then 8 M MeNH$_2$·HCl, 21 °C; (ii) RNH$_2$ or RNH$_2$·HCl, EDCI·HCl, HOBt, DIPEA, DMF, 0–21 °C; and (iii) MeNH$_2$·HCl, HATU, DIPEA, DMF, 21 °C.

Alternatively, the substituted benzamides were prepared directly from the corresponding 2-aminobenzoic acid **7** using standard amide coupling conditions, EDCI/HOBt, or HATU in the presence of DIPEA. The absence of suitable commercially available building blocks necessitated the preparation of 2-amino-N-methyl-4-(trifluoromethoxy)-benzamide (**13**) (Scheme 2). Briefly, 1-bromo-2-nitro-4-(trifluoromethoxy)benzene (**9**) was converted to benzonitrile **10** using CuCN at elevated temperatures. The subsequent hydrolysis of the nitrile group in 55% H$_2$SO$_4$ at 100 °C gave carboxylic acid **11**. The treatment of **11** with methylamine in the presence of EDCI/HOBt and DIPEA gave 2-nitro-N-methylbenzamide **12**, which was subsequently reduced to
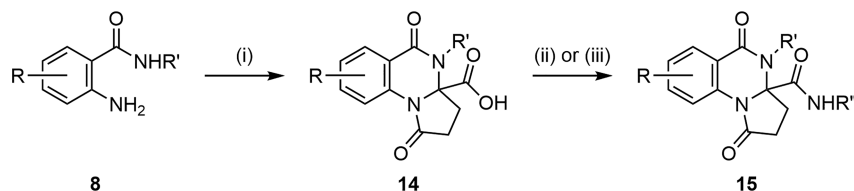
Scheme 2. Synthesis of the 4-Trifluoromethoxy Benzamide Intermediate[a]
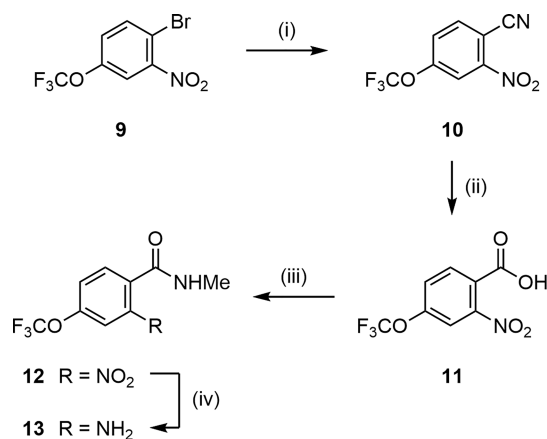
[a]*Reagents and Conditions:* (i) CuCN, DMF, 150 °C, 1 h, then PhCH₃, 110 °C, 1 h, 74%; (ii) 55% H₂SO₄, 100 °C, 15 h, 49%; (iii) MeNH₂· HCl, EDCI·HCl, HOBt, DIPEA, DMF, 0−21 °C, 55%; and (iv) Fe, NH₄Cl, MeOH/H₂O (4:1), 50 °C, 85%.

Scheme 4. Synthesis of the 8-Substituted Quinazolinone Analogues using a Suzuki−Miyaura Reaction[a]

[a]*Reagents and Conditions:* (i) RB(OH)₂, Pd(dppf)Cl₂.CH₂Cl₂ (5−10 mol%), K₃PO₄, PhCH₃/H₂O (9:1), μW, 120 °C, 30 min.
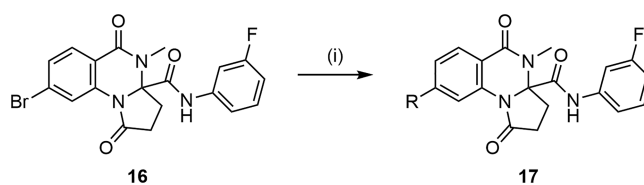
amine **13** using Fe powder and NH₄Cl in MeOH/H₂O at 50 °C.

The 1,5-dioxo-2,3-dihydropyrrolo[1,2-*a*]quinazoline scaffold **14** was formed by condensation with the appropriate 2-aminobenzamides and α-ketoglutaric acid in AcOH at elevated temperatures (Scheme 3).[28] Notably, the cyclization generated a stereocenter at the 3a-position of the pyrrolo[1,2-*a*]-quinazoline scaffold; accordingly, all analogues were isolated as racemic mixtures. The exocyclic carboxamides **15** were then prepared from the corresponding carboxylic acid **14** using either HATU or PyBOP with DIPEA. Alternatively, analogues were also generated using TCFH and 1-methylimidazole (NMI) as reported by Beutner et al.[29] The 8-bromo derivative **16** was prepared using the above methods and then converted to 8-alkyl-substituted analogues **17** using standard Suzuki−Miyaura reaction conditions (Scheme 4).

Structure−Activity Relationship. The SAR was developed using the *P. falciparum* 3D7 asexual blood-stage parasite replication assay. To evaluate the asexual parasite activity of compounds, we employed the previously described assay using LDH activity as the measure of parasite growth.[19] The cytotoxicity of analogues was evaluated against the human HepG2 cell line using CellTitre-Glo as a metabolic marker of cell health.[30] The *in silico* physicochemical parameters, *in vitro* metabolism, and aqueous solubility of analogues were monitored to ensure that the properties of compounds were suitable for *in vivo* administration.

The SAR investigation of the dihydroquinazolinone hit scaffold began with the exploration of the substitution on the exocyclic 3a-carboxamide aryl ring. A cohort of analogues was synthesized with a variety of substituents in the 2-, 3- or 4-position of the aryl ring and then evaluated in the 3D7 asexual parasite growth assay. The results of this assay revealed that analogue **18** with the unsubstituted aryl ring is 5-fold less potent (0.74 μM) than the most potent hit compound **5** (EC₅₀ 0.17 μM) with a 3-methyl substituent on the exocyclic aryl group (Table 1). Analogue **20** with a 3-chloro substituent (EC₅₀ 0.09 μM) was 2-fold more potent than **5** (EC₅₀ 0.17 μM), while analogues **19** and **21** with 3-fluoro and 3-trifluoromethyl substituents were 1.5−2-fold less potent (EC₅₀ 0.23 and 0.36 μM, respectively). These data suggest that the size of the substituent in the 3-positon of the exocyclic ring is important in modulating asexual parasite activity. Substituents such as methoxy, trifluoromethoxy, and nitrile (**6**, **22**, and **23**) were all detrimental to parasite activity (EC₅₀ 0.94, 0.80, and 2.1 μM).

We next examined the impact of substituents in the 4-position of the exocyclic aryl ring on parasite activity. Analogues with 4-fluoro and 4-chloro substituents (**24** and **25**) were significantly less active (EC₅₀ 1.6 and 0.90 μM, respectively) compared to their 3-substituted matched pairs **19** and **20** (Table 1). The presence of methyl, methoxy, and nitrile substituents at the 4-position (**26**, **27**, and **28**, respectively) also led to reduced activity (EC₅₀ 1.1, 2.5, and 2.4 μM, respectively) relative to the unsubstituted analogue **18**. Exploration of the 2-position of the exocyclic aryl group established that a 2-methyl substituent (**31**) was tolerated and was equipotent (EC₅₀ 0.16 μM) with **5**. Conversely, 2-methoxy or 2-halogen substituents (**32**, **29**, and **30**) were all detrimental to asexual parasite activity (EC₅₀ > 10, 2.0, and 0.80 μM) and therefore this position was not investigated further. Overall, the SAR from substitution on the exocyclic arene showed that methyl or halogen substitution in the 3-position of the exocyclic aryl ring was optimal for enhanced asexual parasite activity. Furthermore, analogues **24−26** with this substitution pattern did not exhibit cytotoxicity against the human HepG2

Scheme 3. Synthesis of the 1,5-Dioxo-dihydropyrrolo[1,2-a]quinazoline-3a-carboxylic Acid Scaffold and Analogues[a]

[a]*Reagents and Conditions:* (i) α-Ketoglutaric acid, AcOH, 80 or 118 °C; (ii) R″NH₂, HATU or PyBOP, DIPEA, THF, 21 or 60 °C; and (iii) R′NH₂, TCFH, NMI, MeCN/DMF (1:1), 21 °C.
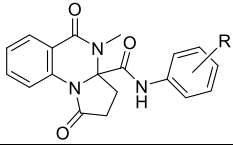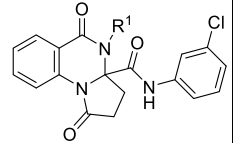
Table 1. Activities of Substituted Aniline Analogues[a,b]

Cmpnd	R	Pf parasite EC$_{50}$ (SD) μM [a]	HepG2 EC$_{50}$ (SD) μM [b]	PSA (Å^2)	cLogP	LipE
18	H	0.74 (0.13)	>40	70	2.0	4.2
19	3-F	0.23 (0.01)	>40	70	2.1	4.5
20	3-Cl	0.09 (0.01)	>40	70	2.6	4.5
5	3-Me	0.17 (0.04)	>40	70	2.5	4.3
21	3-CF$_3$	0.36 (0.08)	>40	70	2.9	3.6
22	3-CF$_3$O	0.80 (0.15)	>40	79	3.4	2.7
6	3-MeO	0.85 (0.30)	>40	79	1.8	4.2
23	3-CN	2.1 (0.45)	>40	94	1.8	3.9
24	4-F	1.6 (0.30)	>40	70	2.1	3.7
25	4-Cl	0.90 (0.08)	>40	70	2.6	3.5
26	4-Me	1.0 (0.13)	>40	70	2.5	3.5
27	4-OMe	2.6 (0.16)	>40	79	1.8	3.8
28	4-CN	2.1 (0.32)	>40	94	1.8	3.9
29	2-F	2.3 (0.39)	>40	70	2.1	3.5
30	2-Cl	0.80 (0.05)	>40	70	2.6	3.5
31	2-Me	0.16 (0.01)	>40	70	2.5	4.3
32	2-OMe	>10	>40	79	1.8	-

[a]EC$_{50}$ data represent means and SDs for three independent experiments using LDH to quantify *P. falciparum* 3D7 parasite growth over 72 h. [b]EC$_{50}$ data represent means and SDs for three independent experiments using Cell Titer-Glo to quantify HepG2 cell growth over 48 h.

Table 2. Activities of 4N-Substituted Analogues[a,b]

Cmpnd	R^1	Pf parasite EC$_{50}$ (SD) μM [a]	HepG2 EC$_{50}$ (SD) μM [b]	PSA (Å^2)	cLogP	LipE
20	Me	0.09 (0.01)	>40	70	2.6	4.5
33	H	5.3 (0.67)	>40	79	2.4	2.9
34	Et	0.42 (0.12)	>40	70	2.9	3.4
35	CH$_2$CF$_3$	0.70 (0.07)	>40	70	3.5	2.6
36	*c*-Pr	0.09 (0.01)	>40	70	3.0	4.0
37	*i*-Pr	2.1 (0.27)	>40	70	3.4	2.3
38	*n*-Pr	0.21 (0.03)	>40	70	3.5	3.2
39	*i*-Bu	0.33 (0.06)	>40	70	3.8	2.7

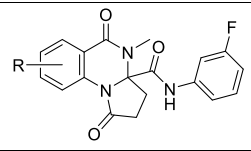[a]EC$_{50}$ data represent means and SDs for three independent experiments using LDH to quantify *P. falciparum* 3D7 parasite growth over 72 h. [b]EC$_{50}$ data represent means and SDs for three independent experiments using Cell Titer-Glo to quantify HepG2 cell growth over 48 h.

cell line at a physiologically relevant concentration (EC$_{50}$s > 40 μM).

To determine whether the N4-methyl substitution in the screening hits **5** and **6** (Figure 1) was required for asexual parasite activity, we exchanged N4-methyl with hydrogen and other aliphatic substituents whil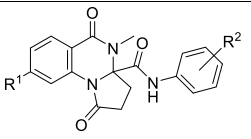e retaining the 3-chloro aryl group on 3a-carboxamide. The absence of N4-methyl (**33**) ablated asexual activity (EC$_{50}$ 4.8 μM) (Table 2), signifying that an alkyl substituent at the N4-position was required. Replacement of the N4-methyl substituent with ethyl (**34**) or a CH$_2$CF$_3$ group (**35**) was detrimental to parasite growth inhibition (EC$_{50}$ 0.45 and 0.67 μM) compared to the

Table 3. Activities of 6-, 7-, 8-, or 9-Halogen-Substituted Analogues[a,b]

Cmpnd	R[1]	Pf parasite EC$_{50}$ (SD) μM [a]	HepG2 EC$_{50}$ (SD) μM [b]	PSA (Å^2)	cLogP	LipE
19	H	0.23 (0.01)	>40	70	2.1	4.5
40	6-F	0.07 (0.01)	>40	70	2.3	4.9
41	7-F	0.97 (0.10)	>40	70	2.3	3.8
42	8-F	0.07 (0.01)	>40	70	2.3	4.9
43	9-F	0.76 (0.09)	>40	70	2.3	3.9
44	6-Cl	0.21 (0.02)	>40	70	2.7	4.0
45	7-Cl	0.92 (0.05)	>40	70	2.7	3.3
46	8-Cl	0.017 (0.004)	>40	70	2.7	5.0
47	9-Cl	0.13 (0.02)	>40	70	2.7	4.2

[a]EC$_{50}$ data represent means and SDs for three independent experiments using LDH to quantify *P. falciparum* 3D7 parasite growth over 72 h. [b]EC$_{50}$ data represent means and SDs for three independent experiments using Cell Titer-Glo to quantify HepG2 cell growth over 48 h.

Table 4. Activity of Anilino-Substituted Analogues against *P. falciparum* Parasites[a,b]
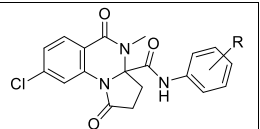

Cmpnd	R[1]	R[2]	Pf parasite EC$_{50}$ (SD) μM [a]	HepG2 EC$_{50}$ (SD) μM [b]	PSA (Å^2)	cLogP	LipE
42	F	3-F	0.067 (0.005)	>40	70	2.3	4.9
46	Cl	3-F	0.017 (0.004)	>40	70	2.7	5.0
48	Me	3-F	0.038 (0.002)	>40	70	2.6	4.8
49	MeO	3-F	0.014 (0.002)	>40	79	2.0	5.9
50	*c*-Pr	3-F	0.039 (0.004)	>40	70	2.9	4.5
51	Ph	3-F	0.010 (0.001)	>40	70	3.8	4.2
52	Cl	3-Cl	0.010 (0.001)	>40	70	3.2	4.8
53	MeO	3-Cl	0.008 (0.001)	>40	79	2.4	5.7
54	CF$_3$	3-Cl	0.014 (0.001)	>40	70	3.5	4.4
55	CN	3-Cl	0.047 (0.008)	>40	94	2.4	4.9
56	CF$_3$O	3-Cl	0.010 (0.002)	>40	79	4.0	4.0

[a]EC$_{50}$ data represent means and SDs for three independent experiments using LDH to quantify *P. falciparum* 3D7 parasite growth over 72 h. [b]EC$_{50}$ data represent means and SDs for three independent experiments using Cell Titer-Glo to quantify HepG2 cell growth over 48 h.

respective N4-methyl orthologue **20**. Interestingly, a cyclopropyl group in the N4-position exhibited equipotent activity (EC$_{50}$ 0.09 μM) compared to **20**, but an isopropyl substituent (**37**) was not tolerated (EC$_{50}$ 2.1 μM), consistent with a cyclopropyl moiety having a smaller steric volume than an isopropyl group. In contrast, an *n*-propyl and an isobutyl group (**38** and **39**) were both moderately tolerated (EC$_{50}$ 0.19 and 0.29 μM). Although the N4-cyclopropyl analogue was equipotent to the N-methyl orthologue, it significantly decreased the LipE (4.5 versus 4.0) and therefore the N4-methyl group was retained for the remainder of the study.
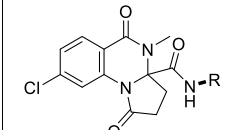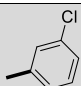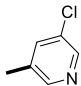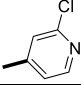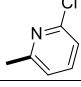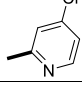
We next investigated whether halogenation was tolerated on each position of the aryl ring on the dihydroquinazolinone scaffold. Incorporation of halogen in these positions was another strategy to potentially mitigate oxidative metabolism of the aryl ring. The addition of fluorine in either the 7- or 9-position (**41** and **43**) gave a decrease in *P. falciparum* activity (EC$_{50}$ 0.97 and 0.76 μM) compared to the non-halogenated orthologue **19** (EC$_{50}$ 0.23 μM) (Table 3). A similar decrease in activity (EC$_{50}$ 0.92 μM) was observed for the 7-chloro analogue **45**, but the 9-chloro analogue **47** was 2-fold more potent (EC$_{50}$ 0.13 μM) than **19**. An approximate 4-fold improvement in parasite activity (EC$_{50}$ 0.07 and 0.07 μM) was

Table 5. Activity of Aniline-Substituted Analogues against *P. falciparum* Parasites[a,b]

Cmpnd	R	Pf parasite EC$_{50}$ (SD) μM [a]	HepG2 EC$_{50}$ (SD) μM [b]	PSA (Å^2)	cLogP	LipE
46	3-F	0.017 (0.004)	>40	70	2.7	5.0
52	3-Cl	0.010 (0.001)	>40	70	3.2	4.8
57	3,4-F$_2$	0.023 (0.001)	>40	70	2.9	4.8
58	3,4-Cl$_2$	0.012 (0.004)	>40	70	3.8	4.1
59	3-Cl,4-F	0.015 (0.001)	>40	70	3.3	4.5
60	4-Cl,3-F	0.060 (0.011)	>40	70	3.3	3.9
61	3,5-F$_2$	0.014 (0.002)	>40	70	2.9	5.0
62	3,5-Cl$_2$	0.062 (0.013)	>40	70	3.8	3.4
63	3-Cl,5-F	0.014 (0.001)	>40	70	3.3	4.5

[a]EC$_{50}$ data represent means and SDs for three independent experiments using LDH to quantify *P. falciparum* 3D7 parasite growth over 72 h. [b]EC$_{50}$ data represent means and SDs for three independent experiments using Cell Titer-Glo to quantify HepG2 cell growth over 48 h.

Table 6. Activity of Anilino-Substituted Analogues against *P. falciparum* Parasites[a,b]

Cmpnd	R	Pf parasite EC$_{50}$ (SD) μM [a]	HepG2 EC$_{50}$ (SD) μM [b]	PSA (Å^2)	cLogP	LipE
52		0.010 (0.001)	>40	70	3.2	4.8
64		0.019 (0.003)	>40	83	2.0	5.8
65		0.054 (0.020)	>40	83	2.2	5.1
66		0.92 (0.20)	>40	83	2.8	3.3
67		0.18 (0.03)	>40	83	2.6	4.2

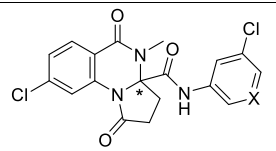[a]EC$_{50}$ data represent means and SDs for three independent experiments using LDH to quantify *P. falciparum* 3D7 parasite growth over 72 h. [b]EC$_{50}$ data represent means and SDs for three independent experiments using Cell Titer-Glo to quantify HepG2 cell growth over 48 h.

observed with both the 6-fluoro and 8-fluoro derivatives **40** and **42**, while analogue **44** with a 6-chloro substituent exhibited similar potency (EC$_{50}$ 0.21 μM) to the comparator compound **19**. Incorporating chloro in the 8-position (**46**) gave a 10-fold increase in potency (EC$_{50}$ 0.02 μM) relative to the activity of **19**. Reassuringly, the increases in parasite activity with the 6- and 8-halogenated analogues **40**, **42**, and **46** were not accompanied by an increase in human cell cytotoxicity (EC$_{50}$ > 40 μM).

The significant increase in asexual activity with the 8-halogen substitution prompted further exploration of the 8-position while retaining 3-fluorophenyl carboxamide. The

compounds **48** and **50** with methyl or cyclopropyl groups in the 8-position exhibited potent activity (EC$_{50}$ 0.038 and 0.039 μM) compared to the 8-chloro derivative **46** (Table 4). Analogue **49** with an 8-methoxy group also displayed potent parasite activity (EC$_{50}$ 0.015 μM), implying that polar substituents are accepted in the 8-position. Analogue **51** with a phenyl substituent in the 8-position also exhibited potent activity (EC$_{50}$ 0.01 μM), highlighting the capacity of this position to accept large functionality. To confirm that the activity imparted by the 3-chloro exocyclic phenyl ring was consistent with 3-fluoro orthologues, we generated 8-chloro and 8-methoxy analogues **52** and **53**. Compounds **52** and **53**

Table 7. Activity of Anilino-Substituted Analogues against *P. falciparum* Parasites[a,b]

Cmpnd	*	X	Pf parasite EC$_{50}$ (SD) μM[a]	HepG2 EC$_{50}$ (SD) μM[b]	PSA (Å^2)	cLogP	LipE
52	*R/S*	CH	0.01 (0.001)	>40	70	3.2	4.8
68	*R*	CH	2.9 (1.1)	>40	70	3.2	2.3
69	*S*	CH	0.007 (0.001)	>40	70	3.2	5.0
64	*R/S*	N	0.019 (0.003)	>40	83	2.0	5.8
70	*R*	N	2.0 (0.1)	>40	83	2.0	3.7
71	*S*	N	0.008 (0.001)	>40	83	2.0	6.1

[a]EC$_{50}$ data represent means and SDs for three independent experiments using LDH to quantify *P. falciparum* 3D7 parasite growth over 72 h. [b]EC$_{50}$ data represent means and SDs for three independent experiments using Cell Titer-Glo to quantify HepG2 cell growth over 48 h.
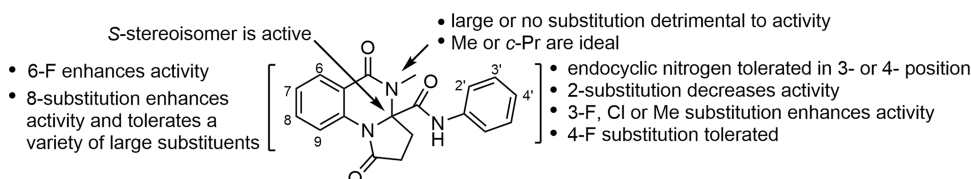

Figure 2. Summary of the structure and activity relationship.

showed similar activity (EC$_{50}$ 0.013 and 0.012 μM) compared to their 3-fluoro exocyclic counterparts **46** and **49**. Further exploring the 8-position, incorporation of the 8-trifluoromethyl (**54**) or 8-nitrile (**55**) functionality led to a 3- to 4-fold decrease in potency (EC$_{50}$ 0.032 and 0.047 μM), while analogue **56** with a 8-trifluoromethoxy group retained activity (EC$_{50}$ 0.012 μM) compared with **53**. This analogue set highlights that a broad array of functionality is tolerated in the 8-position and the possibility to use this position as a handle to enhance physicochemical properties. Notably, substitution in the 8-position increased the clog *P* overall, but the gain in asexual activity offset lipophilicity accordingly, giving significant improvements in LipE and demonstrating that the improvement in activity was not solely attributable to the contribution of hydrophobicity. The exception was the 8-methoxy derivatives **49** and **53**, which had lower clog *P* and showed superior LipE values (5.9 and 5.5). The HepG2 cytotoxicity was not observed for the 8-substituted analogues at the highest concentration tested (EC$_{50}$ > 40 μM), implying that the increase in parasite activity is not causing adverse cytotoxicity to human cells.

It was postulated that bis-halogenation could potentially assist in mitigating metabolic oxidation of the exocyclic aryl group and potentially mitigate the mutagenicity risk of the aniline toxicophore. We therefore explored bis-halogenation of the exocyclic aryl group by preserving halogenation in the 3-position (relative to the carboxamide), while a second halogen was introduced at the 4- and 5-positions. Bis-halogenation was surveyed on the exocyclic arene while retaining the 8-chloro-

substituted tricyclic scaffold to assess the impact on parasite activity. Analogues **57−63** with 3,4-bis-halogen substitution patterns typically exhibited parasite activity (EC$_{50}$ 0.012−0.023 μM) comparable to the corresponding monohalogenated orthologues **46** and **52** (Table 5). The 4-chloro-3-fluoro analogue **60** proved to be an exception, exhibiting a 3-fold decrease in activity (EC$_{50}$ 0.060 μM) versus the 3-fluorophenyl analogue **46**. Analogues **61** and **63** with 3,5-difluoro or 3-chloro-5-fluoro substitution also displayed activity (EC$_{50}$ 0.014 and 0.016 μM) comparable to **46** and **52**, but analogue **62** with 3,5-dichloro substitution was 4-fold less active (EC$_{50}$ 0.062 μM). Overall, none of the dihalogen-substituted combinations improved activity in comparison to the mono 3-fluorinated and 3-chlorinated derivatives **46** and **52**, and consequently, the LipE was reduced with the introduction of an additional halogen.

To improve aqueous solubility and metabolism, we incorporated endocyclic nitrogen into each position of the exocyclic aryl ring while maintaining a chloro substituent in the 3-position relative to the carboxamide group. It was found that analogue **64**, which contains a 5-chloropyridin-3-yl moiety, was 2-fold less active (EC$_{50}$ 0.021 μM) than the carbocyclic benchmark compound **52** (Table 6). The 4-aza-3-chloro analogue (**65**) was also modestly tolerated (EC$_{50}$ 0.054 μM), but the endocyclic nitrogen in the 2-position combined with either a 3- or 5-chloro substituent (**66** and **67**) was detrimental to activity (EC$_{50}$ 0.92 and 0.18 μM, respectively). Collectively, of this set, analogue **64** was the most potent combination on the exocyclic ring and had a favorable LipE of 5.7.

Table 8. Evaluation of Aqueous Solubility, *In Vitro* Metabolism, and eLog D

| | solubility[a] | | | in vitro metabolism[b] | | | | | |
| | | | | liver microsomes | | | hepatocytes | | |
cmpd	SGF (μM)	SIF (μM)	PBS (μM)	human CL_{int} (μL/min/mg)	mouse CL_{int} (μL/min/mg)	rat CL_{int} (μL/min/mg)	rat CL_{int} (μL/min/10^6 cells)	eLog D	cLog P
18	35	39	34	<8	21	295			2.0
40	10	11	10	22	60	>347			2.3
41	9	16	9	44	65	>347			2.3
42	7	31	7	33	76	>347			2.3
46	<4	10	10	76	90	>347	184	3.02	2.7
53			3	107			158	2.86	2.4
55			<4	54			>92	2.58	2.4
56			<4	70			>92	3.93	4.0
58				130	119	70			3.8
62				113	144	100			3.8
64	55	17	5	42	55		18	2.86	2.0
65	54	11	3	56	25		18	2.94	2.2
71			8	28			15	2.89	2.0

[a]Fasted conditions used for SGF (pH 1.2) and SIF (pH 6.5). PBS (pH 7.4). [b]Associated $t_{1/2}$ values are shown in Table S11.

The analogues evaluated in Tables 1−6 were all prepared as racemates with a chiral carbon at the 3a-position. The current synthesis did not allow for the enantioenriched products and therefore the enantiomers of the analogues **52** and **64** were resolved using chiral chromatography. To determine the absolute configuration of the separated isomers, an X-ray crystal structure was obtained on one isomer of **52** (Figure S2). The structure permitted the assignment of *R*-configuration at the chiral center, denoted as compound **68**. The parasite activity of each isomer demonstrated that **68** was the distomer (EC_{50} 0.92 μM), while the *S*-isomer **69** was the eutomer (EC_{50} 0.009 μM) (Table 7). The configuration of the *R*- and *S*-isomers of compound **64** was then assigned according to the parasite activity (EC_{50} 1.7 and 0.011 μM, compounds **70** and **71**, respectively). These data highlighted the enantio-preference for parasite activity (Figure 2). Furthermore, the frontrunner compound **71** (WJM-921) was noncytotoxic to human HepG2 cells (EC_{50} > 40 μM) (Table 7) and showed no inhibition of hERG (IC_{50} > 30 μM) (Table S2).

Aqueous Solubility and *In Vitro* Metabolic Stability. Aqueous solubility and *in vitro* metabolism data were collected on a subset of synthesized analogues to gauge their suitability for evaluation in a mouse model of malaria infection. Aqueous solubility at pH 7 was generally low for all analogues. The introduction of halogen substituents on the scaffold (**40**, **41**, **42**, and **46**) increased the lipophilicity and decreased the solubility in simulated gastrointestinal fluid (SGF) conditions (<10 μM) compared to the undecorated analogue **18** (35 μM) (Table 8). The incorporation of endocyclic nitrogen in the exocyclic ring (**65** and **64**) decreased lipophilicity and modestly increased solubility in SGF conditions (54 and 55 μM).

The unsubstituted analogue **18** was characterized by low intrinsic clearance in human and mouse microsomes (<8 and 21 μL/min/mg) and by high clearance in rat microsomes (295 μL/min/10^6 cells) (Table 8). The addition of halogen substituents to the scaffold (**40**, **41**, **42**, and **46**) to improve parasite activity increased lipophilicity and accordingly increased intrinsic clearance in both human (22−76 μL/min/mg) and mouse microsomes (60−90 μL/min/mg) (Table 8). Metabolite identification following incubation of **46** in mouse liver microsomes revealed that oxidative defluorination of the exocyclic aryl ring was the major metabolic biotransformation, while N-demethylation was also observed (Table S1). The bis-halogen substitution was then introduced into the exocyclic aryl ring (**58** and **62**) to mitigate oxidative dehalogenation, but this change led to an increase in intrinsic clearance (>113 μL/min/mg), and the hypothesis that other metabolic sites were available, and clearance was intrinsically linked to the lipophilicity of the scaffold. The subsequent introduction of endocyclic nitrogen into the exocyclic aryl ring (**65** and **64**) decreased lipophilicity and correspondingly gave a modest improvement in intrinsic clearance in human (56 and 42 μL/min/mg, respectively) and mouse liver microsomes (25 and 55 μL/min/mg, respectively). A significant improvement in metabolic turnover in rat hepatocytes (18 μL/min/10^6 cells) was also observed with both **65** and **64**. Overall, the incorporation of endocyclic nitrogen was beneficial for both aqueous solubility and *in vitro* metabolism and did not overtly impact parasite activity. Therefore, **71** (WJM-921) was considered suitable for evaluation in a malaria mouse model.

Resistance Selection and Whole-Genome Sequencing. To determine the mechanism of action of the dihydroquinazolinone antimalarial class, we performed a minimum inoculum of resistance (MIR) assay using compound **49**.[31] In the MIR assay, an inoculum of 2×10^5 Dd2 parasites was exposed to a concentration three times the EC_{90} of **49** (29 nM) in a 96-well format, and then parasite recrudescence was monitored over 60 days. Resistance selection with **49** resulted in recrudescent parasites in 20 out of 96 wells from day 13 to day 60, with a low EC_{50} fold shift of 1.8−2.3 and a calculated MIR of 9.6×10^5 (Tables S3 and S4). In comparison, DSM265 and KAE609 were used as controls in the experiment and under the same pressure conditions (3 × EC_{90}), yielding 32 recrudescent wells out of 96 with an MIR value of 6×10^5 and 15 recrudescent wells out of 96 wells with an MIR value of 1.3×10^6, respectively. Collectively, the MIR assay data show that compound **49** has a low EC_{50} fold shift of less than 3 and an MIR value of $\leq 10^6$, similar to DSM265 and KAE609. These data position the dihydroquinazolinone class in the medium-risk category for acquiring resistance in the clinic.[18]

Whole-genome sequencing of three Dd2 parasite clones (B2, C5, and C7) from the MIR assay revealed that the C5 population had a single F156L mutation in PfATP4. The B2 population had a D425E mutation in PfATP4 in addition to a V826I mutation in S-adenosyl-L-methionine-dependent tRNA 4-demethylwyosine synthase; in contrast, no SNP was observed for the C7 population (Table S6). No gene amplification was observed for parasite populations B2 and C5, while population C7 had a 2.8-fold amplification in a region that encodes PfATP4 (Table S7 and Figure S8). The observed mutations for populations B2 and C5 were mapped to a homology model of PfATP4 and are located in the cytoplasmic exposed region of PfATP4 (Figure 3). D425E was
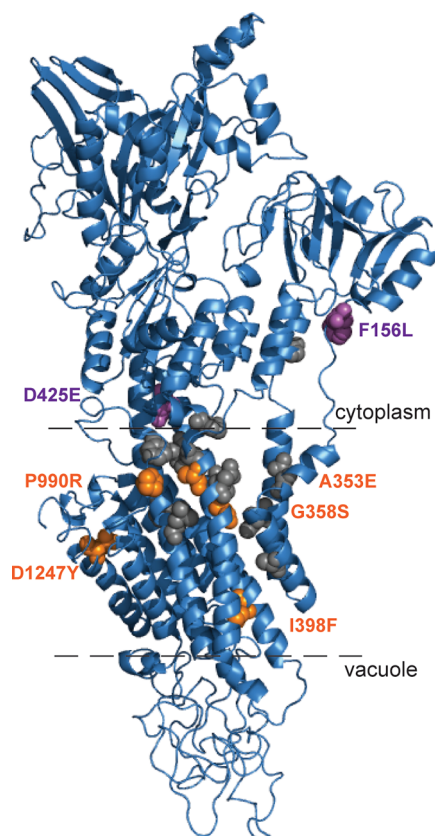

Figure 3. Structure of PfATP4 showing mutations found in **49**-resistant clones (purple) and KAE609 and SJ733-resistant strains (orange) used in this study. Other reported PfATP4 mutations that confer resistance to SJ733 and KAE609[14,20] are shown in gray. The homology model of PfATP4 was created using the crystal structure of the rabbit SERCA pump (PDB 2C88),[32] as previously described.[10,14] The predicted transmembrane region of PfATP4 is shown by the dashed line.

proximal to the mutations located in the intramembrane domain of PfATP4 previously reported for KAE609 and SJ733-resistant strains.[14,20] Notably, the PfATP4 mutations D425E and F156L had not been previously reported. These whole-genome sequencing data implied that PfATP4 was the molecular target of the dihydroquinazolinone antimalarial class.

Rate and Stage of Asexual Stage Arrest. PfATP4 inhibitors are typically characterized by a fast-to-moderate killing rate of the asexual stage parasite.[14] To determine the rate of kill, the dihydroquinazolinone class was benchmarked

against KAE609 in a parasite viability assay.[33] Here, samples of parasites are taken from the treated culture at 0, 24, and 48 h, and the drug is washed out. Drug-free culture is then serially diluted into uninfected RBCs pre-labelled with carboxylfluorescein diacetate succinimidyl ester (CFSE), and cultures are maintained for 48 h before labelling parasites with Hoechst. Viable parasites are then determined at each time point by flow cytometry using double positive staining of CSFE and Hoechst. Parasitemia is determined at each time point by flow cytometry using double positive staining of CSFE and Hoechst. In the parasite viability assay, compounds **5** and **71** showed a fast-to-moderate rate of parasite reduction that was slower than chloroquine and artemisinin but faster than pyrimethamine (Figure 4C). The killing rate profiles of **5** and **71** were consistent with the killing rate of KAE609. The asexual stage of arrest was also determined and showed that **5** and **71** arrested asexual parasites at the early trophozoite stage (Figures 4A,B and S4). Microscopy revealed that the **5**- and **71**-treated parasites were characterized as "swollen," a characteristic phenotype previously observed with PfATP4 inhibitors,[20,26,34] which is attributed to the accumulation of Na^+ inside the parasite cytosol. The asexual phenotype observed was consistent with that for KAE609 and provided further evidence that the dihydroquinazolinone class targeted PfATP4.

Evaluation of Parasite Cytosolic Na^+ Concentration and pH. PfATP4 is an essential P-type ATPase that localizes to the parasite plasma membrane.[14,35] Spillman et al. provided evidence that PfATP4 serves as the parasite's primary Na^+ extruder while also importing H^+ equivalents.[23] Chemically diverse PfATP4 inhibitors have been shown to cause an increase in the parasite $[Na^+]_{cyt}$ and an increase in pH_{cyt}.[20,23] We investigated the effects of the hit compounds **5** and **6** on cytosolic Na^+ concentration ($[Na^+]_{cyt}$) in 3D7 parasites that were isolated from their host erythrocytes and loaded with the Na^+-sensitive fluorescent dye SBFI. Both compounds gave rise to an increase in $[Na^+]_{cyt}$ (Figure S5), consistent with them being PfATP4 inhibitors. The EC_{50} values for dysregulation of $[Na^+]_{cyt}$ by compounds **5** and **6** were 0.23 and 0.32 μM, respectively (Figure S5). These EC_{50} values are comparable to the EC_{50}s determined against asexual parasites of 0.17 and 0.85 μM, respectively (Table 1).

PfATP4 inhibitors can also be detected using pH-based assays. In the assay employed here, 3D7 parasites were isolated from their host erythrocytes, loaded with the pH-sensitive dye BCECF, and depleted of ATP by incubating them in glucose-free saline. They were then suspended in a saline solution containing the test compound (or solvent alone), glucose, and concanamycin A (100 nM), an inhibitor of the parasite's primary pH regulator, the V-type H^+ ATPase.[36,37] Under these conditions, compounds **5** and **6** (tested at 5 μM) and the control PfATP4 inhibitor cipargamin (tested at 0.05 μM) gave rise to a pronounced cytosolic alkalinization (Figure S6). No such alkalinization was observed in the absence of the compound (0.1% v/v DMSO; solvent control; Figure S6).

We next assessed the frontrunner compound **71** (WJM-921) and its distomer **70** to ensure that through structural optimization, the on-target effect (inhibition of PfATP4) was maintained. In Na^+ assays, **71** caused an increase in $[Na^+]_{cyt}$, with the effects observed at each of the two concentrations tested (1 and 0.2 μM) being comparable to that seen with the control PfATP4 inhibitor cipargamin (tested at 0.05 μM; Figure 5). In contrast, the distomer **70** had little effect on
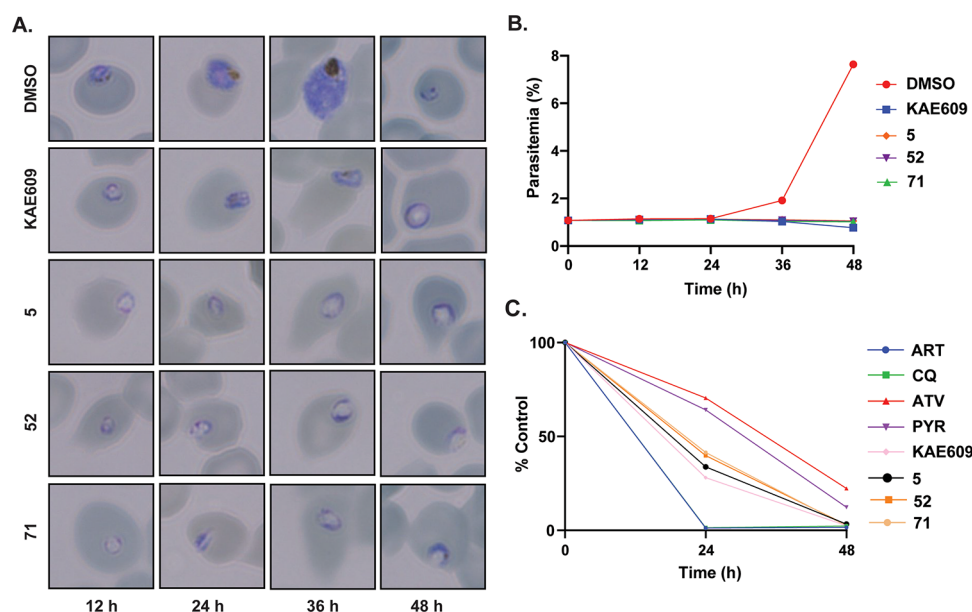
Figure 4. Stage of asexual arrest and killing rate of selected compounds. (A) Parasite morphology was determined by Giemsa-stained blood smears at $10 \times EC_{50}$ of each compound after treatment of ring-stage parasites. Compounds cause vacuolated parasites consistent with the morphology observed with the PfATP4 inhibitor KAE609. (B) Flow cytometry of SYBR green-stained infected RBCs determined that compounds arrest parasites at the early trophozoite stage. Data points represent the mean of three technical replicates. (C) PfATP4 inhibitors have a fast-to-moderate rate of parasite kill in a viability assay measured by flow cytometry of staining erythrocytes pre-labelled with CFSE and parasites stained with Hoechst. Compounds were used at $10 \times EC_{50}$. Data points represent the mean of three technical replicates.
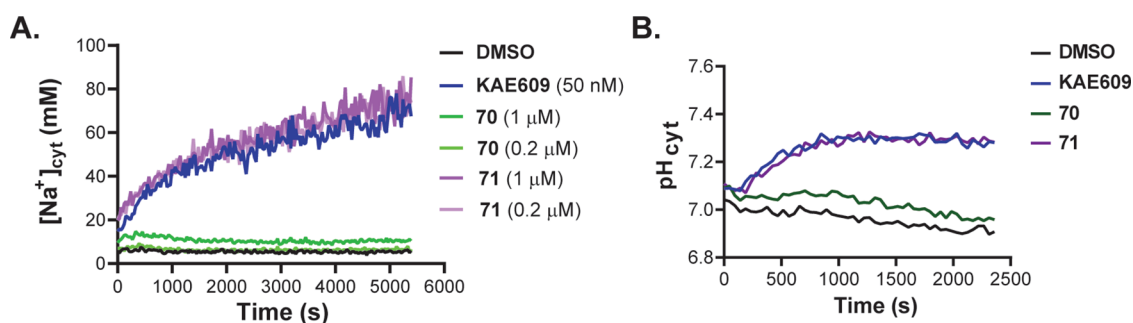

Figure 5. Evaluation of **70** and **71** in Na^+ (A) and pH (B) assays for the detection of PfATP4 inhibition. (A) Fluorescence measurements were performed with isolated SBFI-loaded 3D7 trophozoites suspended at 37 °C at pH 7.1 physiological saline solution containing either **70** or **71** (at concentrations of 1 or 0.2 μM) or cipargamin (50 nM; positive control for PfATP4 inhibition) or DMSO (0.1% v/v; solvent control). (B) Isolated BCECF-loaded 3D7 trophozoites (that prior to the measurements had been ATP-depleted through incubation in glucose-free saline) were suspended in a pH 7.1 saline solution containing glucose, concanamycin A (100 nM), and either **70** (5 μM), **71** (5 μM), cipargamin (50 nM), or DMSO (0.1% v/v; solvent control) at 37 °C and the fluorescence was recorded immediately. The data are from a single experiment, representative of two similar independent experiments.

$[Na^+]_{cyt}$ when tested at 1 or 0.2 μM (Figure 5). In pH assays, under the conditions described above, **71** (tested at 5 μM) and cipargamin (tested at 0.05 μM) gave rise to a cytosolic alkalinization, whereas **70** (tested at 5 μM) and DMSO (0.1% v/v; solvent control) did not (Figure 5). Together, the data imply that the dihydroquinazolinone compounds inhibit PfATP4 and disrupt ion homeostasis in the parasite.

Evaluation of PfATP4 and Multidrug-Resistant Parasite Activity. We next determined whether the **49**-resistant strains were cross-resistant to other representative dihydroquinazolinone analogues and PfATP4 inhibitors, SJ733 and KAE609. It was observed that **71** and **52** showed a 1.5 to 2-fold increase in EC_{50} values against the three **49**-resistant populations (Table 9 and Figure S3), which is approximately the same fold-change observed with **49** against the three **49**-resistant populations. Notably, analogues **71** and **52** showed a

Table 9. Compound 49-Resistant Populations and Activity of Analogues

| | | Dd2 49-resistant strain EC_{50} (SD) (nM)^{a,b} | | |
cmpd	Dd2 EC_{50} (SD) (nM)^a	C5	C7	B2
49	15.0 (0.4)	30.0 (4.3)	25.1 (1.1)	30.1 (7.1)
71	16.6 (4.2)	24.0 (7.6)	24.0 (10.2)	39.6 (13.5)
52	19.4 (6.2)	32.0 (6.9)	35.3 (13.4)	42.8 (11.3)
KAE609	1.9 (0.2)	4.3 (0.5)	3.1 (0.3)	2.1 (0.3)
SJ733	53.9 (6.9)	136 (17)	112 (23)	78.9 (3.0)

^{a}EC_{50} values represent averages and SDs of 3 biological replicates from a 72 h Pf LDH assay. ^{b}Whole-genome sequencing of Dd2 population C5: $2.8 \times$ CNV in PfATP4; C7: F156L SNP in PfATP4; B2: D425E SNP in PfATP4.

2-fold increase in EC$_{50}$ against clone B2, signifying decreased sensitivity in the presence of the D425E mutation. This is in contrast to KAE609 and SJ733, which showed no or little variance in the EC$_{50}$ value between the B2 population and the wildtype Dd2 strain. An approximate 2-fold shift with KAE609 and SJ733 was observed with the **49**-resistant populations C5 and C7.

A variety of dihydroquinazolinone analogues were then evaluated against parasite strains that are resistant to KAE609 and SJ733. KAE609 has a 10-fold decrease in the EC$_{50}$ against a strain with three mutations (I398F, P990R, and D1247Y) in PfATP4 generated in the laboratory,[14] while SJ733 retains potency against this strain (Table 10). Both KAE609 and

Table 10. Evaluation of Selected Compounds against PfATP4 Drug-Resistant *P. falciparum* Strains

| cmpd | Dd2 EC$_{50}$ (nM)[a] | Dd2 PfATP4-resistant EC$_{50}$ (nM)[a] | |
		PfATP4^{I398F,P990R,D1247Y}	PfATP4^{G358S}
5	171	2,860	17
20	63	934	7
36	63	1,440	50
49	16	142	28
52	8	136	13
64	15	173	34
KAE609	2	9	1,340
SJ733	68	85	>11,000

[a]EC$_{50}$ values are an average of two independent experiments in duplicate against the Dd2 parental line, Pf Dd2 PfATP4^{I398F,P990R,D1247Y}[14]- and PfATP4^{G358S}[20]-resistant strains over 72 h using an LDH assay. Table S8 shows EC$_{50}$ values from independent experiments.

SJ733 are greater than 1000-fold less active against a strain with a G358S mutation in PfATP4. The G358S mutation is the same mutation that was detected in recrudescent parasites from patients treated with KAE609 in phase II clinical trials.[27,38] Dihydroquinazolinone analogues generally exhibited a 10-fold decrease in potency against the triple mutant PfATP4 strain, and analogues **20** and **36** exhibited a 20-fold decrease in potency. In contrast, the dihydroquinazolinone analogues were generally equipotent against the PfATP4^{G358S}-resistant strain compared to the Dd2 parental parasite strain, except for compounds **5** and **20** that were 10-fold more potent against the PfATP4^{G358S}-resistant strain. These data argue for different binding site interactions of our analogue series compared to

KAE609, resulting in complex cross-resistance profiles, including instances of collateral hypersensitivity whereby resistance to KAE609 mediated increased sensitivity to **5** and **20**.

Representative dihydroquinazolinone analogues were also evaluated against multidrug-resistant parasite strains found in the clinic, including strains resistant to atovaquone, chloroquine, or mefloquine. It was found that none of the dihydroquinazolinone analogues had reduced potency against these multidrug-resistant strains (Table 11). Overall, the dihydroquinazolinone antimalarial class retained potency against clinical PfATP4 and multidrug-resistant parasite strains signifying that it adheres to the remit of the resistance strategy for the development of new antimalarials.[18]

Evaluation of Transmission Stage Activity. PfATP4 inhibitors have been shown to block the transmission of parasites in preclinical models[20,24] by inhibiting both gametocyte and gamete development.[24,26] To gauge whether the dihydroquinazolinone scaffold has potential as a transmission-blocking agent, we evaluated a representative set of analogues in a dual gamete formation assay (DFGA). In this assay, *P. falciparum* NF54 late-stage gametocytes were treated with compounds for 48 h and then exposed to a drop in temperature and pH, mimicking the mosquito gut conditions to induce male and female gamete formation.[39] After 25 min, the impact of the compound on male exflagellation is quantified by microscopy, and after a further 24 h, the impact on female gamete formation is detected by microscopy using an αPfs25 antibody.[40] The two hit compounds **5** and **6** showed modest inhibition of both male (EC$_{50}$ 1.05 and 4.87 μM, respectively) and female gametes (EC$_{50}$ 0.88 and 4.69 μM, respectively), while the racemic frontrunner compound **64** was more potent against both male and female gametes (EC$_{50}$ 0.50 and 0.19 μM, respectively) (Table 12 and Figure S7), suggesting that this compound class has transmission-blocking potential.

Efficacy in a *Plasmodium berghei* 4-day Mouse Model. The frontrunner compound **71** (WJM-921) was considered to have suitable parasite activity and *in vitro* ADME properties for evaluation in a *P. berghei* 4-day mouse model. The less active isomer **70** was also used to ensure that the activity observed in the mouse model was mediated through the inhibition of PfATP4. This mouse model is an established *in vivo* model for measuring the efficacy of antimalarial compounds at an early stage of development and uses a *Plasmodium* strain that infects mice. In this model, mice are

Table 11. Evaluation of Selected Compounds against Multidrug-Resistant *P. falciparum* Strains

| cmpd | EC$_{50}$ (nM)[a] | | | | | | | | |
	3D7	Dd2	Dd2^{ATV}	K1	K1^{Mef}	PNG^{1776}	W2^{mef}	CAM3^{REV}	CAM3^{RS39T}
5	210	172	177	297	203	148	298	135	143
20	80	63	96	105	96	78	87	77	96
36	84	63	107	111	97	112	100	84	119
49	14	16	16	22	17	14	19	13	15
52	10	7.9	13	17	13	10	13	11	13
64	16	16	21	28	21	17	21	14	16
ATQ	1.7	1.4	14	1.0	0.8	1.7	1.9	0.7	1.0
MFQ	23	35	5.0	3.6	11	4.9	64	9.4	12

[a]EC$_{50}$ values are an average of $n = 2$ experiments in technical replicates measuring the viability of multidrug-resistant parasites over 72 h in an LDH assay. Table S9 shows EC$_{50}$ values from independent experiments. Dd2^{ATV} has an M133I mutation in cyt *b*. ATQ = atovaquone; MFQ = mefloquine.

Table 12. Activity of Selected Compounds in the Dual Gamete Formation Assay

	gamete EC$_{50}$ (μM)[a]	
cmpd	male	female
5	1.05	0.88
6	4.87	4.69
64	0.50	0.19

[a]EC$_{50}$ data represents the mean of four replicate experiments following exposure to compounds for 30 min for *P. falciparum* NF54 male gametes and 24 h for *P. falciparum* NF54 female gametes. The viability of male gametes was quantified by automated microscopy measuring exflagellation and for female gametes measuring fluorescence using an αPfs25 antibody. The assay error is shown in Figure S6.

infected with asexual stage *P. berghei* ANKA GFPcon 259 cl2 parasites[41] that express a green fluorescent protein (GFP) for detection by flow cytometry. The compound was then administered by oral gavage 2 h after the initial infection with *P. berghei* parasites and again at 24, 48, and 72 h after the initial dose, and the level of parasitemia was monitored on days 2, 3, and 4. At 40 mg/kg, **71** suppressed parasitemia by approximately 75−80% on days 2 and 3, and on day 4, an average 30% reduction in parasitemia was observed, although this was not statistically significant (Figure 6A), while parasitemia with **70** was equivalent to the untreated control. Blood plasma analysis was taken 2, 6, and 24 h after the first 40

mg/kg dose in the mouse model and revealed that both **70** and **71** showed reasonable absorption with T_{max} values exceeding 1 μM and plasma concentrations exceeding the *in vitro* EC$_{90}$ for approximately 15 h (Figure 6C). At a dose of 80 mg/kg, **71** suppressed >98% of parasitemia for 3 of the 4 mice on day 4, while there was no statistically significant difference between **70** and the untreated control (Figure 6B). These data imply that further optimization of the dihydroquinazolinone scaffold is required to clear parasitemia at a lower dose. One limitation of using *P. berghei* in an efficacy study is that the sequence of ATP4 is not highly conserved between *P. falciparum* and other *Plasmodium* species[42] and therefore may have contributed to the moderate efficacy observed with **71** in the *P. berghei* model. To circumvent this constraint, antimalarials that target PfATP4 are typically assessed using the *P. falciparum* SCID mouse model.[20]

CONCLUSIONS

We identified a novel antimalarial chemotype by screening the Janssen Jumpstarter library against the *P. falciparum* asexual blood-stage parasite. SAR studies on the dihydroquinazolinone hit scaffold revealed that small nonpolar substituents at the 3-position of the exocyclic ring and substituents at the 8-position of the tricyclic ring system gave appreciable increases in parasite activity (Figure 2). The added hydrophobicity of these substituents generally decreased metabolic stability and aqueous solubility, which was circumvented by the addition
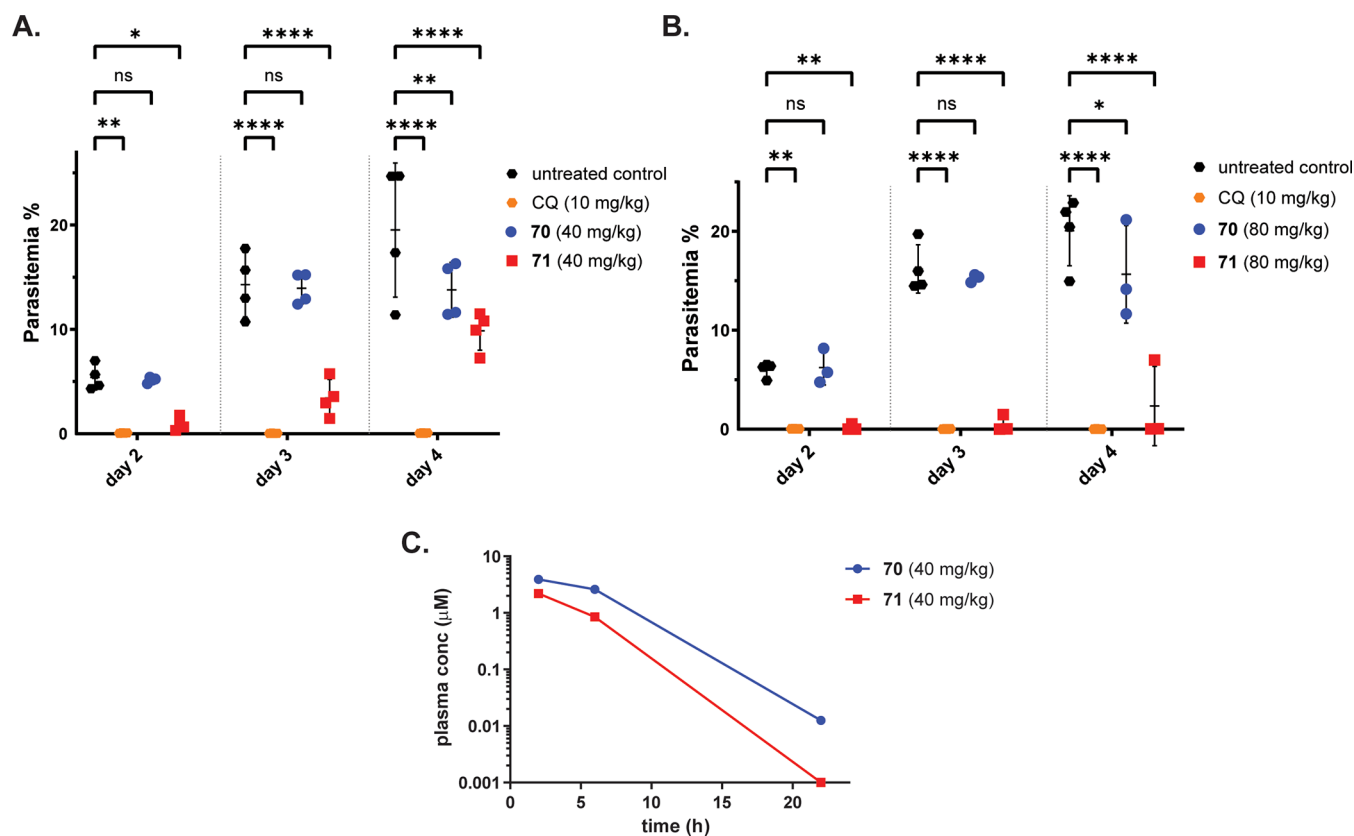

Figure 6. Activity of **71** (WJM-921) (and **70**) in a *P. berghei* 4-day mouse model. To infect mice, *P. berghei* parasites (2 × 10⁷ parasites) were injected into the tail vein. Compounds were administered q.d. (A) 40 mg/kg and (B) 80 mg/kg by p.o. in a HPMC vehicle 2 h after infection (day 0) and then on days 1, 2, and 3. On days 2, 3, and 4, blood smears were taken, and parasitemia was evaluated. Chloroquine (CQ) (10 mg/kg) was used as a positive control. Error bars represent SD. The statistical test was performed using two-way ANOVA. (C) Bioanalysis of **71** (and **70**) concentration in plasma after the first 40 mg/kg dose.

of an endocyclic in the exocyclic ring. It was also found that the stereochemistry at the 3a-position of the tricyclic scaffold was important for parasite activity. These changes culminated in producing the frontrunner compound **71** (WJM-921). **71** had single-digit nanomolar EC_{50} against the asexual parasite, which was devoid of mammalian cellular toxicity and demonstrated oral efficacy in a *P. berghei* mouse model.

Resistance evaluation determined that compound **49** has a MIR of 9.6×10^5 and a low EC_{50} fold shift. Crucially, we also observed that dihydroquinazolinone analogues were not cross-resistant to multidrug-resistant parasite strains found in the clinic, including the PfATP4^{G358S}-resistant strain, classifying the dihydroquinazolinone in the medium-risk category for acquiring resistance in the clinic.[18] Variation in the cross-resistance pattern between analogues was seen with PfATP4^{G358S} and PfATP4^{I398F,P990R,D1247Y} strains and suggests that dihydroquinazolinone analogues other than **49** may have a different MIR and possibly an improved MIR classification.

Whole-genome sequencing of compound **49**-resistant populations revealed an amplification and SNPs in PfATP4. To confirm that PfATP4 was the target, we showed that dihydroquinazolinone analogues display cross-resistance with SJ733 and KAE609 in the PfATP4^{I398F,P990R,D1247Y} strain. These analogues also give rise to ionic perturbations consistent with PfATP4 inhibition. In addition to the moderate to fast killing of asexual parasites, dihydroquinazolinone analogues also killed male and female gametes, consistent with the activity of PfATP4 inhibitors KAE609 and SJ733.[20,24] Collectively, these data imply that PfATP4 is the molecular target of the dihydroquinazolinone antimalarial class.

Further work is required to improve the pharmacokinetic profile of the dihydroquinazolinone class, particularly concentrating on improving the metabolic stability and aqueous solubility to achieve enhanced efficacy in malaria mouse models. The dihydroquinazolinone class, once developed, could have a suitable resistance and pharmacokinetic profile for use as a partner agent in a curative or a transmission-blocking antimalarial therapy.

■ EXPERIMENTAL SECTION

***P. falciparum* 3D7 Asexual Stage LDH Assay.** The asexual growth assay was adapted[43] from the previously described method.[44]

HepG2 Viability Assay. The human HepG2 cell viability assay using CellTitre-Glo was performed as previously described.[30]

Liver Microsome Stability. A solution of compounds in phosphate buffer solution (1μM) was incubated in pooled human or mouse liver microsomes (0.5 mg/mL) for 0, 5, 20, 30, 45, and 60 min at 37 °C in the presence and absence of the NADPH regeneration system. The reaction was terminated with the addition of ice-cold MeCN at designated time points. The samples were then centrifuged (4200 rpm) for 20 min at 20 °C, and the supernatant was half diluted in water and then analyzed by LCMS/MS. The % parent compound remaining, half-life ($t_{1/2}$), and clearance (CL_{int}) were calculated using standard methodology. The experiment was performed in duplicate.

Hepatocyte Stability. A solution of the test compound in Krebs-Henseleit buffer solution (1μM) was incubated in pooled rat hepatocytes (1×10^6 cells/mL) for 0, 15, 30, 45, 60, 75, and 90 min at 37 °C (5% CO_2, 95% relative humidity). The reaction was terminated with the addition of ice-cold MeCN at designated time points. The samples were then centrifuged (4200 rpm) for 20 min at 20 °C, and the supernatant was half diluted in water and then analyzed using LCMS/MS. The % parent compound remaining, half-life ($t_{1/2}$), and clearance (CL_{int}) were calculated using standard methodology. The experiment was carried out in duplicate.

Solubility. The solubility assay was performed using a miniaturized shake flask method. Compound (200μM) was incubated in either a solution of phosphate-buffered saline (PBS pH 7.4), standard FaSSIF (pH 6.5), or FaSSGF (pH 1.2) with constant shaking (600 rpm) at 25 °C for 2 h. The samples were filtered using a multiscreen solubility filter plate. The filtrate was diluted by 50% with MeCN. A five-point linearity curve was prepared in PBS/MeCN (1:1, v/v) at 200, 150, 75, 25, and 2.5 μM. Blank, linearity, and test samples ($n = 2$) were transferred to a UV-readable plate, and the plate was scanned for absorbance. Best-fit calibration curves were constructed using the calibration standards and used to determine the test sample solubility. The experiment was carried out in duplicate.

eLog *D*. eLog D at pH 7.4 was determined using a miniaturized shake flask method. A solution of a pre-saturated mixture of 1-octanol and phosphate-buffered saline (PBS) (1:1, v/v) and the test compound (7.5 μM) was incubated at 25 °C with constant shaking (850 rpm) for 2 h. After incubation, the organic and aqueous phases were separated, and samples of each phase were transferred to a plate for dilution. The organic phase was diluted 1000-fold, and the aqueous phase was diluted 20-fold. The samples were quantitated using LCMS/MS. The experiment was carried out in duplicate.

Minimum Inoculum of Resistance Assay. *P. falciparum* asexual blood-stage parasites were cultured at 3% hematocrit in human O$^+$ RBCs in RPMI-1640 media, supplemented with 25 mM HEPES, 50 mg/L hypoxanthine, 2 mM L-glutamine, 0.21% sodium bicarbonate, 0.5% (wt/vol) AlbuMAX II (Invitrogen), and 10 μg/mL gentamycin, in modular incubator chambers (Billups-Rothenberg) at 5% O_2, 5% CO_2, and 90% N_2 at 37 °C. The Dd2-B2 strain was used in the assay and is a genetically homogenous line that was cloned from Dd2 by limiting dilution. The EC_{50} of asexual parasites was determined by exposing Dd2-B2 ring-stage cultures at 0.2% parasitemia and 1% hematocrit for 72 h to a range of 10 drug concentrations that were 2-fold serially diluted in duplicate along with drug-free controls. Parasite survival was assessed by flow cytometry on an iQue flow cytometer (Sartorius) using SYBR Green and MitoTracker Deep Red FM (Life Technologies) as nuclear stain and vital dyes, respectively. For the MIR assay on compound **49**, a single-step selection was set up using 2 $\times 10^5$ Dd2-B2 parasites in each well of a 96-well plate at a starting concentration of 3 $\times$ EC_{90} (29.1 nM). Parasites cleared from the culture rapidly. Cultures were screened three times weekly by flow cytometry and counted as positive for recrudescence when the overall parasitemia reached 0.3%, and the parasites were able to be seen on a blood smear.

Whole-Genome Sequencing of Compound 49-Resistant Clones. Whole-genome sequencing was performed using an Illumina DNA prep kit with Nextera DNA CD Indexes (Illumina, San Diego, CA) and multiplexed on a MiSeq (MiSeq Reagent Kit V3 600, Illumina, San Diego, CA) to generate 300 bp paired-end reads. Sequences were aligned to the Pf 3D7 reference genome (PlasmoDB-48_Pfalciparum3D7; https://plasmodb.org/plasmo/app/downloads/release-48/Pfalciparum3D7/fasta/) using the Burrows-Wheeler Alignment (BWA version 0.7.17). PCR duplicates and unmapped reads were filtered using Samtools (version 1.13) and Picard MarkDuplicates (GATK version 4.2.2). Base quality scores were recalibrated using the GATK BaseRecalibrator (GATK version 4.2.2). The GATK HaplotypeCaller (GATK version 4.2.2) was used to identify all possible single-nucleotide variants (SNVs) in test parasite lines filtered based on quality scores (variant quality as a function of depth QD > 1.5, mapping quality > 40, min base quality score > 18, read depth > 5) to obtain high-quality single-nucleotide polymorphisms (SNPs) that were annotated using SnpEff version 4.3t.[45] BIC-Seq version 1.1.2 was used to discover copy number variants (CNVs) against the parental strain using the Bayesian statistical model.[46] SNPs and CNVs were visually inspected and confirmed using the Integrative Genome Viewer (IGV). WGS data that support the findings of this study have been deposited in the European Nucleotide Archive (ENA) at EMBL-EBI under accession number: PRJEB58613 (https://www.ebi.ac.uk/ena/browser/view/PRJEB58613).

Stage of Asexual Arrest Assay. The stage of arrest assay using *P. falciparum* 3D7 parasites was performed as previously described[47,48]

using a compound concentration that was 10× the EC_{50}. Parasitemia was determined using SYBR Green staining of cultures.[30] Blood smears were stained with Giemsa, and the morphology of parasites was examined using a Zeiss Axio Observer microscope.

Parasite Viability Rate Assay. An adaptation of the protocol by Linares et al. was undertaken.[33] Briefly, a *P. falciparum* 3D7 culture was treated with the selected drug at 10 × EC_{50} using the EC_{50} that was previously determined using the standard 72 h Pf asexual stage LDH assay. Treatment conditions were similar to the ones used in the standard EC_{50} determinations (2% hematocrit, 0.5% parasitemia). Three time points for drug treatment were assessed, and samples of parasites were taken from the treated culture at 0, 24, and 48 h time points. The drug was renewed every 24 h during the entire treatment period by taking out old media and replenishing with new culture media with a fresh drug. After corresponding drug treatment time, the drug was washed out, and drug-free parasites were cultured by adding fresh erythrocytes pre-labelled with 10 μM carboxylfluorescein diacetate succinimidyl ester (CFSE) and incubated for a further 48 h. Upon completion of the 48 h, parasites were labelled with 2 μM Hoechst and analyzed by flow cytometry (BD FACS Symphony) with blue (515/20) + UV (450/50) laser. Newly invaded parasites were gated by single cell erythrocytes and double positive for CFSE and Hoechst staining (Q2). Viable parasites were calculated as follows: viable parasites (%) = [Q2 (drug treated)/Q2(untreated)] × 100.

***P. falciparum* Cytosolic Na$^+$ Assay.** Na$^+$ assays were performed essentially as described previously.[22,23] Trophozoite-stage 3D7 parasites were isolated by brief exposure to saponin (0.05% w/v) and loaded with SBFI (6 μM; in the presence of 0.01% w/v Pluronic F-127; for 20 min at 37 °C). Measurements were performed using a Tecan Infinite M1000 PRO plate reader with parasites suspended in pH 7.1 physiological saline (125 mM NaCl, 5 mM KCl, 1 mM $MgCl_2$, 20 mM glucose, and 25 mM HEPES) at 37 °C. The ratio of the fluorescence recorded at 340 and 380 nm (with an emission wavelength of 515 nm) was converted to $[Na^+]_{cyt}$ using a calibration procedure described previously.[23]

***P. falciparum* Cytosolic pH Assay.** pH assays were performed with saponin-isolated 3D7 trophozoites that were loaded with the pH-sensitive dye BCECF (5 μM; for 10 min at 37 °C)[36] and then depleted of ATP by washing and resuspending them in glucose-free saline (135 mM NaCl, 5 mM KCl, 1 mM $MgCl_2$, 25 mM HEPES; pH 7.1) for 20 min at 37 °C. In wells of a 96-well plate, aliquots of this parasite suspension (15 μL) were added to 185 μL of (glucose-containing) pH 7.1 physiological saline containing the V-type H$^+$ ATPase inhibitor concanamycin A (to give a final concentration of 100 nM) and the test compound of interest (or solvent alone), and fluorescence measurements were commenced immediately at 37 °C. The excitation wavelengths were 440 and 495 nm, and the emission wavelength was 520 nm. The ratio of the measurements (495/440 nm) provides an indicator of pH, and the fluorescence ratio was converted to pH using a calibration procedure described previously.[36] It should be noted that the cytosolic alkalinization induced by PfATP4 inhibitors can be detected in simple cuvette-based assays in which compounds are added to parasites suspended in pH 7.1 physiological saline (*i.e.*, in assays that do not involve glucose deprivation followed by restoration or inhibition of the V-type H$^+$ ATPase).[21,23] However, in (less sensitive) plate-based assays performed under these conditions, the alkalinization can be difficult to detect,[22] leading us to develop the alternative approach for pH-based detection of PfATP4 inhibitors in 96-well plates used here.

Multidrug- and PfATP4-Resistant Asexual Stage Parasite Viability Assays. The asexual parasite viability was determined using LDH following an assay protocol previously described.[43]

Gamete Assay. *P. falciparum* NF54 Stage V gametocytes for gamete transduction were produced using a protocol by Delves et al.[40] Male and female gamete induction and viability were assessed as previously described.[39] Briefly, compounds are incubated with mature stage V gametocytes for 48 h in 384-well plates before gamete formation is triggered by a drop in temperature and a drop in pH by the addition of xanthurenic acid. After 25 min of further incubation, male gamete exflagellation is recorded and quantified by automated

microscopy. The plates are then incubated at 26 °C for a further 24 h, and then the female gamete formation of the same sample is assessed by live staining using a fluorophore-conjugated αPfs25 antibody specific for female gametes and quantified by automated microscopy. Gentian violet was used in control wells at 12.5 μM.

***P. berghei* Mouse Model.** The use of animals in this model was approved by the Walter and Eliza Hall Institute of Medical Research Animal Ethics Committee under approval number 2020.036 and governance of the Australian code for the care and use of animals for scientific purposes. A total of 38 female ASMU:Swiss mice used in the study were obtained from the Monash Animal Research Platform, Monash University, Australia.

The protocol for the mouse model was followed as previously described,[49] using blood-stage *P. berghei* ANKA GFPcon 259 cl2 parasites.[41] In the first study (Figure 6A,C), four parasite donor mice were required to infect the treatment and control mice on day 1, and four mice were used per 40 mg/kg compound **70** and **71** treatment, untreated control and CQ groups, and two mice/group for plasma collection. In the second study (Figure 6B), two parasite donor mice were required to infect the treatment and control mice, and three mice were used per 80 mg/kg compound **70** and **71** treatment, untreated control and CQ groups. In both study cohorts, a HPMC vehicle was employed for oral administration of compounds 2 h after the initial parasite infection and then once a day for the 3 following days. The HPMC vehicle was prepared according to Gilson et al.[30] GraphPad Prism version 9.0.1 was used for data output and statistical analysis.

Plasma Bioanalysis. Plasma bioanalysis of the first dose from the *P. berghei* mouse model was conducted according to Favuzza et al.[49]

General Chemistry Methods. All general reagents and solvents were purchased from commercial sources and used as supplied. NMR spectra (^1H and ^{13}C) were recorded on a Bruker Avance DRX 300, Bruker BBFO ULTRASHIELD 300 AVANCE III, Agilent MR400, Bruker BBFO ASCEND 400 AVANCE III, or a Varian INOVA 600. Samples were dissolved in DMSO-d_6 with chemical shifts recorded in ppm and referenced to the residual solvent peak (2.50 ppm for ^1H NMR, 39.52 ppm for ^{13}C NMR). Thin-layer chromatography (TLC) was performed using silica gel 60 F_{254} 0.5 mm aluminum-backed plates (Merck) and visualized using UV light (254 nm). Chromatography was performed with silica gel 60 (particle size 0.040−0.063 μm) on a CombiFlash Rf Purification System (Teledyne Isco) with mobile phase gradients as specified. LCMS (Method A) was performed on an Agilent LCMS system using an Agilent G6125B Mass Detector, a 1290 Infinity G71172B Diode Array Detector, and an Agilent G6120B Mass Detector. Conditions for LCMS were as follows: column, Poroshell 120 EC-C18, 2.1 mm × 30 mm 2.7 μm at 30 °C; injection volume, 1 μL; mobile phase A: H_2O containing 0.1% formic acid; mobile phase B: MeCN containing 0.1% formic acid; gradient, 5−100% B over 3 min; flow rate, 1.0 mL min^{-1}; detection, 254 and 214 nm; acquisition time, 4.2 min. LCMS (Method B) was performed on a Shimadzu LC-2020 system with electrospray ionization (ESI). Conditions for LCMS were as follows: column, Ascentis Express C18, 3.0 mm × 50 mm 2.7 μm; injection volume, 2 μL; mobile phase A: H_2O containing 0.05% TFA; mobile phase B: MeCN containing 0.05% TFA; gradient, 5−95% B over 2.7 min; flow rate, 1.5 mL min^{-1}; detection, 254 nm; acquisition time, 3.0 min. These HPLC methods were used to establish the purity of final compounds, which were found to be >95% purity unless otherwise stated. HRMS was performed through the Bio21 Mass Spectrometry and Proteomics Facility and recorded on a Thermo Scientific nano-LC Q Exactive Plus Mass spectrometer with electrospray ionization (ESI). Reverse phase preparative LC was performed on a Waters auto purification instrument. Conditions were as follows: column, REFLECT I-Cellulose (250 mm × 20 mm, 5 μm), operating at 21 °C; diluent, DMSO; mobile phase, A = MeCN, B = 0.1% TFA in H_2O; gradient profile, with the initial composition of 20% A and 80% B, then 30% A and 70% B in 2.5 min, then to 45% A and 55% B in 7 min., then to 75% A and 25% B in 30 min; flow rate, 16 mL min^{-1}. Normal phase preparative LC was performed on an Agilent 1200 series instrument. Conditions were as follows: column, Chiralpak IC

(250 mm × 20 mm, 5 μm); diluent, MeOH/CH$_2$Cl$_2$ (2/8); mobile phase, n-hexane/EtOAc/EtOH (70:15:15); flow rate, 18 mL min^{-1}. Compounds **26**, **27**, **28**, **29**, **31**, and **32** were purchased from Enamine. Compound **33** was purchased from Interbioscreen.

Chemistry Procedures. *General Procedure A. 4-Methyl-N-(m-tolyl)-1,5-dioxo-2,3-dihydropyrrolo[1,2-a]quinazoline-3a-carboxamide (5).* A mixture of **72** (77 mg, 0.30 mmol), 3-methylaniline (40 μL, 0.37 mmol), HATU (143 mg, 0.38 mmol), and DIPEA (90 μL, 0.52 mmol) in THF (0.3 mL) was stirred at 21 °C. The reaction mixture was diluted using MeOH (~1 mL) and H$_2$O (~2 mL) to give a solid that was collected using vacuum filtration. Washing with H$_2$O and MeOH gives **5** (67 mg, 65% yield) as a white powder. ^{1}H NMR (300 MHz, DMSO-d_6) δ 9.82 (s, 1H), 7.90−7.84 (m, 2H), 7.67−7.56 (m, 1H), 7.32 (app. t, J 7.6, 1.2 Hz, 1H), 7.28−7.20 (m, 2H), 7.12 (app t, J 7.8 Hz, 1H), 6.87 (d, J 7.4 Hz, 1H), 3.21 (s, 3H), 2.95−2.53 (m, 4H), 2.21 (s, 3H). ^{13}C NMR (75 MHz, DMSO-d_6) δ 173.4, 168.4, 162.0, 137.70, 137.66, 135.0, 132.8, 128.3, 127.8, 125.5, 125.0, 121.5, 121.2, 121.0, 118.1, 80.7, 30.4, 29.5, 27.1, 20.9. LCMS (Method A): t_R = 1.93 min, m/z = 350.2 (M + H$^+$). HRMS m/z: [M + H$^+$] calcd for C$_{20}$H$_{19}$N$_3$O$_3$ 350.1500; found 350.1498.

N-(3-Methoxyphenyl)-4-methyl-1,5-dioxo-2,3-dihydropyrrolo-[1,2-a]quinazoline-3a-carboxamide (6). General procedure A was reproduced using **72** (74 mg, 0.28 mmol), 3-methoxyaniline (40 μL, 0.36 mmol), HATU (149 mg, 0.392 mmol), and DIPEA (90 μL, 0.52 mmol) in THF (0.3 mL) at 21 °C for 3 h, which affords **6** (77 mg, 74% yield) as a white powder. ^{1}H NMR (300 MHz, DMSO-d_6) δ 9.85 (s, 1H), 7.88 (dd, J 7.8, 1.5 Hz, 1H), 7.86−7.77 (m, 1H), 7.62 (ddd, J 8.2, 7.4, 1.6 Hz, 1H), 7.32 (td, J 7.6, 1.2 Hz, 1H), 7.21−7.08 (m, 2H), 7.04 (ddd, J 8.1, 2.0, 1.0 Hz, 1H), 6.63 (ddd, J 8.1, 2.6, 1.0 Hz, 1H), 3.67 (s, 3H), 3.21 (s, 3H), 2.95−2.55 (m, 4H). ^{13}C NMR (75 MHz, DMSO-d_6) δ 173.5, 168.5, 162.1, 159.3, 139.0, 135.0, 132.9, 129.2, 127.8, 125.6, 121.3, 121.0, 113.0, 110.0, 106.5, 80.8, 55.1, 30.4, 29.5, 27.0. LCMS (Method A): t_R = 1.83 min, m/z = 364.2 (M + H$^+$). HRMS m/z: [M + H$^+$] calcd for C$_{20}$H$_{19}$N$_3$O$_4$ 366.1449; found 366.1449.

8-Bromo-N-(3-fluorophenyl)-4-methyl-1,5-dioxo-2,3-dihydropyrrolo[1,2-a]quinazoline-3a-carboxamide (16). General procedure A was reproduced using **73** (679 mg, 2.00 mmol), 3-fluoroaniline (250 μL, 2.60 mmol), HATU (986 mg, 2.59 mmol), and DIPEA (700 μL, 4.02 mmol) in THF (2 mL) at 60 °C for 17 h, which affords **16** (857 mg, 99% yield) as a gray powder. ^{1}H NMR (400 MHz, DMSO-d_6) δ 10.03 (s, 1H), 8.12−8.03 (m, 1H), 7.82 (d, J 8.4 Hz, 1H), 7.57−7.50 (m, 1H), 7.42 (d, J 11.4 Hz, 1H), 7.37−7.25 (m, 2H), 6.97−6.88 (m, 1H), 3.20 (s, 3H), 2.94−2.60 (m, 4H).

4-Methyl-N-phenyl-1,5-dioxo-2,3-dihydropyrrolo[1,2-a]-quinazoline-3a-carboxamide (18). General procedure A was reproduced using **72** (505 mg, 1.94 mmol), aniline (240 μL, 2.65 mmol), and HATU (991 mg, 2.61 mmol) in THF (2 mL) at 21 °C and was treated with DIPEA (700 μL, 4.02 mmol) for 1 h. Additional purification using column chromatography, eluting with 50−100% EtOAc in n-heptane and then 0−50% MeOH in EtOAc, affords **18** (459 mg, 71% yield) as a white solid. ^{1}H NMR (300 MHz, DMSO-d_6) δ 9.89 (s, 1H), 7.90−7.84 (m, 2H), 7.65−7.59 (m, 1H), 7.42 (d, J 7.6 Hz, 2H), 7.34−7.22 (m, 3H), 7.05 (app. t, J 7.4, 1H), 3.22 (s, 3H), 2.97−2.54 (m, 4H). LCMS (Method A): t_R = 1.77 min, m/z = 336.2 (M + H$^+$). HRMS m/z: [M − H$^+$] calcd for C$_{19}$H$_{17}$N$_3$O$_3$ 334.1196; found 334.1211.

N-(3-Chlorophenyl)-4-methyl-1,5-dioxo-2,3-dihydropyrrolo[1,2-a]quinazoline-3a-carboxamide (20). General procedure A was reproduced using **72** (66 mg, 0.25 mmol), 3-chloroaniline (40 μL, 0.38 mmol), HATU (130 mg, 0.34 mmol), and DIPEA (90 μL, 0.52 mmol) in THF (0.25 mL) at 21 °C for 18 h. Purification using preparative LC gives **20** (17 mg, 18% yield) as a white powder. ^{1}H NMR (600 MHz, DMSO-d_6) δ 10.04 (s, 1H), 7.89 (d, J 6.8 Hz, 1H), 7.85 (d, J 8.0 Hz, 1H), 7.63−7.60 (m, 2H), 7.43 (d, J 8.2 Hz, 1H), 7.32 (app. t, J 7.3 Hz, 1H), 7.28 (app. t, J 8.1 Hz, 1H), 7.12 (d, J 7.8 Hz, 1H), 3.21 (s, 3H), 2.94−2.81 (m, 2H), 2.77−2.68 (m, 1H), 2.67−2.58 (m, 1H). LCMS (Method A): t_R = 1.76 min, m/z = 370.2 (M + H$^+$). HRMS: m/z: [M − H$^+$] calcd for C$_{19}$H$_{16}$ClN$_3$O$_3$ 368.0806; found 368.0789.

4-Methyl-N-(3-[trifluoromethyl]phenyl)-1,5-dioxo-2,3-dihydropyrrolo[1,2-a]quinazoline-3a-carboxamide (21). General procedure A was reproduced using **72** (132 mg, 0.51 mmol), 3-(trifluoromethyl)aniline (80 μL, 0.64 mmol), HATU (279 mg, 0.73 mmol), and DIPEA (180 μL, 2.01 mmol) in THF (0.5 mL) at 60 °C for 21 h, which affords **21** (144 mg, 70% yield) as a white powder. ^{1}H NMR (600 MHz, DMSO-d_6) δ 10.18 (s, 1H), 7.93−7.84 (m, 3H), 7.79 (d, J 8.2 Hz, 1H), 7.66−7.58 (m, 1H), 7.50 (app. t, J 8.1 Hz, 1H), 7.42 (d, J 7.7 Hz, 1H), 7.32 (app. t, J 7.6 Hz, 1H), 3.22 (s, 3H), 2.95−2.83 (m, 2H), 2.79−2.60 (m, 2H). ^{13}C NMR (75 MHz, DMSO-d_6) δ 173.5, 169.2, 162.0, 138.6, 134.9, 133.0, 129.8, 129.4 (q, J 31.5 Hz), 127.9, 125.7, 124.5, 124.0 (q, J 270.7 Hz), 121.2, 120.9, 120.7 (q, J 3.8 Hz), 117.1 (q, J 4.0 Hz), 80.7, 30.4, 29.5, 27.0. LCMS (Method A): t_R = 1.94 min, m/z = 404.2 (M + H$^+$). HRMS: m/z: [M − H$^+$] calcd for C$_{20}$H$_{16}$F$_3$N$_3$O$_3$ 404.1218; found 404.1216.

4-Methyl-N-(3-[trifluoromethoxy]phenyl)-1,5-dioxo-2,3-dihydropyrrolo[1,2-a]quinazoline-3a-carboxamide (22). General procedure A was reproduced using **72** (75 mg, 0.29 mmol), 3-(trifluoromethoxy)aniline (45 μL, 0.34 mmol), HATU (123 mg, 0.32 mmol), and DIPEA (90 μL, 0.52 mmol) in THF (0.25 mL) at 21 °C for 48 h, which affords **22** (36 mg, 30%) as an off-white powder. ^{1}H NMR (400 MHz, DMSO-d_6) δ 10.13 (s, 1H), 7.89 (d, J 7.7 Hz, 1H), 7.85 (d, J 8.2 Hz, 1H), 7.62 (app. t, J 7.5 Hz, 1H), 7.57 (s, 1H), 7.49 (d, J 8.1 Hz, 1H), 7.39 (app. t, J 8.1 Hz, 1H), 7.32 (app. t, J 7.6 Hz, 1H), 7.06 (d, J 8.0 Hz, 1H), 3.21 (s, 3H), 2.95−2.80 (m, 2H), 2.79−2.61 (m, 2H). ^{13}C NMR (75 MHz, DMSO-d_6) δ 173.4, 169.0, 162.0, 148.1 (q, J 1.9 Hz), 139.4, 134.8, 132.9, 130.2, 127.8, 125.7, 121.2, 120.9, 120.0 (q, J 254.8 Hz), 119.6, 116.6, 113.1, 80.8, 30.4, 29.5, 26.9. LCMS (Method A): t_R = 1.91 min, m/z = 420.0 (M + H$^+$). HRMS: m/z: [M − H$^+$] calcd for C$_{20}$H$_{16}$F$_3$N$_3$O$_4$ 418.1019; found 418.1003.

N-(3-Cyanophenyl)-4-methyl-1,5-dioxo-2,3-dihydropyrrolo[1,2-a]quinazoline-3a-carboxamide (23). General procedure A was reproduced using **72** (79 mg, 0.30 mmol), 3-aminobenzonitrile (44 mg, 0.37 mmol), HATU (128 mg, 0.34 mmol), and DIPEA (90 μL, 0.52 mmol) in THF (0.25 mL) at 21 °C for 48 h. Purification using preparative LC gives **23** (23 mg, 21%) as a white solid. ^{1}H NMR (400 MHz, DMSO-d_6) δ 10.18 (s, 1H), 7.92−7.86 (m, 2H), 7.77 (d, J 8.2 Hz, 1H), 7.62 (app. t, J 7.7 Hz, 1H), 7.58−7.42 (m, 2H), 7.32 (app. t, J 7.6 Hz, 1H), 3.22 (s, 2H), 2.96−2.81 (m, 2H), 2.81−2.58 (m, 2H). LCMS (Method A): t_R = 1.41 min, m/z = 361.2 (M + H$^+$). HRMS: m/z: [M − H$^+$] calcd for C$_{20}$H$_{16}$N$_4$O$_3$ 359.1148; found 359.1132.

N-(4-Fluorophenyl)-4-methyl-1,5-dioxo-2,3-dihydropyrrolo[1,2-a]quinazoline-3a-carboxamide (24). General procedure A was reproduced using **72** (63 mg, 0.24 mmol), 4-fluoroaniline (40 μL, 0.42 mmol), HATU (120 mg, 0.32 mmol), and DIPEA (90 μL, 0.52 mmol) in THF (0.25 mL) at 21 °C for 43 h, which affords **24** (39 mg, 46% yield) as a light tan-colored powder. ^{1}H NMR (400 MHz, DMSO-d_6) δ 9.94 (s, 1H), 7.88 (t, J 6.9 Hz, 2H), 7.62 (app. t, J 7.8 Hz, 1H), 7.43 (dd, J 9.0, 5.0 Hz, 2H), 7.32 (app. t, J 7.6 Hz, 1H), 7.09 (app. t, J 8.9 Hz, 2H), 3.21 (s, 3H), 2.94−2.79 (m, 2H), 2.78−2.56 (m, 2H). ^{13}C NMR (75 MHz, DMSO-d_6) δ 173.3, 168.5, 162.0, 158.7 (d, J 239.8 Hz), 134.9, 134.0 (d, J 2.6 Hz), 132.9, 127.8, 125.5, 123.1 (d, J 8.0 Hz), 121.1, 120.9, 115.0 (d, J 22.2 Hz), 80.6, 30.4, 29.5, 27.1. LCMS (Method A): t_R = 1.50 min, m/z = 352.2 (M − H$^+$). HRMS: m/z: [M + H$^+$] calcd for C$_{19}$H$_{16}$FN$_3$O$_3$ 354.1250; found 354.1247.

N-(2-Chlorophenyl)-4-methyl-1,5-dioxo-2,3-dihydropyrrolo[1,2-a]quinazoline-3a-carboxamide (30). General procedure A was reproduced using **72** (65 mg, 0.25 mmol), 2-chloroaniline (40 μL, 0.38 mmol), HATU (140 mg, 0.38 mmol), and DIPEA (90 μL, 0.52 mmol) in THF (0.25 mL) at 60 °C for 20 h. Additional purification using preparative LC affords **30** (66 mg, 71%) as a white solid. ^{1}H NMR (300 MHz, DMSO-d_6) δ 9.75 (s, 1H), 7.99 (dd, J 8.2, 1.1 Hz, 1H), 7.90 (dd, J 7.8, 1.5 Hz, 1H), 7.66−7.60 (m, 1H), 7.46−7.37 (m, 1H), 7.37−7.17 (m, 4H), 3.21 (s, 3H), 2.97−2.61 (m, 4H). ^{13}C NMR (75 MHz, DMSO-d_6) δ 172.9, 168.9, 161.8, 135.2, 133.9, 132.8, 129.6, 129.4, 128.4, 128.1, 127.8, 127.4, 125.3, 120.6, 120.5, 80.4, 30.1, 29.7, 27.5. LCMS (Method A): t_R = 2.06 min, m/z = 370.2 (M + H$^+$). HRMS m/z: [M + H$^+$] calcd for C$_{19}$H$_{16}$ClN$_3$O$_3$ 370.0954; found 370.0956.

N-(3-Chlorophenyl)-4-ethyl-1,5-dioxo-2,3-dihydropyrrolo[1,2-a]-quinazoline-3a-carboxamide (34). General procedure A was reproduced using **74** (135 mg, 0.49 mmol), 3-chloroaniline (80 μL, 0.76 mmol), HATU (247 mg, 0.65 mmol), and DIPEA (170 μL, 0.98 mmol) in THF (0.5 mL) at 60 °C for 66 h. The crude solid was washed further with EtOAc to give **34** (58 mg, 31% yield) as a white powder. ¹H NMR (300 MHz, DMSO-d_6) δ 10.07 (s, 1H), 7.88 (dd, J 7.8, 1.5 Hz, 1H), 7.81 (d, J 7.5 Hz, 1H), 7.68−7.55 (m, 2H), 7.42 (d, J 8.7 Hz, 1H), 7.37−7.22 (m, 2H), 7.12 (dd, J 7.9, 1.3 Hz, 1H), 4.08 (dq, J 14.2, 7.0 Hz, 1H), 3.24 (dq, J 14.2, 7.0 Hz, 1H), 2.92−2.57 (m, 4H), 1.21 (t, J 7.0 Hz, 3H). ¹³C NMR (75 MHz, DMSO-d_6) δ 173.4, 169.0, 162.1, 139.3, 134.8, 132.9, 132.8, 130.3, 127.7, 125.7, 124.0, 121.5, 121.1, 120.2, 119.0, 81.4, 40.0,* 29.5, 26.7, 15.2. LCMS (Method A): t_R = 2.14 min, m/z = 384.2 (M + H⁺). HRMS m/z: [M + H⁺] calcd for $C_{20}H_{18}ClN_3O_3$ 384.1111; found 384.1109. *Determined by HSQC.

N-(3-Chlorophenyl)-4-(2,2,2-trifluoroethyl)-1,5-dioxo-2,3-dihydropyrrolo[1,2-a]quinazoline-3a-carboxamide (35). General procedure A was reproduced using **75** (370 mg, 1.13 mmol), 3-chloroaniline (180 μL, 1.69 mmol), HATU (857 mg, 2.25 mmol), and DIPEA (590 μL, 3.38 mmol) in THF (10 mL) at 60 °C for 16 h. Purification using column chromatography, eluting with 50% EtOAc in *n*-hexane, gives a solid that was further purified by trituration in MeOH/CH₂Cl₂/*n*-pentane (1:2:5). The solid was collected using vacuum filtration to give **35** (70 mg, 14%) as a white solid. ¹H NMR (400 MHz, DMSO-d_6) δ 10.38 (s, 1H), 7.95 (dd, J 8.0, 0.8 Hz, 1H), 7.76 (d, J 8.0 Hz, 1H), 7.70 (td, J 8.0, 1.2 Hz, 1H), 7.57 (app. t, J 2.0 Hz, 1H), 7.41−7.35 (m, 2H), 7.29 (app. t, J 8.0 Hz, 1H), 7.12 (dd, J 8.0, 0.8 Hz, 1H), 4.89−4.74 (m, 1H), 4.48−4.30 (m, 1H), 2.92−2.80 (m, 2H), 2.72−2.61 (m, 2H). LCMS (Method A): t_R = 1.97 min, m/z = 438.10 (M + H⁺). HRMS m/z: [M + H⁺] calcd for $C_{20}H_{15}ClF_3N_3O_3$ 438.0828; found 438.0825.

N-(3-Chlorophenyl)-4-cyclopropyl-1,5-dioxo-2,3-dihydropyrrolo[1,2-a]quinazoline-3a-carboxamide (36). General procedure A was reproduced using **76** (75 mg, 0.26 mmol), 3-chloroaniline (40 μL, 0.45 mmol), HATU (130 mg, 0.34 mmol), and DIPEA (90 μL, 0.52 mmol) in THF (0.25 mL) at 21 °C for 5 days. Additional purification using preparative LC gives **36** (7.0 mg, 7% yield) as a white powder. ¹H NMR (300 MHz, DMSO-d_6) 10.13 (s, 1H), 7.86 (d, J 7.8 Hz, 1H), 7.73 (d, J 8.0 Hz, 1H), 7.64−7.52 (m, 2H), 7.39−7.24 (m, 3H), 7.11 (d, J 8.0 Hz, 1H), 3.36−3.30 (m, 1H),* 2.84−2.79 (m, 2H), 2.72−2.55 (m, 3H), 0.98−0.81 (m, 4H). LCMS (Method A): t_R = 2.38 min, m/z = 394.2 (M − H+). HRMS: m/z [M − H⁺] calcd for $C_{21}H_{18}ClN_3O_3$ 396.1111; found 396.1113. * Determined by HSQC.

N-(3-Chlorophenyl)-4-isopropyl-1,5-dioxo-2,3-dihydropyrrolo[1,2-a]quinazoline-3a-carboxamide (37). General procedure A was reproduced using **77** (270 mg, 0.94 mmol), 3-chloroaniline (120 μL, 1.12 mmol), HATU (1.07 g, 2.81 mmol), and DIPEA (820 μL, 4.68 mmol) in THF (10 mL) at 60 °C for 16 h. Purification using column chromatography, eluting with 30−60% EtOAc in *n*-hexane, gives a solid that was further purified by trituration in Et₂O/*n*-pentane (6:1). The solid was collected using vacuum filtration to give **37** (124 mg, 33%) as a white solid. ¹H NMR (400 MHz, DMSO-d_6) δ 9.87 (s, 1H), 7.88 (d, J 8.0 Hz, 1H), 7.82 (d, J 8.0 Hz, 1H), 7.64−7.56 (m, 2H), 7.44 (d, J 8.0 Hz, 1H), 7.32−7.26 (m, 2H), 7.13 (d, J 8.0 Hz, 1H), 3.97−3.90 (m, 1H), 2.90−2.71 (m, 3H), 2.72−2.64 (m, 1H), 1.65 (d, J 6.4 Hz, 1H), 1.46 (d, J 6.4 Hz, 1H). LCMS (Method A): t_R = 2.91 min, m/z = 398.33 (M + H⁺). HRMS m/z: [M + H⁺] calcd for $C_{21}H_{20}ClN_3O_3$ 398.1267; found 398.1268.

N-(3-Chlorophenyl)-4-propyl-1,5-dioxo-2,3-dihydropyrrolo[1,2-a]quinazoline-3a-carboxamide (38). General procedure A was reproduced using **78** (260 mg, 0.90 mmol), 3-chloroaniline (110 μL, 1.02 mmol), HATU (649 mg, 1.71 mmol), and DIPEA (300 μL, 1.71 mmol) in THF (5 mL) at 60 °C for 16 h. Purification using column chromatography, eluting with 30−60% EtOAc in *n*-hexane, gives a solid that was further purified by trituration in MeOH/CH₂Cl₂/*n*-pentane (1:2:5). The solid was collected using vacuum filtration to give **38** (51 mg, 14%) as a white solid. ¹H NMR (400 MHz, DMSO-d_6) δ 10.07 (s, 1H), 7.88 (d, J 8.0 Hz, 1H), 7.81 (d, J 8.0 Hz, 1H), 7.63−7.57 (m, 2H), 7.41 (d, J 8.0 Hz, 1H), 7.37−7.25

(m, 2H), 7.11 (d, J 8.0 Hz, 1H), 4.00−3.93 (m, 1H), 3.17−3.09 (m, 1H), 2.90−2.70 (m, 3H), 2.69−2.60 (m, 1H), 1.75−1.66 (m, 1H), 1.65−1.47 (m, 1H), 0.91 (t, J 7.2 Hz, 3H). LCMS (Method A): t_R = 1.90 min, m/z = 398.22 (M + H⁺). HRMS m/z: [M + H⁺] calcd for $C_{21}H_{20}ClN_3O_3$ 398.1267; found 398.1269.

N-(3-Chlorophenyl)-4-isobutyl-1,5-dioxo-2,3-dihydropyrrolo[1,2-a]quinazoline-3a-carboxamide (39). General procedure A was reproduced using **79** (450 mg, 1.49 mmol), 3-chloroaniline (240 μL, 2.23 mmol), HATU (1.132 g, 2.98 mmol), and DIPEA (780 μL, 4.47 mmol) in THF (10 mL) at 60 °C for 16 h. Purification using column chromatography, eluting with 40−60% EtOAc in *n*-hexane, gives a solid that was further purified by trituration in MeOH/CH₂Cl₂/*n*-pentane (1:2:5). The solid was collected using vacuum filtration to give **39** (101 mg, 16%) as a white solid. ¹H NMR (400 MHz, DMSO-d_6) δ 10.16 (s, 1H), 7.89 (d, J 8.0 Hz, 1H), 7.78 (d, J 7.6 Hz, 1H), 7.63 (app. t, J 7.6 Hz, 1H), 7.58 (s, 1H), 7.39 (d, J 7.6 Hz, 1H), 7.35−7.24 (m, 2H), 7.11 (d, J 7.6 Hz, 1H), 3.95−3.90 (m, 1H), 3.03−2.92 (m, 1H), 2.90−2.49 (m, 4H), 2.02−1.91 (m, 1H), 0.94 (d, J 6.4 Hz, 3H), 0.88 (d, J 6.4 Hz, 3H). LCMS (Method A): t_R = 1.96 min, m/z = 412.20 (M + H⁺). HRMS m/z: [M + H⁺] calcd for $C_{22}H_{22}ClN_3O_3$ 412.1424; found 412.1427.

8-Chloro-N-(3-fluorophenyl)-4-methyl-1,5-dioxo-2,3-dihydropyrrolo[1,2-a]quinazoline-3a-carboxamide (46). General procedure A was reproduced using **80** (585 mg, 1.99 mmol), 3-fluoroaniline (250 μL, 2.60 mmol), HATU (1.01 g, 2.65 mmol), and DIPEA (700 μL, 4.02 mmol) in THF (2 mL) at 21 °C for 18.5 h, which affords **46** (711 mg, 92% yield) as an off-white powder. ¹H NMR (400 MHz, DMSO-d^6) δ 10.04 (s, 1H), 7.94−7.87 (m, 2H), 7.45−7.37 (m, 2H), 7.36−7.26 (m, 2H), 6.94−6.89 (m, 1H), 3.21 (s, 3H), 2.95−2.60 (m, 4H). ¹³C NMR (75 MHz, DMSO-d_6) δ 173.5, 168.6, 161.8 (d, J 240.4 Hz), 161.1, 139.4 (d, J 10.8 Hz), 137.2, 135.9, 130.1 (d, J 9.3 Hz), 129.8, 125.8, 120.5, 119.5, 116.9 (d, J 2.9 Hz), 111.1 (d, J 20.9 Hz), 108.0 (d, J 25.9 Hz), 80.7, 30.4, 29.5, 27.2. LCMS (Method A): t_R = 2.27 min, m/z = 388.2 (M + H⁺). HRMS: m/z: [M − H⁺] calcd for $C_{19}H_{15}ClFN_3O_3$ 386.0712; found 386.073.

N-(3-Fluorophenyl)-8-methoxy-4-methyl-1,5-dioxo-2,3-dihydropyrrolo[1,2-a]quinazoline-3a-carboxamide (49). General procedure A was reproduced using **81** (74 mg, 0.255 mmol), 3-fluoroaniline (40 μL, 0.416 mmol), DIPEA (90 μL, 0.517 mmol), and HATU (134 mg, 0.352 mmol) in THF (0.25 mL) and was stirred at 21 °C for 48 h. Additional purification by preparative LC gives **49** (17 mg, 17% yield) as a white solid. ¹H NMR (600 MHz, DMSO-d_6) δ 9.99 (s, 1H), 7.81 (d, J 8.6 Hz, 1H), 7.44−7.41 (m, 2H), 7.31−7.29 (m, 2H), 6.90−6.89 (m, 2H), 3.82 (s, 3H), 3.19 (s, 3H), 2.91−2.79 (m, 2H), 2.77−2.65 (m, 1H), 2.63−2.54 (m, 1H). ¹³C NMR (75 MHz, DMSO-d_6) δ 173.4, 169.0, 162.5, 161.9, 161.8 (d, J 240.2 Hz), 139.5 (d, J 10.8 Hz), 136.4, 130.1 (d, J 9.3 Hz), 129.7, 116.7 (d, J 2.8 Hz), 113.7, 111.6, 110.9 (d, J 20.9 Hz), 107.8 (d, J 25.9 Hz), 106.0, 80.8, 55.6, 30.1, 29.6, 27.0. LCMS (Method A): t_R = 1.64 min, m/z = 382.2 (M − H⁺). HRMS: m/z: [M − H⁺] calcd for $C_{20}H_{18}FN_3O_4$ 382.1207; found 382.1192.

8-Chloro-N-(3-chlorophenyl)-4-methyl-1,5-dioxo-2,3-dihydropyrrolo[1,2-a]quinazoline-3a-carboxamide (52). General procedure A was reproduced using **80** (72 mg, 0.24 mmol), 3-chloroaniline (40 μL, 0.38 mmol), HATU (131 mg, 0.35 mmol), and DIPEA (90 μL, 0.52 mmol) in THF (0.25 mL) at 21 °C for 15 h. Additional purification using column chromatography, eluting with 50−100% EtOAc in cyclohexane, gives **52** (66 mg, 67% yield) as a white powder. ¹H NMR (600 MHz, DMSO-d_6) δ 10.02 (s, 1H), 7.98−7.85 (m, 2H), 7.62 (s, 1H), 7.44 (d, J 7.6 Hz, 1H), 7.40 (d, J 8.0 Hz, 1H), 7.30 (app. t, J 8.1 Hz, 1H), 7.14 (d, J 7.1 Hz, 1H), 3.20 (s, 3H), 2.91−2.85 (m, 2H), 2.80−2.62 (m, 2H). ¹³C NMR (75 MHz, DMSO-d_6) δ 173.4, 168.6, 161.1, 139.1, 137.3, 135.9, 132.8, 130.2, 129.8, 125.8, 124.3, 120.8, 120.5, 119.6, 119.4, 80.7, 30.4, 29.5, 27.3. LCMS (Method A): t_R = 2.06 min, m/z = 402.0 (M − H⁺). HRMS m/z: [M + H⁺] calcd for $C_{19}H_{15}Cl_2N_3O_3$ 404.0564; found 404.0564.

Reverse phase chiral HPLC was performed to give both enantiomers of **52** as follows:

(R)-8-Chloro-N-(3-chlorophenyl)-4-methyl-1,5-dioxo-2,3-dihydropyrrolo[1,2-a]quinazoline-3a-carboxamide (R-enantiomer,

68). t_R = 22.50 min, ee >99%. LCMS (Method A): t_R = 1.95 min, m/z = 404.2 (M + H⁺). HRMS m/z: [M + H⁺] calcd for $C_{19}H_{15}Cl_2N_3O_3$ 404.0564; found 404.0563.

(S)-8-Chloro-N-(3-chlorophenyl)-4-methyl-1,5-dioxo-2,3-dihydropyrrolo[1,2-a]quinazoline-3a-carboxamide (S-enantiomer, 69). t_R = 23.89 min, ee 99.7%. LCMS (Method A): t_R = 1.88 min, m/z = 402.2 (M − H⁺). HRMS: m/z: [M + H⁺] calcd for $C_{19}H_{15}Cl_2N_3O_3$ 404.0564; found 404.0563.

N-(3-Chlorophenyl)-8-methoxy-4-methyl-1,5-dioxo-2,3-dihydropyrrolo[1,2-a]quinazoline-3a-carboxamide (53). General procedure A was reproduced using **81** (71 mg, 0.245 mmol), 3-chloroaniline (40 µL, 0.378 mmol), DIPEA (90 µL, 0.517 mmol), and HATU (135 mg, 0.355 mmol) in THF (0.25 mL) at 21 °C for 48 h. Additional purification by preparative LC gives **53** (11 mg, 11% yield) as a white solid. ¹H NMR (600 MHz, DMSO-d_6) δ 9.97 (s, 1H), 7.82 (d, J 8.7 Hz, 1H), 7.64 (s, 1H), 7.46 (d, J 8.3 Hz, 1H), 7.42 (s, 1H), 7.29 (app. t, J 8.1 Hz, 1H), 7.13 (d, J 7.5 Hz, 1H), 6.89 (d, J 6.6 Hz, 1H), 3.82 (s, 3H), 3.19 (s, 3H), 2.90−2.79 (m, 2H), 2.77−2.67 (m, 1H), 2.64−2.54 (m, 1H). LCMS (Method A): t_R = 1.91 min, m/z = 398.2 (M − H⁺). HRMS: m/z: [M − H⁺] calcd for $C_{20}H_{18}ClN_3O_4$ 398.0912; found 398.0899.

N-(3-Chlorophenyl)-4-methyl-8-(trifluoromethyl)-1,5-dioxo-2,3-dihydropyrrolo[1,2-a]quinazoline-3a-carboxamide (54). General procedure A was reproduced using **82** (280 mg, 0.85 mmol), 3-chloroaniline (110 µL, 1.02 mmol), HATU (649 mg, 1.71 mmol), and DIPEA (300 µL, 1.71 mmol) in DMF (5 mL) at 21 °C for 3 h. Upon completion, the mixture was diluted with EtOAc (25 mL), washed with H_2O (3 × 20 mL), dried (Na_2SO_4), filtered, and reduced *in vacuo*. Purification using column chromatography, eluting with 25−50% EtOAc in *n*-hexane, gives a solid that was purified further by trituration from MeOH/CH_2Cl_2/*n*-pentane (1:2:5) to afford **54** (80 mg, 21%) as a white solid. ¹H NMR (400 MHz, DMSO-d_6): δ 10.03 (s, 1H), 8.26 (s, 1H), 8.11 (d, J 8.0 Hz, 1H), 7.69 (d, J 8.0 Hz, 1H), 7.62−7.61 (m, 1H), 7.44−7.42 (m, 1H), 7.30 (app. t, J 8.0 Hz, 1H), 7.14 (dd, J 8.0, 1.2 Hz, 1H), 3.24 (s, 3H), 2.96−2.86 (m, 2H), 2.81−2.69 (m, 2H). LCMS (Method A): t_R = 1.97 min, m/z = 438.2 (M + H+). HRMS m/z: [M + H⁺] calcd for $C_{20}H_{15}ClF_3N_3O_3$ 438.0828; found 438.0826.

N-(3-Chlorophenyl)-8-cyano-4-methyl-1,5-dioxo-2,3-dihydropyrrolo[1,2-a]quinazoline-3a-carboxamide (55). General procedure A was reproduced using **83** (160 mg, 0.56 mmol), 3-chloroaniline (120 µL, 1.12 mmol), PyBOP (584 mg, 1.12 mmol), and DIPEA (290 µL, 1.68 mmol) in DMF (3 mL) at 21 °C for 16 h. Upon completion, the mixture was diluted with EtOAc (20 mL), washed with H_2O (3 × 15 mL), dried (Na_2SO_4), filtered, and reduced *in vacuo*. Purification using column chromatography, eluting with 30−60% EtOAc in *n*-hexane, gives a solid that was purified further by trituration from MeOH/CH_2Cl_2/*n*-pentane (1:2:5) to afford **55** (51 mg, 23%) as a white solid. ¹H NMR (400 MHz, DMSO-d_6) δ 10.05 (s, 1H), 8.24 (s, 1H), 8.06 (d, J 8.0 Hz, 1H), 7.78 (dd, J 8.0, 1.2 Hz, 1H), 7.62−7.61 (m, 1H), 7.45−7.43 (m, 1H), 7.30 (t, J 8.0 Hz, 1H), 7.15 (dd, J 8.0, 1.2 Hz, 1H), 3.22 (s, 3H), 2.96−2.86 (m, 2H), 2.81−2.68 (m, 2H). ¹³C NMR (75 MHz, DMSO-d_6) δ 173.5, 168.2, 160.5, 139.0, 135.2, 132.8, 130.2, 129.11, 129.08, 124.38, 124.36, 124.1, 120.9, 119.7, 117.8, 115.0, 80.5, 30.6, 29.4, 27.3. LCMS (Method A): t_R = 1.82 min, m/z = 395.2 (M + H⁺). HRMS m/z: [M + H⁺] calcd for $C_{20}H_{15}ClN_4O_3$ 395.0907; found 393.0904.

N-(3-Chlorophenyl)-4-methyl-8-(trifluoromethoxy)-1,5-dioxo-2,3-dihydropyrrolo[1,2-a]quinazoline-3a-carboxamide (56). General procedure A was reproduced using **84** (280 mg, 0.81 mmol), 3-chloroaniline (173 µL, 1.63 mmol), HATU (464 mg, 1.22 mmol), and DIPEA (710 µL, 4.07 mmol) in THF (6 mL) at 21 °C for 3 h. Upon completion, the mixture was reduced *in vacuo*, diluted with H_2O (15 mL), and extracted using EtOAc (3 × 15 mL). The combined organic phase was washed with brine (15 mL), dried (Na_2SO_4), filtered, and reduced *in vacuo*. Purification using column chromatography, eluting with 30−70% EtOAc in *n*-hexane, gives a solid that was purified further by trituration from MeOH/CH_2Cl_2/*n*-pentane (1:2:5) to afford **56** (81 mg, 22%) as an off-white solid. ¹H NMR (400 MHz, DMSO-d_6) δ 10.00 (s, 1H), 8.01 (d, J 8.4 Hz, 1H),

7.88 (s, 1H), 7.63−7.58 (m, 1H), 7.44−7.41 (m, 1H), 7.30 (m, 2H), 7.15 (d, J 8.0 Hz, 1H), 3.22 (s, 3H), 2.93−2.85 (m, 2H), 2.79−2.65 (m, 2H). LCMS (Method A): t_R = 2.02 min, m/z = 454.2 (M + H⁺). HRMS m/z: [M + H⁺] calcd for $C_{20}H_{15}ClF_3N_3O_4$ 454.0777; found 454.0776.

8-Chloro-N-(3-chloro-4-fluorophenyl)-4-methyl-1,5-dioxo-2,3-dihydropyrrolo[1,2-a]quinazoline-3a-carboxamide (59). General procedure A was reproduced using **80** (74 mg, 0.25 mmol), 3-chloro-4-fluoroaniline (45 mg, 0.31 mmol), HATU (120 mg, 0.32 mmol), and DIPEA (90 µL, 0.504 mmol) in THF (0.25 mL) at 21 °C for 22 h, which affords **59** (100 mg, 94% yield) as a gray powder. ¹H NMR (400 MHz, DMSO-d_6) δ 10.03 (s, 1H), 7.94 (d, J 1.5 Hz, 1H), 7.90 (d, J 8.4 Hz, 1H), 7.74 (dd, J 6.8, 2.3 Hz, 1H), 7.50−7.42 (m, 1H), 7.40 (dd, J 8.4, 1.7 Hz, 1H), 7.33 (app. t, J 9.1 Hz, 1H), 3.20 (s, 3H), 2.94−2.80 (m, 2H), 2.80−2.62 (m, 3H). ¹³C NMR (75 MHz, DMSO-d_6) δ 173.4, 168.5, 161.0, 153.9 (d, J 242.8 Hz), 137.3, 135.9, 134.8 (d, J 3.2 Hz), 129.8, 125.7, 123.0, 121.8 (d, J 7.1 Hz), 120.3, 119.3, 118.9 (d, J 18.3 Hz), 116.6 (d, J 21.6 Hz), 80.6, 30.4, 29.5, 27.4. LCMS (Method A): t_R = 2.08 min, m/z = 422.2 (M + H⁺). HRMS: m/z: [M − H⁺] calcd for $C_{19}H_{14}Cl_2FN_3O_3$ 420.0322; found 420.0309.

8-Chloro-N-(4-chloro-3-fluorophenyl)-4-methyl-1,5-dioxo-2,3-dihydropyrrolo[1,2-a]quinazoline-3a-carboxamide (60). General procedure A was reproduced using **80** (75 mg, 0.25 mmol), 4-chloro-3-fluoroaniline (53 mg, 0.36 mmol), HATU (120 mg, 0.33 mmol), and DIPEA (90 µL, 0.52 mmol) in THF (0.25 mL) at 21 °C for 22 h. Additional purification using column chromatography, eluting with 50−100% EtOAc in cyclohexane, gives **60** (75 mg, 70% yield) as a white solid. ¹H NMR (400 MHz, DMSO-d_6) δ 10.13 (s, 1H), 7.99−7.83 (m, 2H), 7.63 (dd, J 11.8, 2.0 Hz, 1H), 7.49 (app. t, J 8.6 Hz, 1H), 7.40 (d, J 8.4 Hz, 1H), 7.34 (d, J 8.7 Hz, 1H), 3.20 (s, 3H), 2.94−2.60 (m, 4H). ¹³C NMR (75 MHz, DMSO-d_6) δ 173.4, 168.7, 161.0, 156.6 (d, J 243.1 Hz), 138.1 (d, J 10.0 Hz), 137.2, 135.8, 130.3, 129.8, 125.8, 120.4, 119.4, 118.1 (d, J 3.3 Hz), 114.4 (d, J 17.5 Hz), 109.4 (d, J 25.5 Hz), 80.7, 30.4, 29.5, 27.2. LCMS (Method A): t_R = 2.18 min, m/z = 420.2 (M − H⁺). HRMS: m/z: [M − H⁺] calcd for $C_{19}H_{14}Cl_2FN_3O_3$ 420.0322; found 420.0308.

8-Chloro-N-(3,5-difluorophenyl)-4-methyl-1,5-dioxo-2,3-dihydropyrrolo[1,2-a]quinazoline-3a-carboxamide (61). General procedure A was reproduced using **80** (73 mg, 0.25 mmol), 3,5-difluoroaniline (41 mg, 0.32 mmol), HATU (130 mg, 0.34 mmol), and DIPEA (90 µL, 0.52 mmol) in THF (0.25 mL) at 21 °C for 15 h. Additional purification using column chromatography, eluting with 50−100% EtOAc in cyclohexane, gives **61** (51 mg, 51%) as a white powder. ¹H NMR (600 MHz, DMSO-d_6) δ 10.15 (s, 1H), 7.90 (dd, J 8.4, 5.7 Hz, 2H), 7.40 (dd, J 8.4, 2.0 Hz, 1H), 7.30 (d, J 8.5 Hz, 2H), 6.96 (s, 1H), 3.20 (s, 3H), 2.91−2.85 (m, 2H), 2.80−2.70 (m, 1H), 2.68−2.63 (m, 1H). LCMS (Method A): t_R = 2.04 min, m/z = 406.0 (M + H⁺). HRMS: m/z: [M − H⁺] calcd for $C_{19}H_{14}ClF_2N_3O_3$ 404.0618; found 404.0600.

8-Chloro-N-(3,5-dichlorophenyl)-4-methyl-1,5-dioxo-2,3-dihydropyrrolo[1,2-a]quinazoline-3a-carboxamide (62). General procedure A was reproduced using **80** (285 mg, 0.97 mmol), 3,5-dichloroaniline (130 µL, 1.27 mmol), HATU (500 mg, 1.32 mmol), and DIPEA (350 µL, 2.01 mmol) in THF (1 mL) at 21 °C for 18 h. Additional purification using column chromatography, eluting 30−90% EtOAc in *n*-heptane, gives **62** (368 mg, 87%) as an off-white powder. ¹H NMR (300 MHz, DMSO-d_6) d 10.12 (s, 1H), 7.97−7.84 (m, 2H), 7.65 (d, J 1.9 Hz, 2H), 7.40 (dd, J 8.4, 2.1 Hz, 1H), 7.33 (app. t, J 1.9 Hz, 1H), 3.20 (s, 3H), 2.98−2.59 (m, 4H). ¹³C NMR (75 MHz, DMSO-d_6) d 173.4, 168.9, 161.0, 140.0, 137.3, 135.7, 133.8, 129.8, 125.8, 123.7, 120.4, 119.3, 119.2, 80.6, 30.4, 29.4, 27.2. LCMS (Method A): t_R = 2.57 min, m/z = 438.0 (M + H⁺). HRMS: m/z: [M − H⁺] calcd for $C_{19}H_{14}Cl_3N_3O_3$ 436.0027; found 436.0046.

8-Chloro-N-(3-chloro-5-fluorophenyl)-4-methyl-1,5-dioxo-2,3-dihydropyrrolo[1,2-a]quinazoline-3a-carboxamide (63). General procedure A was reproduced using **80** (76 mg, 0.26 mmol), 3-chloro-5-fluoroaniline (40 µL, 0.40 mmol), HATU (140 mg, 0.36 mmol), and DIPEA (90 µL, 0.52 mmol) in THF (0.25 mL) at 21 °C for 22 h. Additional purification using column chromatography,

eluting with 30−80% EtOAc in cyclohexane, affords **63** (79 mg, 73% yield) as a white powder. ^{1}H NMR (400 MHz, DMSO-d_6) δ 10.13 (s, 1H), 7.96−7.86 (m, 2H), 7.53−7.36 (m, 3H), 7.16 (d, J 8.5 Hz, 1H), 3.20 (s, 3H), 2.95−2.60 (m, 4H). ^{13}C NMR (75 MHz, DMSO-d_6) δ 173.4, 168.9, 161.8 (d, J 243.6 Hz), 161.0, 140.2 (d, J 12.4 Hz), 137.3, 135.8, 133.7 (d, J 12.7 Hz), 129.8, 125.8, 120.5, 119.3, 116.8 (d, J 10.2 Hz), 111.7 (d, J 25.2 Hz), 106.6 (d, J 26.3 Hz), 80.7, 30.4, 29.4, 27.2. LCMS (Method A): t_R = 2.23 min, m/z = 420.2 (M − H$^+$). HRMS: m/z: [M − H$^+$] calcd for C$_{19}$H$_{14}$Cl$_2$FN$_3$O$_3$ 420.0322; found 420.0309.

8-Chloro-N-(5-chloropyrid-3-yl)-4-methyl-1,5-dioxo-2,3-dihydropyrrolo[1,2-a]quinazoline-3a-carboxamide (64). General procedure A was reproduced using **80** (148 mg, 0.502 mmol), 5-chloropyridin-3-amine (86 mg, 0.67 mmol), HATU (234 mg, 0.615 mmol), and DIPEA (150 μL, 0.86 mmol) in THF (500 μL) at 21 °C for 22 h, which affords **64** (149 mg, 73% yield) as an off-white powder. ^{1}H NMR (300 MHz, DMSO-d_6) δ 10.24 (s, 1H), 8.64 (s, 1H), 8.36 (s, 1H), 8.08 (app. t, J 2.2 Hz, 1H), 7.95 (d, J 2.0 Hz, 1H), 7.91 (d, J 8.4 Hz, 1H), 7.41 (dd, J 8.4, 2.1 Hz, 1H), 3.21 (s, 3H), 3.00−2.64 (m, 4H). ^{13}C NMR (75 MHz, DMSO-d_6) δ 173.4, 169.2, 161.0, 143.6, 140.8, 137.3, 135.8, 135.3, 130.3, 129.9, 127.8, 125.8, 120.4, 119.2, 80.6, 30.4, 29.5, 27.3. LCMS (Method A): t_R = 2.02 min, m/z = 405.0 (M + H$^+$). HRMS m/z: [M + H$^+$] calcd for C$_{18}$H$_{14}$Cl$_2$N$_4$O$_3$ 405.0517; found 405.0518.

Normal phase chiral HPLC was performed to give both enantiomers of **64** as follows:

8-Chloro-N-(5-chloropyrid-3-yl)-4-methyl-1,5-dioxo-2,3-dihydropyrrolo[1,2-a]quinazoline-3a-carboxamide (R-Enantiomer, 70). t_R = 10.55 min, ee >99%. LCMS (Method A): t_R = 2.01 min, m/z = 403.2 (M − H$^+$). HRMS m/z: [M + H$^+$] calcd for C$_{18}$H$_{14}$Cl$_2$N$_4$O$_3$ 405.0517; found 405.0520.

8-Chloro-N-(5-chloropyrid-3-yl)-4-methyl-1,5-dioxo-2,3-dihydropyrrolo[1,2-a]quinazoline-3a-carboxamide (S-Enantiomer, 71, WJM-921). t_R = 22.94 min, ee >99%. LCMS (Method A): t_R = 2.01 min, m/z = 403.2 (M − H$^+$). HRMS m/z: [M + H$^+$] calcd for C$_{18}$H$_{14}$Cl$_2$N$_4$O$_3$ 405.0517; found 405.0520.

8-Chloro-N-(2-chloropyrid-4-yl)-4-methyl-1,5-dioxo-2,3-dihydropyrrolo[1,2-a]quinazoline-3a-carboxamide (65). General procedure A was reproduced using **80** (71 mg, 0.24 mmol), 2-chloropyridin-4-amine (46 mg, 0.36 mmol), HATU (140 mg, 0.37 mmol), and DIPEA (90 μL, 0.52 mmol) in THF (0.5 mL) at 21 °C for 22 h. Additional purification using column chromatography, eluting with 0−20% MeOH in EtOAc, gives **65** (40 mg, 41%) as a purple solid. ^{1}H NMR (300 MHz, DMSO-d_6) δ 10.37 (s, 1H), 8.25 (d, J 5.6 Hz, 1H), 7.95−7.85 (m, 2H), 7.69 (d, J 1.8 Hz, 1H), 7.57 (dd, J 5.7, 1.8 Hz, 1H), 7.41 (dd, J 8.4, 2.1 Hz, 1H), 3.20 (s, 3H), 2.98−2.61 (m, 4H). LCMS (Method A): t_R = 2.22 min, m/z = 405.0 (M + H$^+$). HRMS m/z: [M + H$^+$] calcd for C$_{18}$H$_{14}$Cl$_2$N$_4$O$_3$ 405.0517; found 405.0521.

8-Chloro-N-(6-chloropyrid-2-yl)-4-methyl-1,5-dioxo-2,3-dihydropyrrolo[1,2-a]quinazoline-3a-carboxamide (66). General procedure A was reproduced using **80** (72 mg, 0.24 mmol), 6-chloropyridin-2-amine (45 mg, 0.35 mmol), HATU (120 mg, 0.33 mmol), and DIPEA (90 μL, 0.52 mmol) in THF (0.25 mL) at 21 °C for 22 h. Additional purification using preparative LC gives **66** (11 mg, 11%) as a tan solid. ^{1}H NMR (300 MHz, DMSO-d_6) δ 11.16 (s, 1H), 7.90 (d, J 8.4 Hz, 1H), 7.85−7.71 (m, 3H), 7.39 (dd, J 8.4, 2.1 Hz, 1H), 7.23 (dd, J 6.9, 1.6 Hz, 1H), 3.20 (s, 3H), 2.98−2.58 (m, 4H). LCMS (Method A): t_R = 2.35 min, m/z = 405.0 (M + H$^+$). HRMS m/z: [M + H$^+$] calcd for C$_{18}$H$_{14}$Cl$_2$N$_4$O$_3$ 405.0517; found 405.0520.

8-Chloro-N-(4-chloropyrid-2-yl)-4-methyl-1,5-dioxo-2,3-dihydropyrrolo[1,2-a]quinazoline-3a-carboxamide (67). General procedure A was reproduced using **80** (72 mg, 0.24 mmol), 4-chloropyridin-2-amine (48 mg, 0.37 mmol), HATU (125 mg, 0.33 mmol), and DIPEA (90 μL, 0.52 mmol) in THF (0.25 mL) at 21 °C for 25 h. Additional purification using preparative LC gives **67** (22 mg, 22%) as a tan powder. ^{1}H NMR (300 MHz, DMSO-d_6) δ 11.20 (s, 1H), 8.32 (d, J 5.4 Hz, 1H), 7.94−7.84 (m, 2H), 7.81 (d, J 2.1 Hz, 1H), 7.40 (dd, J 8.4, 2.1 Hz, 1H), 7.29 (dd, J 5.4, 1.9 Hz, 1H), 3.20 (s, 3H), 2.97−2.62 (m, 4H). ^{13}C NMR (75 MHz, DMSO-d_6) δ 173.6,

169.3, 161.5, 152.4, 149.3, 144.0, 137.2, 136.0, 129.9, 125.8, 120.8, 120.4, 119.6, 114.5, 81.1, 30.4, 29.4, 26.5. LCMS (Method A): t_R = 2.33 min, m/z = 405.0 (M + H$^+$). HRMS m/z: [M + H$^+$] calcd for C$_{18}$H$_{14}$Cl$_2$N$_4$O$_3$ 405.0517; found 405.0517.

General Procedure B. N-(3-Fluorophenyl)-4-methyl-1,5-dioxo-2,3-dihydropyrrolo[1,2-a]quinazoline-3a-carboxamide (19). An 8 mL vial, equipped with a stir bar, was charged with **72** (104 mg, 0.40 mmol), 3-fluoroaniline (44 mg, 0.40 mmol), 1-methylimidazole (94 mg, 1.10 mmol), and TCFH (129 mg, 0.46 mmol) in MeCN/DMF (1:1, 2 mL) at 21 °C. Upon completion of the reaction, the mixture was purified by preparative LC to afford **19** (69 mg, 49% yield) as a white solid. ^{1}H NMR (300 MHz, DMSO-d_6) δ 10.06 (s, 1H), 7.91−7.83 (m, 2H), 7.65−7.60 (m, 1H), 7.43−7.28 (m, 4H), 6.92−6.88 (m, 1H), 3.22 (s, 3H), 2.92−2.60 (m, 4H). LCMS (Method A): t_R = 1.89 min, m/z = 352.2 (M − H$^+$). HRMS m/z: [M − H$^+$] calcd for C$_{19}$H$_{16}$FN$_3$O$_3$ 352.1102; found 352.1117.

N-(4-Chlorophenyl)-4-methyl-1,5-dioxo-2,3-dihydropyrrolo[1,2-a]quinazoline-3a-carboxamide (25). General procedure B was reproduced using **72** (104 mg, 0.40 mmol), 4-chloroaniline (51 mg, 0.40 mmol), 1-methylimidazole (90 mg, 1.10 mmol), and TCFH (140 mg, 0.50 mmol) in MeCN/DMF (1:1, 2 mL) at 21 °C, which affords **25** (22 mg, 15% yield) as a white solid. ^{1}H NMR (300 MHz, DMSO-d_6) δ 10.02 (s, 1H), 7.91−7.85 (m, 2H), 7.66−7.63 (m, 1H), 7.60−7.45 (m, 2H), 7.36−7.29 (m, 3H), 3.22 (s, 3H), 2.94−2.57 (m, 4H). LCMS (Method A): t_R = 2.02 min, m/z = 368.2 (M − H$^+$). HRMS: m/z: [M − H$^+$] calcd for C$_{19}$H$_{16}$ClN$_3$O$_3$ 368.0806; found 368.0822.

6-Fluoro-N-(3-fluorophenyl)-4-methyl-1,5-dioxo-2,3-dihydropyrrolo[1,2-a]quinazoline-3a-carboxamide (40). General procedure B was reproduced using **85** (111 mg, 0.40 mmol), 3-fluoroaniline (44 mg, 0.40 mmol), 1-methylimidazole (90 mg, 1.10 mmol), and TCFH (140 mg, 0.50 mmol) in MeCN/DMF (1:1, 2 mL) at 21 °C, which affords **40** (73 mg, 27% yield) as a white solid. ^{1}H NMR (300 MHz, DMSO-d_6) δ 10.10 (s, 1H), 7.73−7.60 (m, 2H), 7.43−7.29 (m, 3H), 7.17−7.10 (m, 1H), 6.95−6.89 (m, 1H), 3.19 (s, 3H), 2.91−2.58 (m, 4H). LCMS (Method A): t_R = 1.89 min, m/z = 370.2 (M − H$^+$). HRMS: m/z: [M − H$^+$] calcd for C$_{19}$H$_{15}$F$_2$N$_3$O$_3$ 370.1008; found 370.1023.

7-Fluoro-N-(3-fluorophenyl)-4-methyl-1,5-dioxo-2,3-dihydropyrrolo[1,2-a]quinazoline-3a-carboxamide (41). General procedure B was reproduced using **86** (111 mg, 0.40 mmol), 3-fluoroaniline (44 mg, 0.40 mmol), 1-methylimidazole (90 mg, 1.10 mmol), and TCFH (140 mg, 0.50 mmol) in MeCN/DMF (1:1, 2 mL) at 21 °C, which affords **41** (52 mg, 19%) as a white solid. ^{1}H NMR (400 MHz, DMSO-d_6) δ 10.11 (br, 1H), 7.88−7.85 (m, 1H), 7.63−7.60 (m, 1H), 7.55−7.50 (m, 1H), 7.43−7.40 (m, 1H), 7.32−7.29 (m, 2H), 6.93−6.91 (m, 1H), 3.22 (s, 3H), 2.92−2.82 (m, 2H), 2.79−2.61 (m, 2H). LCMS (Method A): t_R = 2.29 min, m/z = 370.2 (M − H$^+$). HRMS: m/z: [M − H$^+$] calcd for C$_{19}$H$_{15}$F$_2$N$_3$O$_3$ 370.1008; found 370.1024.

8-Fluoro-N-(3-fluorophenyl)-4-methyl-1,5-dioxo-2,3-dihydropyrrolo[1,2-a]quinazoline-3a-carboxamide (42). General procedure B was reproduced using **87** (111 mg, 0.40 mmol), 3-fluoroaniline (44 mg, 0.40 mmol), 1-methylimidazole (90 mg, 1.10 mmol), and TCFH (140 mg, 0.50 mmol) in MeCN/DMF (1:1, 2 mL) at 21 °C, which affords **42** (44 mg, 16%) as a white solid. ^{1}H NMR (400 MHz, DMSO-d_6) δ 10.05 (br, 1H), 7.98−7.94 (m, 1H), 7.68−7.65 (m, 1H) 7.44−7.41 (m, 1H), 7.32−7.30 (m, 2H), 7.21−7.16 (m, 1H), 6.94−6.90 (m, 1H), 3.22 (s, 3H), 2.91−2.84 (m, 2H), 2.79−2.65 (m, 2H). LCMS (Method A): t_R = 2.01 min, m/z = 370.2 (M − H$^+$). HRMS: m/z: [M − H$^+$] calcd for C$_{19}$H$_{15}$F$_2$N$_3$O$_3$ 370.1008; found 370.1024.

9-Fluoro-N-(3-fluorophenyl)-4-methyl-1,5-dioxo-2,3-dihydropyrrolo[1,2-a]quinazoline-3a-carboxamide (43). General procedure B was reproduced using **88** (200 mg, 0.70 mmol), 3-fluoroaniline (120 mg, 1.10 mmol), 1-methylimidazole (177 mg, 2.20 mmol), and TCFH (303 mg, 1.10 mmol) in MeCN/DMF (1:1, 2 mL) at 21 °C for 4 h, which affords **43** (65 mg, 24%) as an off-white solid. ^{1}H NMR (400 MHz, DMSO-d_6) δ 10.45 (s, 1H), 7.74 (d, J 7.6 Hz, 1H), 7.55 (d, J 8.0 Hz, 1H), 7.48−7.37 (m, 2H), 7.36−7.26 (m,

1H), 7.24 (d, J 8.0 Hz, 1H), 6.91 (t, J 8.0 Hz, 1H), 3.19 (s, 3H), 3.06–2.91 (m, 1H), 2.90–2.67 (m, 3H). LCMS (Method A): t_R = 1.95 min, m/z = 370.2 (M − H$^+$). HRMS: m/z: [M − H$^+$] calcd for C$_{19}$H$_{15}$F$_2$N$_3$O$_3$ 370.1008; found 370.1024.

6-Chloro-N-(3-fluorophenyl)-4-methyl-1,5-dioxo-2,3-dihydropyrrolo[1,2-a]quinazoline-3a-carboxamide (44). General procedure B was reproduced using **89** (118 mg, 0.40 mmol), 3-fluoroaniline (44 mg, 0.40 mmol), 1-methylimidazole (90 mg, 1.10 mmol), and TCFH (140 mg, 0.50 mmol) in MeCN/DMF (1:1, 2 mL) at 21 °C, which affords **44** (70 mg, 27%) as an off-white solid. ^{1}H NMR (300 MHz, DMSO-d_6) δ 10.12 (s, 1H), 7.86–7.83 (m, 1H), 7.58 (app. t, J 10.8 Hz, 1H), 7.43–7.35 (m, 2H), 7.33–7.26 (m, 2H), 6.95–6.88 (m, 1H), 3.22 (s, 3H), 2.96–2.72 (m, 3H), 2.69–2.59 (m, 1H). LCMS (Method A): t_R = 2.02 min, m/z = 386.2 (M − H$^+$). HRMS: m/z: [M − H$^+$] calcd for C$_{19}$H$_{15}$ClFN$_3$O$_3$ 386.0712; found 386.0731.

7-Chloro-N-(3-fluorophenyl)-4-methyl-1,5-dioxo-2,3-dihydropyrrolo[1,2-a]quinazoline-3a-carboxamide (45). General procedure B was reproduced using **90** (118 mg, 0.40 mmol), 3-fluoroaniline (44 mg, 0.40 mmol), 1-methylimidazole (90 mg, 1.10 mmol), and TCFH (140 mg, 0.50 mmol) in MeCN/DMF (1:1, 2 mL) at 21 °C, which affords **45** (126 mg, 46%) as an off-white solid. ^{1}H NMR (400 MHz, DMSO-d_6) δ 10.09 (s, 1H), 7.89 (d, J 8.8 Hz, 1H), 7.84 (d, J 2.4 Hz, 1H), 7.72–7.70 (m, 1H), 7.43–7.39 (m, 1H), 7.32–7.29 (m, 2H), 6.94–6.90 (m, 1H), 3.22 (s, 3H), 2.90–2.85 (m, 2H), 2.77–2.69 (m, 2H). LCMS (Method A): t_R = 2.17 min, m/z = 386.2 (M − H$^+$). HRMS: m/z: [M − H$^+$] calcd for C$_{19}$H$_{15}$ClFN$_3$O$_3$ 386.0712; found 386.0731.

9-Chloro-N-(3-fluorophenyl)-4-methyl-1,5-dioxo-2,3-dihydropyrrolo[1,2-a]quinazoline-3a-carboxamide (47). General procedure B was reproduced using **91** (118 mg, 0.40 mmol), 3-fluoroaniline (44 mg, 0.40 mmol), 1-methylimidazole (90 mg, 1.10 mmol), and TCFH (140 mg, 0.50 mmol) in MeCN/DMF (1:1, 2 mL) at 21 °C, which affords **47** (52 mg, 20%) as a white solid. ^{1}H NMR (300 MHz, DMSO-d_6) δ 10.30 (s, 1H), 7.85 (d, J 7.5 Hz, 1H), 7.71 (d, J 8.1 Hz, 1H), 7.48–7.15 (m, 4H), 6.96–6.83 (m, 1H), 3.19 (s, 3H), 3.04–2.70 (m, 4H). LCMS (Method A): t_R = 2.03 min, m/z = 386.2 (M − H$^+$). HRMS: m/z: [M − H$^+$] calcd for C$_{19}$H$_{15}$ClFN$_3$O$_3$ 386.0712; found 386.0731.

N-(3-Fluorophenyl)-4,8-dimethyl-1,5-dioxo-2,3-dihydropyrrolo[1,2-a]quinazoline-3a-carboxamide (48). General procedure B was reproduced using **92** (110 mg, 0.40 mmol), 3-fluoroaniline (44 mg, 0.40 mmol), 1-methylimidazole (90 mg, 1.10 mmol), and TCFH (140 mg, 0.50 mmol) in MeCN/DMF (1:1, 2 mL) at 21 °C, which affords **48** (88 mg, 32%) as an off-white solid. ^{1}H NMR (400 MHz, DMSO-d_6) δ 10.05 (br s, 1H), 7.78 (d, J 7.6 Hz, 1H), 7.67 (s, 1H), 7.45–7.42 (m, 1H), 7.32–7.29 (m, 2H), 7.15–7.13 (m, 1H), 6.91–6.89 (m, 1H), 3.20 (s, 3H), 2.90–2.81 (m, 2H), 2.76–2.70 (m, 2H), 2.37 (s, 3H). LCMS (Method A): t_R = 2.00 min, m/z = 366.2 (M − H$^+$). HRMS: m/z: [M − H$^+$] calcd for C$_{20}$H$_{18}$FN$_3$O$_3$ 366.1258; found 366.1274.

8-Chloro-N-(3,4-difluorophenyl)-4-methyl-1,5-dioxo-2,3-dihydropyrrolo[1,2-a]quinazoline-3a-carboxamide (57). General procedure B was reproduced using **80** (118 mg, 0.40 mmol), 3,4-difluoroaniline (52 mg, 0.40 mmol), 1-methylimidazole (90 mg, 1.10 mmol), and TCFH (140 mg, 0.50 mmol) in MeCN/DMF (1:1, 2 mL) at 21 °C, which affords **57** (62 mg, 43%) as an off-white solid. ^{1}H NMR (400 MHz, DMSO-d_6) δ 10.07 (s, 1H), 7.94–7.90 (m, 2H), 7.66–7.60 (m, 1H), 7.42–7.27 (m, 3H), 3.21 (s, 3H), 2.92–2.84 (m, 2H), 2.79–2.65 (m, 2H). LCMS (Method A): t_R = 2.22 min, m/z = 404.0 (M − H$^+$). HRMS: m/z: [M − H$^+$] calcd for C$_{19}$H$_{14}$ClF$_2$N$_3$O$_3$ 404.0618; found 404.0637.

8-Chloro-N-(3,4-dichlorophenyl)-4-methyl-1,5-dioxo-2,3-dihydropyrrolo[1,2-a]quinazoline-3a-carboxamide (58). General procedure B was reproduced using **80** (118 mg, 0.40 mmol), 3,4-difluoroaniline (52 mg, 0.40 mmol), 1-methylimidazole (90 mg, 1.10 mmol), and TCFH (140 mg, 0.50 mmol) in MeCN/DMF (1:1, 2 mL) at 21 °C, which affords **58** (81 mg, 54%) as a solid. ^{1}H NMR (400 MHz, DMSO-d_6) δ 10.12 (s, 1H), 7.94–7.90 (m, 2H), 7.83 (s,

1H), 7.56–7.49 (m, 2H), 7.40 (d, J 8.4 Hz, 1H), 3.21 (s, 3H), 2.93–2.85 (m, 2H), 2.80–2.64 (m, 2H)

LCMS (Method A): t_R = 2.49 min, m/z = 436.0 (M − H$^+$). HRMS: m/z: [M − H$^+$] calcd for C$_{19}$H$_{14}$Cl$_3$N$_3$O$_3$ 436.0027; found 436.0047.

General Procedure C. 8-Cyclopropyl-N-(3-fluorophenyl)-4-methyl-1,5-dioxo-2,3-dihydropyrrolo[1,2-a]quinazoline-3a-carboxamide (50). A 10 mL microwave vial was charged with **18** (63 mg, 0.15 mmol), cyclopropyl boronic acid (24 mg, 0.28 mmol), K$_3$PO$_4$ (62 mg, 0.29 mmol), Pd(dppf)Cl$_2$·CH$_2$Cl$_2$ (17 mg, 0.014 mmol), and PhCH$_3$/H$_2$O (9:1, 1.5 mL). The vial was capped, and the solution was sparged with N$_2$ for 15 min before the mixture was heated at 120 °C for 30 min using microwave irradiation. The resultant mixture was diluted with EtOAc and filtered over Celite. The filtrate was then dry-loaded onto Celite and purified using column chromatography, eluting with 50–100% EtOAc in n-heptane to afford **50** (19 mg, 33%) as a tan powder. ^{1}H NMR (300 MHz, DMSO-d^6) δ 9.99 (s, 1H), 7.74 (d, J 8.1 Hz, 1H), 7.57 (d, J 1.7 Hz, 1H), 7.45–7.40 (m, 1H), 7.37–7.22 (m, 2H), 6.98 (dd, J 8.2, 1.8 Hz, 1H), 6.93–6.87 (m, 1H), 3.19 (s, 3H), 2.97–2.53 (m, 4H), 2.05–1.93 (m, 1H), 1.10–1.01 (m, 2H), 0.76–0.68 (m, 2H). LCMS (Method A): t_R = 1.88 min, m/z = 394.2 (M + H$^+$). HRMS: m/z: [M − H$^+$] calcd for C$_{22}$H$_{20}$FN$_3$O$_3$ 392.1415; found 392.1401.

N-(3-Fluorophenyl)-4-methyl-1,5-dioxo-8-phenyl-2,3-dihydropyrrolo[1,2-a]quinazoline-3a-carboxamide (51). General procedure C was reproduced using **18** (64 mg, 0.15 mmol), phenylboronic acid (26 mg, 0.21 mmol), K$_3$PO$_4$ (64 mg, 0.30 mmol), Pd(dppf)Cl$_2$·CH$_2$Cl$_2$ (18 mg, 0.02 mmol), and PhCH$_3$/H$_2$O (9:1, 1.5 mL). Gives **51** (41 mg, 64%) as an off-white solid. ^{1}H NMR (300 MHz, DMSO) δ 10.07 (s, 1H), 8.15 (d, J 1.7 Hz, 1H), 7.96 (d, J 8.2 Hz, 1H), 7.73–7.57 (m, 3H), 7.57–7.38 (m, 4H), 7.33–7.24 (m, 2H), 6.93–6.86 (m, 1H), 3.24 (s, 3H), 3.00–2.57 (m, 4H). ^{13}C NMR (75 MHz, DMSO) δ 173.5, 168.9, 161.78, 161.77 (d, J 241.9 Hz), 144.4, 139.46 (d, J 11.0 Hz), 138.7, 135.4, 130.11 (d, J 9.4 Hz), 129.2, 128.6, 126.9, 124.0, 119.6, 119.0, 116.74 (d, J 3.0 Hz), 110.93 (d, J 20.6 Hz), 107.79 (d, J 26.2 Hz), 80.8, 30.4, 29.5, 27.1. LCMS (Method A): t_R = 2.16 min, m/z = 428.2 (M − H$^+$). HRMS: m/z: [M + H$^+$] calcd for C$_{25}$H$_{20}$FN$_3$O$_3$ 430.1563; found 430.1563.

General Procedure D. 4-Methyl-1,5-dioxo-2,3-dihydropyrrolo[1,2-a]quinazoline-3a-carboxylic Acid (72). A stirring mixture of 2-amino-N-methylbenzamide (3.43 g, 22.8 mmol) and α-ketoglutaric acid (4.00 g, 27.4 mmol) in AcOH (20 mL) was heated at 118 °C for 24 h. The resultant mixture was diluted with H$_2$O (25 mL) to give a solid that was collected using vacuum filtration. Washing with H$_2$O affords **72** (5.47 g, 92%) as an off-white solid. ^{1}H NMR (400 MHz, DMSO-d_6) δ 8.23 (d, J 8.2 Hz, 1H), 7.91 (dd, J 7.8, 1.6 Hz, 1H), 7.65–7.57 (m, 1H), 7.33–7.24 (m, 1H), 3.07 (s, 3H), 2.82–2.56 (m, 4H). LCMS (Method A): t_R = 0.66 min, m/z = 261.2 (M + H$^+$).

8-Bromo-4-methyl-1,5-dioxo-2,3-dihydropyrrolo[1,2-a]quinazoline-3a-carboxylic Acid (73). General procedure D was reproduced using **93** (1.87 g, 8.16 mmol) and α-ketoglutaric acid (1.41 g, 9.63 mmol) in AcOH (7 mL) at 118 °C for 10 min, which affords **73** (2.51 g, 91%) as an off-white powder. ^{1}H NMR (400 MHz, DMSO-d_6) δ 8.43 (d, J 1.9 Hz, 1H), 7.84 (d, J 8.4 Hz, 1H), 7.51 (dd, J 8.4, 1.9 Hz, 1H), 3.06 (s, 3H), 2.85–2.52 (m, 4H). ^{13}C NMR (101 MHz, DMSO-d_6) δ 172.9, 170.9, 161.1, 136.6, 130.1, 127.9, 126.7, 120.3, 117.9, 79.4, 30.1, 29.1, 28.0. LCMS (Method A): t_R = 1.19 min, m/z = 338.2 (M + H$^+$).

4-Ethyl-1,5-dioxo-2,3-dihydropyrrolo[1,2-a]quinazoline-3a-carboxylic Acid (74). General procedure D was reproduced using 2-amino-N-ethylbenzamide (1.74 g, 10.6 mmol) and α-ketoglutaric acid (1.84 g, 12.6 mmol) in AcOH (9 mL) at 118 °C for 19.5 h, which affords **74** (2.55 g, 88% yield) over two crops as an off-white solid. ^{1}H NMR (600 MHz, DMSO-d_6) δ 8.24 (d, J 8.1 Hz, 1H), 7.90 (dd, J 7.2, 1.2 Hz, 1H), 7.62–7.59 (m, 1H), 7.30–7.27 (m, 1H), 3.83 (dq, J 14.1, 7.1 Hz, 1H), 3.20 (dq, J 14.1, 7.1 Hz, 1H), 2.79–2.54 (m, 4H), 1.22 (dd, J 7.1, 7.1 Hz, 3H). ^{13}C NMR (101 MHz, DMSO-d_6) δ 172.7, 171.5, 161.7, 135.7, 133.3, 127.9, 124.7, 119.0, 118.0, 79.8, 39.0, 30.1, 27.6, 15.1. LCMS (Method A): t_R = 0.78 min, m/z = 275.2 (M + H$^+$).

4-(2,2,2-Trifluoroethyl)-1,5-dioxo-2,3-dihydropyrrolo[1,2-a]-quinazoline-3a-carboxylic Acid (75). General procedure D was reproduced using **94** (320 mg, 1.47 mmol) and α-ketoglutaric acid (257 mg, 1.76 mmol) in AcOH (5 mL) at 118 °C for 2 h. The solvent was removed under reduced pressure, and the resultant residue was triturated with Et$_2$O/n-pentane (7:3, 15 mL). The resultant precipitate was collected using vacuum filtration to give **75** (370 mg, 77%) as an off-white powder. ^{1}H NMR (400 MHz, DMSO-d_6) δ 14.27 (br s, 1H), 8.31 (d, J 8.0 Hz, 1H), 7.97 (d, J 8.0 Hz, 1H), 7.69 (app. t, J 8.0 Hz, 1H), 7.34 (app. t, J 7.2 Hz, 1H), 4.69–4.56 (m, 1H), 4.32–4.20 (m, 1H), 2.88–2.71 (m, 3H), 2.61–2.50 (m, 1H). LCMS: t_R = 1.73 min, m/z = 329.2 (M + H$^+$).

4-Cyclopropyl-1,5-dioxo-2,3-dihydropyrrolo[1,2-a]quinazoline-3a-carboxylic Acid (76). General procedure D was reproduced using 2-amino-N-cyclopropylbenzamide (936 mg, 5.31 mmol) and α-ketoglutaric acid (946 mg, 6.48 mmol) in AcOH (5 mL) at 118 °C for 27 h, which affords **76** (1.21 g, 79%) as a white powder. ^{1}H NMR (400 MHz,) δ 8.14 (d, J 8.2 Hz, 1H), 7.86 (d, J 7.6 Hz, 1H), 7.58 (t, J 7.9 Hz, 1H), 7.28 (t, J 7.6 Hz, 1H), 2.94 (dt, J 11.0, 9.2 Hz, 1H), 2.83–2.58 (m, 4H), 1.03–0.73 (m, 4H). ^{13}C NMR (101 MHz, DMSO-d_6) δ 172.6, 172.3, 162.5, 135.4, 133.2, 128.1, 125.0, 120.6, 118.3, 80.2, 30.3, 27.3, 25.7, 8.9, 6.4. LCMS (Method A): t_R = 0.82 min, m/z = 287.2 (M + H$^+$).

4-Isopropyl-1,5-dioxo-2,3-dihydropyrrolo[1,2-a]quinazoline-3a-carboxylic Acid (77). General procedure D was reproduced using **95** (400 mg, 2.24 mmol) and α-ketoglutaric acid (393 mg, 2.69 mmol) in AcOH (5 mL) at 118 °C for 4 h, which affords **77** (525 mg, 81%) as an off-white powder. ^{1}H NMR (400 MHz, DMSO-d_6) δ 13.86 (br s, 1H), 8.16 (d, J 8.0 Hz, 1H), 7.84 (d, J 7.2 Hz, 1H), 7.56 (app. t, J 7.2 Hz, 1H), 7.26 (app. t, J 7.6 Hz, 1H), 3.77–3.70 (m, 1H), 2.81–2.67 (m, 2H), 2.66–2.51 (m, 2H), 1.57 (d, J 6.4 Hz, 1H), 1.46 (d, J 6.4 Hz, 1H). LCMS: t_R = 1.49 min, m/z = 289.21 (M + H$^+$).

4-Propyl-1,5-dioxo-2,3-dihydropyrrolo[1,2-a]quinazoline-3a-carboxylic Acid (78). General procedure D was reproduced using **96** (550 mg, 3.09 mmol) and α-ketoglutaric acid (541 mg, 3.70 mmol) in AcOH (5 mL) at 118 °C for 3 h, which affords **78** (760 mg, 85%) as an off-white powder. ^{1}H NMR (400 MHz, DMSO-d_6) δ 13.94 (br s, 1H), 8.24 (d, J 8.0 Hz, 1H), 7.90 (dd, J 8.0, 1.6 Hz, 1H), 7.63–758 (m, 1H), 7.31–7.26 (m, 1H), 3.76–3.67 (m, 1H), 3.10–3.01 (m, 1H), 2.80–2.62 (m, 3H), 2.61–2.49 (m, 1H), 1.80–1.65 (m, 1H), 1.64–1.50 (m, 1H), 0.89 (t, J 7.6 Hz, 3H). LCMS: t_R = 1.52 min, m/z = 289.18 (M + H$^+$).

4-Isobutyl-1,5-dioxo-2,3-dihydropyrrolo[1,2-a]quinazoline-3a-carboxylic Acid (79). General procedure D was reproduced using **97** (370 mg, 1.92 mmol) and α-ketoglutaric acid (337 mg, 2.31 mmol) in AcOH (6 mL) at 118 °C for 2 h, which affords **79** (360 mg, 62%) as an off-white powder. ^{1}H NMR (400 MHz, DMSO-d_6) δ 13.94 (br s, 1H), 8.29 (d, J 8.0 Hz, 1H), 7.91 (dd, J 7.6, 1.2 Hz, 1H), 7.61 (td, J 7.6, 1.2 Hz, 1H), 7.28 (app. t, J 7.2 Hz, 1H), 3.79–3.68 (m, 1H), 2.92–2.80 (m, 1H), 2.79–2.61 (m, 3H), 2.60–2.49 (m, 1H), 2.20–2.02 (m, 1H), 0.95–0.79 (m, 6H). LCMS: t_R = 1.82 min, m/z = 303.2 (M + H$^+$).

8-Chloro-4-methyl-1,5-dioxo-2,3-dihydropyrrolo[1,2-a]-quinazoline-3a-carboxylic Acid (80). General procedure D was reproduced using **98** (1.56 g, 8.46 mmol) and α-ketoglutaric acid (1.48 g, 10.1 mmol) in AcOH (7 mL) at 118 °C for 16 h. Gives **80** (2.21 g, 89% yield) as a light yellow crystalline solid. ^{1}H NMR (600 MHz,) δ 8.28 (d, J 1.9 Hz, 1H), 7.92 (d, J 8.4 Hz, 1H), 7.37 (dd, J 8.4, 2.0 Hz, 1H), 3.07 (s, 3H), 2.76 (ddd, J 16.4, 10.8, 8.9 Hz, 1H), 2.72–2.56 (m, 3H). ^{13}C NMR (101 MHz, DMSO-d_6) δ 172.9, 170.9, 161.0, 137.8, 136.6, 130.1, 124.9, 117.5, 117.4, 79.4, 30.1, 29.1, 28.0. LCMS (Method A): t_R = 0.98 min, m/z = 293.2 (M − H$^+$).

8-Methoxy-4-methyl-1,5-dioxo-2,3-dihydropyrrolo[1,2-a]-quinazoline-3a-carboxylic Acid (81). General procedure D was reproduced using **99** (1.35 g, 7.51 mmol) and α-ketoglutaric acid (1.33 g, 9.12 mmol) in AcOH (7 mL) at 80 °C for 40 min. Gives **81** (1.91 g, 84% yield) as a white solid. ^{1}H NMR (400 MHz, DMSO-d_6) δ 7.88–7.77 (m, 2H), 6.86 (dd, J 8.8, 2.4 Hz, 1H), 3.82 (s, 3H), 3.04 (s, 3H), 2.81–2.55 (m, 4H). ^{13}C NMR (101 MHz, DMSO-d_6) δ 172.8, 171.3, 162.9, 161.8, 137.3, 130.0, 111.7, 110.9, 102.7, 79.6,

55.6, 30.2, 28.9, 28.1. LCMS (Method A): t_R = 0.80 min, m/z = 289.2 (M − H$^+$).

4-Methyl-8-(trifluoromethyl)-1,5-dioxo-2,3-dihydropyrrolo[1,2-a]quinazoline-3a-carboxylic Acid (82). General procedure D was reproduced using **100** (370 mg, 1.70 mmol) and α-ketoglutaric acid (273 mg, 1.87 mmol) in AcOH (5 mL) at 118 °C for 2 h, which affords **82** (470 mg, 84%) as an off-white powder. ^{1}H NMR (400 MHz, DMSO-d_6) δ 14.21 (br s, 1H), 8.57 (s, 1H), 8.13 (d, J 8.0 Hz, 1H), 7.66 (d, J 8.0 Hz, 1H), 3.17 (s, 3H), 2.78–2.60 (m, 4H). LCMS: t_R = 1.45 min, m/z = 329.06 (M + H$^+$).

8-Cyano-4-methyl-1,5-dioxo-2,3-dihydropyrrolo[1,2-a]-quinazoline-3a-carboxylic Acid (83). General procedure D was reproduced using **101** (205 mg, 1.17 mmol) and α-ketoglutaric acid (205 mg, 1.404 mmol) in AcOH (2 mL) at 118 °C for 4 h, which affords **83** (301 mg, 90%) as an off-white solid. ^{1}H NMR (400 MHz, DMSO-d_6): δ 8.58 (s, 1H), 8.06 (d, J 8.0 Hz, 1H), 7.74 (d, J 8.0 Hz, 1H), 3.08 (s, 3H), 2.84–2.56 (m, 4H). LCMS: t_R = 1.38 min, m/z = 286.36 (M + H$^+$).

4-Methyl-8-(trifluoromethoxy)-1,5-dioxo-2,3-dihydropyrrolo[1,2-a]quinazoline-3a-carboxylic Acid (84). General procedure D was reproduced using **13** (305 mg, 1.302 mmol) and α-ketoglutaric acid (228 mg, 1.563 mmol) in AcOH (3 mL) at 118 °C for 4 h, which affords **84** (296 mg, 66%) as an off-white solid. ^{1}H NMR (400 MHz, DMSO-d_6) δ 14.23 (br s, 1H), 8.22 (s, 1H), 8.04 (d, J 8.4 Hz, 1H), 7.28 (d, J 8.4 Hz, 1H), 3.08 (s, 3H), 2.91–2.58 (m, 4H). LCMS: t_R = 1.58 min, m/z = 289.18 (M + H$^+$).

6-Fluoro-4-methyl-1,5-dioxo-2,3-dihydropyrrolo[1,2-a]-quinazoline-3a-carboxylic Acid (85). General procedure D was reproduced using 2-amino-6-fluoro-N-methylbenzamide **102** (1.00 g, 5.95 mmol), α-ketoglutaric acid (869 mg, 5.95 mmol), and AcOH (10 mL) at 118 °C for 6 h. After cooling to ambient temperature, the reaction mixture was poured into cold H$_2$O and extracted with EtOAc (3 × 50 mL). The combined organic phase was washed with brine (5 × 50 mL), dried (NaSO$_4$), filtered, and reduced *in vacuo* to give **85** (600 mg, 36%) as a yellow solid. LCMS (Method B): t_R = 0.64 min, m/z = 279.1 (M + H$^+$).

7-Fluoro-4-methyl-1,5-dioxo-2,3-dihydropyrrolo[1,2-a]-quinazoline-3a-carboxylic Acid (86). General procedure D was reproduced using 2-amino-5-fluoro-N-methylbenzamide **103** (1.90 g, 11.30 mmol), α-ketoglutaric acid (1.65 g, 11.30 mmol), and AcOH (40 mL) at 118 °C for 6 h. After cooling to ambient temperature, the reaction mixture was poured into cold H$_2$O and extracted with EtOAc (3 × 50 mL). The combined organic phase was washed with brine (5 × 50 mL), dried (NaSO$_4$), filtered, and reduced *in vacuo* to give **86** (2.00 g, 64%) as an off-white solid. LCMS (Method B): t_R = 0.71 min, m/z = 279.1 (M + H$^+$).

8-Fluoro-4-methyl-1,5-dioxo-2,3-dihydropyrrolo[1,2-a]-quinazoline-3a-carboxylic Acid (87). General procedure D was reproduced using 2-amino-4-fluoro-N-methylbenzamide **104** (1.37 g, 8.13 mmol) and α-ketoglutaric acid (1.42 g, 9.72 mmol) in AcOH (7 mL) at 118 °C for 21.5 h. After cooling to ambient temperature, the reaction mixture was poured into cold H$_2$O and extracted with EtOAc (3 × 50 mL). The combined organic phase was washed with brine (5 × 50 mL), dried (NaSO$_4$), filtered, and reduced *in vacuo* to give **87** (1.91 g, 84% yield) as a light yellow crystalline solid. ^{1}H NMR (400 MHz, DMSO-d_6) δ 8.02 (dd, J 10.7, 2.4 Hz, 1H), 7.97 (dd, J 8.7, 6.5 Hz, 1H), 7.15 (td, J 8.6, 2.4 Hz, 1H), 3.06 (s, 3H), 2.82–2.55 (m, 4H). ^{13}C NMR (75 MHz, DMSO-d_6) δ 173.0, 171.1, 164.6 (d, J 248.3 Hz), 161.1, 137.4 (d, J 12.6 Hz), 131.1 (d, J 10.8 Hz), 115.4, (d, J 2.6 Hz), 112.2 (d, J 22.3 Hz), 104.8 (d, J 27.8 Hz), 79.5, 30.1, 29.1, 28.1. LCMS (Method A): t_R = 0.78 min, m/z = 277.2 (M − H$^+$).

9-Fluoro-4-methyl-1,5-dioxo-2,3-dihydropyrrolo[1,2-a]-quinazoline-3a-carboxylic Acid (88). General procedure D was reproduced using 2-amino-3-fluoro-N-methylbenzamide **105** (2.0 g, 11.9 mmol), α-ketoglutaric acid (1.7 g, 11.9 mmol), and AcOH (50 mL) at 118 °C for 6 h. After cooling to ambient temperature, the reaction mixture was poured into cold H$_2$O and extracted with EtOAc (3 × 50 mL). The combined organic phase was washed with brine (5 × 50 mL), dried (NaSO$_4$), filtered, and reduced *in vacuo* to give **88**

(1.50 g, 45%) as a yellow solid. LCMS (Method B): t_R = 0.33 min, m/z = 279.1 (M + H$^+$).

6-Chloro-4-methyl-1,5-dioxo-2,3-dihydropyrrolo[1,2-a]-quinazoline-3a-carboxylic Acid (89). General procedure D was reproduced using 2-amino-6-chloro-N-methylbenzamide **106** (800 mg, 4.33 mmol), α-ketoglutaric acid (633 mg, 4.33 mmol), and AcOH (50 mL) at 118 °C for 6 h. After cooling to ambient temperature, the reaction mixture was poured into cold H$_2$O and extracted with EtOAc (3 × 50 mL). The combined organic phase was washed with brine (5 × 50 mL), dried (NaSO$_4$), filtered, and reduced *in vacuo* to give **89** (600 mg, 47%) as a yellow solid. LCMS (Method B): t_R = 0.69 min, m/z = 295.2 (M + H$^+$).

7-Chloro-4-methyl-1,5-dioxo-2,3-dihydropyrrolo[1,2-a]-quinazoline-3a-carboxylic Acid (90). General procedure D was reproduced using 2-amino-5-chloro-N-methylbenzamide **107** (500 mg, 2.71 mmol), α-ketoglutaric acid (396 mg, 2.71 mmol), and AcOH (20 mL) at 118 °C for 6 h. After cooling to ambient temperature, the reaction mixture was poured into cold H$_2$O and extracted with EtOAc (3 × 50 mL). The combined organic phase was washed with brine (5 × 50 mL), dried (NaSO$_4$), filtered, and reduced *in vacuo* to give **90** (420 mg, 52%) as a white solid. LCMS (Method B): t_R = 1.08 min, m/z = 295.2 (M + H$^+$).

9-Chloro-4-methyl-1,5-dioxo-2,3-dihydropyrrolo[1,2-a]-quinazoline-3a-carboxylic Acid (91). General procedure D was reproduced using 2-amino-3-chloro-N-methylbenzamide **108** (700 mg, 3.79 mmol), α-ketoglutaric acid (554 g, 3.79 mmol), and AcOH (20 mL) at 118 °C for 6 h. After cooling to ambient temperature, the reaction mixture was poured into cold H$_2$O and extracted with EtOAc (3 × 50 mL). The combined organic phase was washed with brine (5 × 50 mL), dried (NaSO$_4$), filtered, and reduced *in vacuo* to give **91** (500 mg, 45%) as a yellow solid. LCMS (Method B): t_R = 0.43 min, m/z = 295.1 (M + H$^+$).

4,8-Dimethyl-1,5-dioxo-2,3-dihydropyrrolo[1,2-a]quinazoline-3a-carboxylic Acid (92). General procedure D was reproduced using 2-amino-4-methyl-N-methylbenzamide **109** (900 mg, 5.48 mmol), α-ketoglutaric acid (800 mg, 5.48 mmol), and AcOH (20 mL) at 118 °C for 6 h. After cooling to ambient temperature, the reaction mixture was poured into cold H$_2$O and extracted with EtOAc (3 × 50 mL). The combined organic phase was washed with brine (5 × 50 mL), dried (NaSO$_4$), filtered, and reduced *in vacuo* to give **92** (900 mg, 61%) as a yellow solid. LCMS (Method B): t_R = 0.88 min, m/z = 275.2 (M + H$^+$).

General Procedure E. 2-Amino-4-bromo-N-methylbenzamide (93). A stirring mixture of 2-amino-4-bromobenzoic acid (2.16 g, 9.98 mmol) in THF (15 mL) under a N$_2$ atmosphere was treated with CDI (1.67 g, 10.3 mmol) at 0 °C and then stirred at ambient temperature for 200 min. A solution of 8 M MeNH$_2$ in EtOH (2.5 mL, 20 mmol) was added, and the mixture was stirred for two weeks. After this time, the reaction mixture was diluted in EtOAc (50 mL), washed using H$_2$O (50 mL) and brine (50 mL), dried (MgSO$_4$), filtered, and reduced *in vacuo* to give **93** (1.94 g, 85% yield) as a tan solid. ^{1}H NMR (400 MHz, DMSO-d_6) δ 8.23 (d, J 5.0 Hz, 1H), 7.37 (d, J 8.4 Hz, 1H), 6.90 (d, J 2.0 Hz, 1H), 6.65–6.62 (m, 3H), 2.71 (d, J 5.0 Hz, 3H).

2-Amino-4-chloro-N-methylbenzamide (98). General procedure E was reproduced using 2-amino-4-chloro-benzoic acid (1.74 g, 10.1 mmol) and CDI (1.30 g, 8.01 mmol) in THF (15 mL) and was stirred at 21 °C for 23 h before an additional portion of CDI (358 mg, 2.21 mmol) was added. After stirring for a further 25 h, a solution of 8 M MeNH$_2$ in EtOH (2.50 mL, 20.0 mmol) was added to the reaction mixture, which was then stirred for 25 h. After this time, the reaction mixture was reduced *in vacuo* to give an oil that was taken up in EtOAc (50 mL), washed using H$_2$O (50 mL) and brine (50 mL), dried (MgSO$_4$), filtered, and reduced *in vacuo* to give **98** (1.59 g, 85% yield) as an off-white solid. ^{1}H NMR (600 MHz, DMSO) δ 8.22 (s, 1H), 7.45 (d, J 8.5 Hz, 1H), 6.74 (d, J 2.0 Hz, 1H), 6.67 (s, 2H), 6.51 (dd, J 8.4, 2.0 Hz, 1H), 2.71 (d, J 4.4 Hz, 3H).

2-Amino-4-methoxy-N-methylbenzamide (99). General procedure E was reproduced using 2-amino-4-methoxybenzoic acid (1.80 g, 10.8 mmol) and CDI (1.66 g, 10.2 mmol) in THF (15 mL) for 19 h,

followed by 8 M MeNH$_2$ in EtOH (2.5 mL, 20.0 mmol) for 3.5 h, which affords **99** (1.35 g, 70% yield) as a light brown-colored powder. ^{1}H NMR (400 MHz, DMSO-d6) δ 7.96 (d, J 4.2 Hz, 1H), 7.41 (d, J 8.8 Hz, 1H), 6.59 (s, 2H), 6.20 (d, J 2.4 Hz, 1H), 6.08 (dd, J 8.8, 2.4 Hz, 1H), 3.69 (s, 3H), 2.69 (d, J 4.2 Hz, 3H).

2-Amino-4-fluoro-N-methylbenzamide (104). General procedure E was reproduced using 2-amino-4-fluorobenzoic acid (1.55 g, 9.97 mmol) and CDI (1.68 g, 10.4 mmol) in THF (15 mL) for 21 h, followed by 8 M MeNH$_2$ in EtOH (2.5 mL, 20.0 mmol) for 19 h, which affords **104** (1.367 g, 82%) as a light orange-colored oil. ^{1}H NMR (400 MHz, DMSO) δ 8.13 (s, 1H), 7.48 (dd, J 8.6, 6.9 Hz, 1H), 6.72 (s, 2H), 6.42 (dd, J 11.9, 2.5 Hz, 1H), 6.30–6.25 (m, 1H), 2.69 (d, J 4.5 Hz, 3H).

General Procedure F. 2-Amino-N-(2,2,2-trifluoroethyl)-benzamide (94). To a solution of 2-aminobenzoic acid (500 mg, 3.65 mmol) in DMF (10.0 ml) at 0 °C were successively added EDCI·HCl (1.05 g, 1.92 mmol), HOBt·H$_2$O (591 mg, 4.38 mmol), and DIPEA (4.45 ml, 25.52 mmol). The mixture was stirred for 15 min under an atmosphere of N$_2$ before the addition of 2,2,2-trifluoroethan-1-amine (988 mg, 7.29 mmol). After stirring for an additional 4 h at 21 °C, the reaction mixture was diluted with EtOAc (25 mL), washed with H$_2$O (3 × 20 mL) and brine (20 mL), dried (Na$_2$SO$_4$), filtered, and concentrated under reduced pressure. The residue was purified by column chromatography, eluting with 30% EtOAc in n-hexane to give **94** (320 mg, 40%) as an off-white solid. ^{1}H NMR (400 MHz, DMSO-d_6) δ 8.75 (s, 1H), 7.53 (d, J 8.0 Hz, 1H), 7.17 (app. t, J 8.0 Hz, 1H), 6.72 (d, J 8.0 Hz, 1H), 6.53 (app. t, J 7.2 Hz, 1H), 6.46 (br s, 2H), 4.02 (m, 2H). LCMS: t_R = 1.62 min, m/z = 219.15 (M + H$^+$).

2-Amino-N-isopropylbenzamide (95). General Procedure F was reproduced using 2-aminobenzoic acid (1.50 g, 10.94 mmol), isopropylamine (1.88 mL, 21.87 mmol), EDCI·HCl (4.19 g, 21.87 mmol), HOBt·H$_2$O (1.77 g, 13.12 mmol), and DIPEA (9.53 ml, 54.68 mmol) in DMF (20 mL) for 4 h. Purification using column chromatography, eluting with 10–25% EtOAc in n-hexane, gives **95** (1.41 g, 72%) as an off-white solid. ^{1}H NMR (400 MHz, DMSO-d_6) δ 7.92 (d, J 7.6 Hz, 1H), 7.45 (dd, J 8.0, 1.0 Hz, 1H), 7.13–7.09 (m, 1H), 6.66 (d, J 8.0 Hz, 1H), 6.67–6.54 (m, 1H), 6.32 (br s, 2H), 4.04 (septet, J 6.6 Hz, 1H), 1.13 (d, J 6.6 Hz, 1H). LCMS: t_R = 1.55 min, m/z = 179.2 (M + H$^+$).

2-Amino-N-propylbenzamide (96). General Procedure F was reproduced using 2-aminobenzoic acid (500 mg, 3.65 mmol), propylamine hydrochloride (697 mg, 7.29 mmol), EDCI·HCl (1.40 g, 7.29 mmol), HOBt·H$_2$O (591 mg, 4.38 mmol), and DIPEA (3.18 ml, 18.23 mmol) in DMF (8 mL) for 4 h. Purification using column chromatography, eluting with 20% EtOAc in n-hexane, gives **96** (550 mg, 84%) as an off-white solid. ^{1}H NMR (400 MHz, DMSO-d_6) δ 8.14 (s, 1H), 7.42 (d, J 8.0 Hz, 1H), 7.09 (app. t, J 7.6 Hz, 1H), 6.64 (d, J 8.0 Hz, 1H), 6.47 (app. t, J 7.6 Hz, 1H), 6.32 (br s, 2H), 3.13 (q, J 7.2 Hz, 2H), 1.48 (m, 2H), 0.85 (t, J 7.2 Hz, 3H). LCMS: t_R = 2.74 min, m/z = 179.2 (M + H$^+$).

2-Amino-N-isobutylbenzamide (97). General Procedure F was reproduced using 2-aminobenzoic acid (600 mg, 4.38 mmol), isobutylamine (878 mg, 8.75 mmol), EDCI·HCl (1.1 g, 5.25 mmol), HOBt·H$_2$O (650 mg, 4.81 mmol), and DIPEA (2.27 ml, 13.13 mmol) in DMF (10 mL) for 4 h. Purification using column chromatography, eluting with 20% EtOAc in n-hexane, gives **97** (380 mg, 45%) as an off-white solid. ^{1}H NMR (400 MHz, DMSO-d_6) δ 8.18 (br s, 1H), 7.47 (d, J 7.6 Hz, 1H), 7.12 (app. t, J 7.6 Hz, 1H), 6.67 (d, J 8.0 Hz, 1H), 6.50 (app. t, J 7.2 Hz, 1H), 6.32 (br s, 2H), 3.02 (t, J 6.4 Hz, 2H), 1.90–1.75 (m, 1H), 0.88 (d, J 6.8 Hz, 6H). LCMS: t_R = 1.64 min, m/z = 193.18 (M + H$^+$).

2-Amino-N-methyl-4-(trifluoromethyl)benzamide (100). General Procedure F was reproduced using 2-amino-4-(trifluoromethyl)-benzoic acid (500 mg, 2.44 mmol), MeNH$_2$·HCl (494 mg, 7.312 mmol), EDCI·HCl (701 mg, 3.66 mmol), HOBt·H$_2$O (395 mg, 2.93 mmol), and DIPEA (1.27 ml, 7.31 mmol) in DMF (3 mL) for 4 h. Purification using column chromatography, eluting with 5–25% EtOAc in n-hexane, gives **100** (373 mg, 70%) as an off-white solid. ^{1}H NMR (400 MHz, DMSO-d_6) δ 8.34 (br s, 1H), 7.61 (d, J 8.0 Hz,

1H), 7.03 (s, 1H), 6.77 (d, J 8.0 Hz, 1H), 6.69 (br s, 2H), 2.74 (d, J 4.4 Hz, 3H). MS (ESI) m/z: 219.35 [M + H]$^+$. LCMS: t_R = 1.66 min, m/z = 219.35 (M + H$^+$).

2-Amino-4-cyano-N-methylbenzamide (101). General Procedure F was reproduced using 2-amino-4-cyanobenzoic acid (240 mg, 1.48 mmol), MeNH$_2$·HCl (250 mg, 3.70 mmol), EDCI·HCl (567 mg, 2.96 mmol), HOBt·H$_2$O (240 mg, 1.78 mmol), and DIPEA (1.30 ml, 7.40 mmol) in DMF (3 mL) for 3 h. Purification using column chromatography, eluting with 10−30% EtOAc in *n*-hexane, gives **101** (205 mg, 79%) as an off-white solid. ^{1}H NMR (400 MHz, DMSO-d_6) δ 8.42 (br s, 1H), 7.56 (d, J 8.0 Hz, 1H), 7.07 (s, 1H), 6.89 (d, J 8.0 Hz, 1H), 6.69 (br s, 2H), 2.73 (d, J 4.4 Hz, 3H). LCMS: t_R = 2.01 min, m/z = 174.0 (M + H$^+$).

General Procedure G. 2-Amino-6-fluoro-N-methylbenzamide (102). 2-Amino-6-fluorobenzoic acid (2.0 g, 12.9 mmol), MeNH$_2$·HCl (8.7 g, 128.9 mmol), HATU (7.4 g, 19.3 mmol), and DIPEA (21.7 g, 167.6 mmol) were added to DMF (100 mL). The resulting mixture was stirred at room temperature for 2 h. Upon completion of the reaction, the mixture was poured into H$_2$O and extracted with EtOAc (3 × 100 mL). The combined organic phase was washed with brine (2 × 100 mL), dried (Na$_2$SO$_4$), filtered, and reduced *in vacuo* to afford **102** (2.05 g, 95%) as a yellow solid. LCMS (Method B): t_R = 0.49 min, m/z = 169.2 (M + H$^+$).

2-Amino-5-fluoro-N-methylbenzamide (103). General procedure G was reproduced using 2-amino-5-fluorobenzoic acid (2.00 g, 12.9 mmol), MeNH$_2$·HCl (8.70 g, 128.9 mmol), HATU (7.34 g, 19.3 mmol), DIPEA (21.66 g, 167.6 mmol), and DMF (100 mL) at ambient temperature for 2 h. Gives **103** (1.90 g, 88%) as a white solid. LCMS (Method B): t_R = 0.95 min, m/z = 169.1 (M + H$^+$).

2-Amino-3-fluoro-N-methylbenzamide (105). General procedure G was reproduced using 2-amino-3-fluorobenzoic acid (2.00 g, 12.9 mmol), MeNH$_2$·HCl (8.70 g, 128.9 mmol), HATU (7.34 g, 19.3 mmol), DIPEA (21.66 g, 167.6 mmol), and DMF (100 mL) at ambient temperature for 2 h. Gives **105** (2.10 g, 97%) as a yellow solid. LCMS (Method B): t_R = 0.60 min, m/z = 169.1 (M + H$^+$).

2-Amino-6-chloro-N-methylbenzamide (106). General procedure G was reproduced using 2-amino-6-chlorobenzoic acid (2.21 g, 12.9 mmol), MeNH$_2$·HCl (8.70 g, 128.9 mmol), HATU (7.34 g, 19.3 mmol), DIPEA (21.66 g, 167.6 mmol), and DMF (100 mL) at ambient temperature for 2 h. Gives **106** (800 g, 74%) as a white solid. LCMS (Method B): t_R = 0.66 min, m/z = 185.1 (M + H$^+$).

2-Amino-5-chloro-N-methylbenzamide (107). General procedure G was reproduced using 2-amino-5-chlorobenzoic acid (2.21 g, 12.9 mmol), MeNH$_2$·HCl (8.70 g, 128.9 mmol), HATU (7.34 g, 19.3 mmol), DIPEA (21.66 g, 167.6 mmol), and DMF (100 mL) at ambient temperature for 2 h. Gives **107** (1.10 g, 96%) as a white solid. LCMS (Method B): t_R = 1.19 min, m/z = 185.2 (M + H$^+$).

2-Amino-3-chloro-N-methylbenzamide (108). General procedure G was reproduced using 2-amino-3-chlorobenzoic acid (2.21 g, 12.9 mmol), MeNH$_2$·HCl (8.70 g, 128.9 mmol), HATU (7.34 g, 19.3 mmol), DIPEA (21.66 g, 167.6 mmol), and DMF (100 mL) at ambient temperature for 2 h. Gives **108** (800 g, 74%) as a white solid. LCMS (Method B): t_R = 0.65 min, m/z = 185.1 (M + H$^+$).

2-Amino-4,N-dimethylbenzamide (109). General procedure G was reproduced using 2-amino-4-methylbenzoic acid (1.95 g, 12.9 mmol), MeNH$_2$·HCl (8.70 g, 128.9 mmol), HATU (7.34 g, 19.3 mmol), DIPEA (21.66 g, 167.6 mmol), and DMF (100 mL) at ambient temperature for 2 h. Gives **109** (800 g, 74%) as a white solid. LCMS (Method B): t_R = 0.65 min, m/z = 165.3 (M + H$^+$).

2-Nitro-4-(trifluoromethoxy)benzonitrile (10). To a stirred solution of 1-bromo-2-nitro-4-(trifluoromethoxy)benzene (**9**) (2.00 g, 6.99 mmol) in DMF (3.5 mL) was added CuCN (626 mg, 6.99 mmol) and the mixture was stirred at 150 °C for 1 h. The reaction mixture was cooled, diluted with PhCH$_3$ (19.0 mL), and refluxed for another 1 h. The mixture was diluted with EtOAc (40 mL), washed with H$_2$O (2 × 40 mL), dried (Na$_2$SO$_4$), filtered, and concentrated under reduced pressure. The residue was purified using column chromatography, eluting with 10−30% EtOAc in *n*-hexane to give **10** (1.20 g, 74%) as a light yellow solid. ^{1}H NMR (400 MHz, DMSO-d_6)

δ 8.39−8.34 (m, 2H), 8.04 (d, J 8.0 Hz, 1H). LCMS: t_R = 9.41 min, m/z = 232.0 (M$^+$).

2-Nitro-4-(trifluoromethoxy)benzoic acid (11). A mixture of **10** (1.50 g, 6.46 mmol) in 55% H$_2$SO$_4$ (20 mL) was stirred under reflux overnight. The reaction mixture was poured onto ice H$_2$O (30 mL) and extracted with EtOAc (3 × 25 mL). The combined organic phase was extracted using 1 M NaOH (3 × 15 mL). The aqueous fractions were combined, acidified with 10% HCl, and extracted with EtOAc (3 × 25 mL). The combined organic phase was dried (Na$_2$SO$_4$), filtered, and concentrated under reduced pressure to afford **11** (798 mg, 49%) as an off-white solid. ^{1}H NMR (400 MHz, DMSO-d_6) δ 14.00 (br s, 1H), 8.12 (s, 1H), 7.96 (d, J 8.0 Hz, 1H), 7.81 (d, J 8.0 Hz, 1H). LCMS: t_R = 1.72 min, m/z = 250.14 (M − H$^+$).

N-Methyl-2-nitro-4-(trifluoromethoxy)benzamide (12). To a solution of **11** (600 mg, 2.39 mmol) in DMF (6 mL) under an atmosphere of N$_2$ were added EDCI·HCl (916 mg, 4.78 mmol), HOBt·H$_2$O (387 mg, 2.87 mmol), and DIPEA (2.1 mL, 11.95 mmol) sequentially and stirred at ambient temperature for 15 min, before the addition of MeNH$_2$·HCl (484 mg, 7.17 mmol). Stirring was continued for 3 h before the reaction mixture was diluted with EtOAc (30 mL), and the solution was washed with H$_2$O (3 × 20 mL) and brine, dried (Na$_2$SO$_4$), filtered, and concentrated under reduced pressure. The residue was purified by column chromatography, eluting with 20−30% EtOAc in *n*-hexane to give **12** (348 mg, 55%) as a light yellow solid. ^{1}H NMR (400 MHz, DMSO-d_6) δ 8.68 (br s, 1H), 8.11 (s, 1H), 7.84 (d, J 8.0 Hz, 1H), 7.76 (d, J 8.0 Hz, 1H), 2.76 (d, J 4.4 Hz, 3H). LCMS: t_R = 3.25 min, m/z = 265.2 (M + H$^+$).

2-Amino-N-methyl-4-(trifluoromethoxy)benzamide (13). To a stirred solution of **12** (350 mg, 1.33 mmol) in MeOH/H$_2$O (4:1, 8.0 mL) was added Fe powder (370 mg, 6.63 mmol), followed by NH$_4$Cl (709 mg, 13.25 mmol), and the resulting mixture was heated at a reflux temperature for 2 h. The reaction mixture was cooled to ambient temperature, filtered through Celite, and the filtrate was concentrated under reduced pressure. The residue was diluted with H$_2$O and extracted with CH$_2$Cl$_2$ (3 × 15 mL). The combined organic phase was washed with brine, dried (Na$_2$SO$_4$), filtered, and concentrated under reduced pressure. The residue was purified by column chromatography, eluting with 10−25% EtOAc in *n*-hexane to give **13** (265 mg, 85%) as an off-white solid. ^{1}H NMR (400 MHz, DMSO-d_6): δ 8.25 (br s, 1H), 7.54 (d, J 8.0 Hz, 1H), 6.75 (br s, 2H), 6.63 (s, 1H), 6.41 (d, J 8.0 Hz, 1H), 2.72 (d, J 4.4 Hz, 3H). LCMS: t_R = 2.92 min, m/z = 235.0 (M + H$^+$).

X-ray Crystallography. Single colorless needle-shaped crystals of compound **68** recrystallized from a mixture of chloroform and ethanol by slow evaporation. A suitable crystal with dimensions 0.56 mm × 0.04 mm × 0.03 mm was selected and mounted on a loop with Paratone on a Synergy-S diffractometer. The crystal was kept at a constant T = 108(6) K during data collection. The structure was solved with the ShelXT 2018/2[50] solution program using dual methods and using Olex2 1.3-$α$[51] as the graphical interface. The model was refined with olex2.refine 1.3-$α$[52] using full matrix least squares minimization on F^2. Crystal Data. C$_{19}$H$_{15}$Cl$_2$N$_3$O$_3$, M_r = 404.254, monoclinic, C2 (No. 5), a = 22.0349(9) Å, b = 6.8614(3) Å, c = 24.5146(10) Å, $β$ = 108.177(4)°, $α$ = $γ$ = 90°, V = 3521.4(3) Å^3, T = 108(6) K, Z = 8, Z' = 2, m(Cu K$α$) = 3.551 mm^{-1}, 13450 reflections measured, 4814 unique (R_{int} = 0.0526), which were used in all calculations. The final wR_2 was 0.0781 (all data) and R_1 was 0.0385 ($I ≥ 2σ(I)$). CCDC Deposition number: 2224865.

■ ASSOCIATED CONTENT

ⓈI Supporting Information

The Supporting Information is available free of charge at https://pubs.acs.org/doi/10.1021/acs.jmedchem.2c02092.

> *P. falciparum* asexual parasite (3D7 and resistant lines) and DGFA data, microscopy, parasite cytosolic pH and Na$^+$ data, MIR and whole-genome sequencing data, X-ray crystal data, metabolism identification data, and compound spectra (PDF)

Molecular formula strings (CSV)

AUTHOR INFORMATION

Corresponding Author

Brad E. Sleebs − *The Walter and Eliza Hall Institute of Medical Research, Parkville 3052, Australia; Department of Medical Biology, The University of Melbourne, Parkville 3010, Australia;* ⓞ orcid.org/0000-0001-9117-1048; Phone: 61 3 9345 2718; Email: sleebs@wehi.edu.au

Authors

Trent D. Ashton − *The Walter and Eliza Hall Institute of Medical Research, Parkville 3052, Australia; Department of Medical Biology, The University of Melbourne, Parkville 3010, Australia;* ⓞ orcid.org/0000-0002-6707-6064

Madeline G. Dans − *The Walter and Eliza Hall Institute of Medical Research, Parkville 3052, Australia; Department of Medical Biology, The University of Melbourne, Parkville 3010, Australia*

Paola Favuzza − *The Walter and Eliza Hall Institute of Medical Research, Parkville 3052, Australia; Department of Medical Biology, The University of Melbourne, Parkville 3010, Australia*

Anna Ngo − *The Walter and Eliza Hall Institute of Medical Research, Parkville 3052, Australia; Department of Medical Biology, The University of Melbourne, Parkville 3010, Australia*

Adele M. Lehane − *Research School of Biology, Australian National University, Canberra 2601, Australia;* ⓞ orcid.org/0000-0002-0050-9101

Xinxin Zhang − *Research School of Biology, Australian National University, Canberra 2601, Australia*

Deyun Qiu − *Research School of Biology, Australian National University, Canberra 2601, Australia*

Bikash Chandra Maity − *TCG Lifesciences Pvt. Ltd., Kolkata 700091 West Bengal, India*

Nirupam De − *TCG Lifesciences Pvt. Ltd., Kolkata 700091 West Bengal, India*

Kyra A. Schindler − *Department of Microbiology & Immunology, Columbia University, Irving Medical Center, New York, New York 10032, United States*

Tomas Yeo − *Department of Microbiology & Immunology, Columbia University, Irving Medical Center, New York, New York 10032, United States*

Heekuk Park − *Department of Microbiology & Immunology, Columbia University, Irving Medical Center, New York, New York 10032, United States*

Anne-Catrin Uhlemann − *Department of Microbiology & Immunology, Columbia University, Irving Medical Center, New York, New York 10032, United States;* ⓞ orcid.org/0000-0002-9798-4768

Alisje Churchyard − *Department of Life Sciences, Imperial College London, South Kensington SW7 2AZ, U.K.*

Jake Baum − *Department of Life Sciences, Imperial College London, South Kensington SW7 2AZ, U.K.; School of Biomedical Sciences, University of New South Wales, Sydney 2031, Australia*

David A. Fidock − *Department of Microbiology & Immunology, Columbia University, Irving Medical Center, New York, New York 10032, United States; Center for Malaria Therapeutics and Antimicrobial Resistance, Division of Infectious Diseases, Department of Medicine, Columbia*

University, Irving Medical Center, New York, New York 10032, United States

Kate E. Jarman − *The Walter and Eliza Hall Institute of Medical Research, Parkville 3052, Australia; Department of Medical Biology, The University of Melbourne, Parkville 3010, Australia*

Kym N. Lowes − *The Walter and Eliza Hall Institute of Medical Research, Parkville 3052, Australia; Department of Medical Biology, The University of Melbourne, Parkville 3010, Australia*

Delphine Baud − *Medicines for Malaria Venture, ICC, 1215 Geneva, Switzerland*

Stephen Brand − *Medicines for Malaria Venture, ICC, 1215 Geneva, Switzerland*

Paul F. Jackson − *Global Public Health, Janssen R&D LLC, La Jolla, California 92121, United States*

Alan F. Cowman − *The Walter and Eliza Hall Institute of Medical Research, Parkville 3052, Australia; Department of Medical Biology, The University of Melbourne, Parkville 3010, Australia*

Complete contact information is available at:
https://pubs.acs.org/10.1021/acs.jmedchem.2c02092

Author Contributions

✉T.D.A. and M.G.D. contributed equally.

Notes

The authors declare no competing financial interest.

ABBREVIATIONS USED

ABS, asexual blood stage; ACTs, artemisinin combination therapies (ACTs); ART, artemisinin; ATQ, atovaquone; BCECF, 2,7-bis(2-carboxyethyl)-5(6)-carboxyfluorescein; CNV, copy number variant; CCCP, carbonyl cyanide m-chlorophenylhydrazone; CQ, chloroquine; DGFA, dual gamete formation assay; DHODH, dihydroorotate dehydrogenase; DIDS, 4,4′-diisothiocyano-2,2′-stilbene disulfonic acid; DIPEA, *N,N*-diisopropylethylamine; FNT, formate−nitrite transporter; FaSSGF, fasted state simulated gastrointestinal fluid; FaSSIF, fasted state simulated intestinal fluid; HPMC, hydroxypropyl methylcellulose; LDH, lactate dehydrogenase; MIR, minimum inoculum of resistance; MFQ, mefloquine; MMV, Medicines for Malaria Venture; HT1, hexose transport 1; Pf, *P. falciparum*; RBC, red blood cell; SNP, single-nucleotide polymorphism; TCFH, N,N,N′,N′-tetramethyl-

chloroformamidinium hexafluorophosphate; PBS, phosphate-buffered saline; PRR, parasite reduction ratio; PYR, pyrimethamine; RBC, red blood cell; SAR, structure−activity relationship; SBFI, sodium-binding benzofuran isophthalate; SCID, severe combined immunodeficiency; SERCA, sarcoendoplasmic reticulum calcium ATPase; WJM, WEHI-Janssen-MMV

■ REFERENCES

(1) *World Malaria Report*; World Health Organisation: Geneva, 2022.

(2) Dhiman, S. Are malaria elimination efforts on right track? An analysis of gains achieved and challenges ahead. *Infect. Dis. Poverty* **2019**, *8*, No. 14.

(3) Mendis, K.; Sina, B. J.; Marchesini, P.; Carter, R. The neglected burden of *Plasmodium vivax* malaria. *Am. J. Trop. Med. Hyg.* **2001**, *64*, 97−106.

(4) Sutherland, C. J. Persistent parasitism: The adaptive biology of *malariae* and *ovale* Malaria. *Trends Parasitol.* **2016**, *32*, 808−819.

(5) Millar, S. B.; Cox-Singh, J. Human infections with *Plasmodium knowlesi*–zoonotic malaria. *Clin. Microbiol. Infect.* **2015**, *21*, 640−648.

(6) Sabbatani, S.; Fiorino, S.; Manfredi, R. *Plasmodium knowlesi*: from Malaysia, a novel health care threat. *Infez. Med.* **2012**, *20*, 5−11.

(7) Ashley, E. A.; Dhorda, M.; Fairhurst, R. M.; Amaratunga, C.; Lim, P.; Suon, S.; Sreng, S.; Anderson, J. M.; Mao, S.; Sam, B.; Sopha, C.; Chuor, C. M.; Nguon, C.; Sovannaroth, S.; Pukrittayakamee, S.; Jittamala, P.; Chotivanich, K.; Chutasmit, K.; Suchatsoonthorn, C.; Runcharoen, R.; Hien, T. T.; Thuy-Nhien, N. T.; Thanh, N. V.; Phu, N. H.; Htut, Y.; Han, K. T.; Aye, K. H.; Mokuolu, O. A.; Olaosebikan, R. R.; Folaranmi, O. O.; Mayxay, M.; Khanthavong, M.; Hongvanthong, B.; Newton, P. N.; Onyamboko, M. A.; Fanello, C. I.; Tshefu, A. K.; Mishra, N.; Valecha, N.; Phyo, A. P.; Nosten, F.; Yi, P.; Tripura, R.; Borrmann, S.; Bashraheil, M.; Peshu, J.; Faiz, M. A.; Ghose, A.; Hossain, M. A.; Samad, R.; Rahman, M. R.; Hasan, M. M.; Islam, A.; Miotto, O.; Amato, R.; MacInnis, B.; Stalker, J.; Kwiatkowski, D. P.; Bozdech, Z.; Jeeyapant, A.; Cheah, P. Y.; Sakulthaew, T.; Chalk, J.; Intharabut, B.; Silamut, K.; Lee, S. J.; Vihokhern, B.; Kunasol, C.; Imwong, M.; Tarning, J.; Taylor, W. J.; Yeung, S.; Woodrow, C. J.; Flegg, J. A.; Das, D.; Smith, J.; Venkatesan, M.; Plowe, C. V.; Stepniewska, K.; Guerin, P. J.; Dondorp, A. M.; Day, N. P.; White, N. J. Spread of Artemisinin resistance in *Plasmodium falciparum* Malaria. *N. Engl. J. Med.* **2014**, *371*, 411−423.

(8) Dondorp, A. M.; Nosten, F.; Yi, P.; Das, D.; Phyo, A. P.; Tarning, J.; Lwin, K. M.; Ariey, F.; Hanpithakpong, W.; Lee, S. J.; Ringwald, P.; Silamut, K.; Imwong, M.; Chotivanich, K.; Lim, P.; Herdman, T.; An, S. S.; Yeung, S.; Singhasivanon, P.; Day, N. P. J.; Lindegardh, N.; Socheat, D.; White, N. J. Artemisinin resistance in *Plasmodium falciparum* malaria. *N. Eng. J. Med.* **2009**, *361*, 455−467.

(9) Uwimana, A.; Legrand, E.; Stokes, B. H.; Ndikumana, J.-L. M.; Warsame, M.; Umulisa, N.; Ngamije, D.; Munyaneza, T.; Mazarati, J.-B.; Munguti, K.; Campagne, P.; Criscuolo, A.; Ariey, F.; Murindahabi, M.; Ringwald, P.; Fidock, D. A.; Mbituyumuremyi, A.; Menard, D. Emergence and clonal expansion of in vitro artemisinin-resistant *Plasmodium falciparum* kelch13 R561H mutant parasites in Rwanda. *Nat. Med.* **2020**, *26*, 1602−1608.

(10) Ashton, T. D.; Devine, S. M.; Möhrle, J. J.; Laleu, B.; Burrows, J. N.; Charman, S. A.; Creek, D. J.; Sleebs, B. E. The development process for discovery and clinical advancement of modern antimalarials. *J. Med. Chem.* **2019**, *62*, 10526−10562.

(11) McCarthy, J. S.; Lotharius, J.; Ruckle, T.; Chalon, S.; Phillips, M. A.; Elliott, S.; Sekuloski, S.; Griffin, P.; Ng, C. L.; Fidock, D. A.; Marquart, L.; Williams, N. S.; Gobeau, N.; Bebrevska, L.; Rosario, M.; Marsh, K.; Mohrle, J. J. Safety, tolerability, pharmacokinetics, and activity of the novel long-acting antimalarial DSM265: a two-part first-in-human phase 1a/1b randomised study. *Lancet Infect. Dis.* **2017**, *17*, 626−635.

(12) Phillips, M. A.; Lotharius, J.; Marsh, K.; White, J.; Dayan, A.; White, K. L.; Njoroge, J. W.; El Mazouni, F.; Lao, Y.; Kokkonda, S.; Tomchick, D. R.; Deng, X.; Laird, T.; Bhatia, S. N.; March, S.; Ng, C. L.; Fidock, D. A.; Wittlin, S.; Lafuente-Monasterio, M.; Benito, F. J.; Alonso, L. M.; Martinez, M. S.; Jimenez-Diaz, M. B.; Bazaga, S. F.; Angulo-Barturen, I.; Haselden, J. N.; Louttit, J.; Cui, Y.; Sridhar, A.; Zeeman, A. M.; Kocken, C.; Sauerwein, R.; Dechering, K.; Avery, V. M.; Duffy, S.; Delves, M.; Sinden, R.; Ruecker, A.; Wickham, K. S.; Rochford, R.; Gahagen, J.; Iyer, L.; Riccio, E.; Mirsalis, J.; Bathhurst, I.; Rueckle, T.; Ding, X.; Campo, B.; Leroy, D.; Rogers, M. J.; Rathod, P. K.; Burrows, J. N.; Charman, S. A. A long-duration dihydroorotate dehydrogenase inhibitor (DSM265) for prevention and treatment of malaria. *Sci. Transl. Med.* **2015**, *7*, No. 296ra111.

(13) Sulyok, M.; Ruckle, T.; Roth, A.; Murbeth, R. E.; Chalon, S.; Kerr, N.; Samec, S. S.; Gobeau, N.; Calle, C. L.; Ibanez, J.; Sulyok, Z.; Held, J.; Gebru, T.; Granados, P.; Bruckner, S.; Nguetse, C.; Mengue, J.; Lalremruata, A.; Sim, B. K. L.; Hoffman, S. L.; Mohrle, J. J.; Kremsner, P. G.; Mordmuller, B. DSM265 for *Plasmodium falciparum* chemoprophylaxis: a randomised, double blinded, phase 1 trial with controlled human malaria infection. *Lancet Infect. Dis.* **2017**, *17*, 636−644.

(14) Rottmann, M.; McNamara, C.; Yeung, B. K.; Lee, M. C.; Zou, B.; Russell, B.; Seitz, P.; Plouffe, D. M.; Dharia, N. V.; Tan, J.; Cohen, S. B.; Spencer, K. R.; Gonzalez-Paez, G. E.; Lakshminarayana, S. B.; Goh, A.; Suwanarusk, R.; Jegla, T.; Schmitt, E. K.; Beck, H. P.; Brun, R.; Nosten, F.; Renia, L.; Dartois, V.; Keller, T. H.; Fidock, D. A.; Winzeler, E. A.; Diagana, T. T. Spiroindolones, a potent compound class for the treatment of malaria. *Science* **2010**, *329*, 1175−1180.

(15) Leong, F. J.; Li, R.; Jain, J. P.; Lefevre, G.; Magnusson, B.; Diagana, T. T.; Pertel, P. A first-in-human randomized, double-blind, placebo-controlled, single- and multiple-ascending oral dose study of novel antimalarial Spiroindolone KAE609 (Cipargamin) to assess its safety, tolerability, and pharmacokinetics in healthy adult volunteers. *Antimicrob. Agents Chemother.* **2014**, *58*, 6209−6214.

(16) White, N. J.; Pukrittayakamee, S.; Phyo, A. P.; Rueangweerayut, R.; Nosten, F.; Jittamala, P.; Jeeyapant, A.; Jain, J. P.; Lefevre, G.; Li, R.; Magnusson, B.; Diagana, T. T.; Leong, F. J. Spiroindolone KAE609 for falciparum and vivax malaria. *N. Engl. J. Med.* **2014**, *371*, 403−410.

(17) Flannery, E. L.; McNamara, C. W.; Kim, S. W.; Kato, T. S.; Li, F.; Teng, C. H.; Gagaring, K.; Manary, M. J.; Barboa, R.; Meister, S.; Kuhen, K.; Vinetz, J. M.; Chatterjee, A. K.; Winzeler, E. A. Mutations in the P-type cation-transporter ATPase 4, PfATP4, mediate resistance to both aminopyrazole and spiroindolone antimalarials. *ACS Chem. Biol.* **2015**, *10*, 413−420.

(18) Duffey, M.; Blasco, B.; Burrows, J. N.; Wells, T. N. C.; Fidock, D. A.; Leroy, D. Assessing risks of *Plasmodium falciparum* resistance to select next-generation antimalarials. *Trends Parasitol.* **2021**, *37*, 709−721.

(19) Nguyen, W.; Hodder, A. N.; de Lezongard, R. B.; Czabotar, P. E.; Jarman, K. E.; O'Neill, M. T.; Thompson, J. K.; Jousset Sabroux, H.; Cowman, A. F.; Boddey, J. A.; Sleebs, B. E. Enhanced antimalarial activity of plasmepsin V inhibitors by modification of the P(2) position of PEXEL peptidomimetics. *Eur. J. Med. Chem.* **2018**, *154*, 182−198.

(20) Jiménez-Díaz, M. B.; Ebert, D.; Salinas, Y.; Pradhan, A.; Lehane, A. M.; Myrand-Lapierre, M.-E.; O'Loughlin, K. G.; Shackleford, D. M.; Justino de Almeida, M.; Carrillo, A. K.; Clark, J. A.; Dennis, A. S. M.; Diep, J.; Deng, X.; Duffy, S.; Endsley, A. N.; Fedewa, G.; Guiguemde, W. A.; Gómez, M. G.; Holbrook, G.; Horst, J.; Kim, C. C.; Liu, J.; Lee, M. C. S.; Matheny, A.; Martínez, M. S.; Miller, G.; Rodríguez-Alejandre, A.; Sanz, L.; Sigal, M.; Spillman, N. J.; Stein, P. D.; Wang, Z.; Zhu, F.; Waterson, D.; Knapp, S.; Shelat, A.; Avery, V. M.; Fidock, D. A.; Gamo, F.-J.; Charman, S. A.; Mirsalis, J. C.; Ma, H.; Ferrer, S.; Kirk, K.; Angulo-Barturen, I.; Kyle, D. E.; DeRisi, J. L.; Floyd, D. M.; Guy, R. K. (+)-SJ733, a clinical candidate for malaria that acts through ATP4 to induce rapid host-mediated clearance of Plasmodium. *Proc. Natl. Acad. Sci. U.S.A.* **2014**, *111*, E5455−E5462.

(21) Lehane, A. M.; Ridgway, M. C.; Baker, E.; Kirk, K. Diverse chemotypes disrupt ion homeostasis in the malaria parasite. *Mol. Microbiol.* **2014**, *94*, 327−339.

(22) Dennis, A. S. M.; Rosling, J. E. O.; Lehane, A. M.; Kirk, K. Diverse antimalarials from whole-cell phenotypic screens disrupt malaria parasite ion and volume homeostasis. *Sci. Rep.* **2018**, *8*, No. 8795.

(23) Spillman, N. J.; Allen, R. J.; McNamara, C. W.; Yeung, B. K.; Winzeler, E. A.; Diagana, T. T.; Kirk, K. Na(+) regulation in the malaria parasite *Plasmodium falciparum* involves the cation ATPase PfATP4 and is a target of the spiroindolone antimalarials. *Cell Host Microbe* **2013**, *13*, 227−237.

(24) van Pelt-Koops, J. C.; Pett, H. E.; Graumans, W.; van der Vegte-Bolmer, M.; van Gemert, G. J.; Rottmann, M.; Yeung, B. K. S.; Diagana, T. T.; Sauerwein, R. W. The spiroindolone drug candidate NITD609 potently inhibits gametocytogenesis and blocks *Plasmodium falciparum* transmission to *Anopheles* mosquito vector. *Antimicrobi. Agents Chemother.* **2012**, *56*, 3544.

(25) Burrows, J. N.; Duparc, S.; Gutteridge, W. E.; Hooft van Huijsduijnen, R.; Kaszubska, W.; Macintyre, F.; Mazzuri, S.; Möhrle, J. J.; Wells, T. N. C. New developments in anti-malarial target candidate and product profiles. *Malar. J.* **2017**, *16*, No. 26.

(26) Vaidya, A. B.; Morrisey, J. M.; Zhang, Z.; Das, S.; Daly, T. M.; Otto, T. D.; Spillman, N. J.; Wyvratt, M.; Siegl, P.; Marfurt, J.; Wirjanata, G.; Sebayang, B. F.; Price, R. N.; Chatterjee, A.; Nagle, A.; Stasiak, M.; Charman, S. A.; Angulo-Barturen, I.; Ferrer, S.; Belén Jiménez-Díaz, M.; Martínez, M. S.; Gamo, F. J.; Avery, V. M.; Ruecker, A.; Delves, M.; Kirk, K.; Berriman, M.; Kortagere, S.; Burrows, J.; Fan, E.; Bergman, L. W. Pyrazoleamide compounds are potent antimalarials that target Na+ homeostasis in intraerythrocytic *Plasmodium falciparum*. *Nat. Commun.* **2014**, *5*, No. 5521.

(27) Qiu, D.; Pei, J. V.; Rosling, J. E. O.; Thathy, V.; Li, D.; Xue, Y.; Tanner, J. D.; Penington, J. S.; Aw, Y. T. V.; Aw, J. Y. H.; Xu, G.; Tripathi, A. K.; Gnadig, N. F.; Yeo, T.; Fairhurst, K. J.; Stokes, B. H.; Murithi, J. M.; Kümpornsin, K.; Hasemer, H.; Dennis, A. S. M.; Ridgway, M. C.; Schmitt, E. K.; Straimer, J.; Papenfuss, A. T.; Lee, M. C. S.; Corry, B.; Sinnis, P.; Fidock, D. A.; van Dooren, G. G.; Kirk, K.; Lehane, A. M. A G358S mutation in the *Plasmodium falciparum* Na+ pump PfATP4 confers clinically-relevant resistance to cipargamin. *Nat. Commun.* **2022**, *13*, No. 5746.

(28) Tverdokhlebov, A. V.; Tverdokhlebov, A.; Tolmachev, A.; Volovenko, Y.; Kostyuk, A.; Chernega, A.; Rusanov, E. Simple and convenient synthesis of 2,3,4,5-tetrahydro-1,5-dioxopyrrolo[1,2-a]-quinazoline- 3a(1H)-carboxylic acids in multi-gram scale. *Heterocycles* **2008**, *75*, 1673−1680.

(29) Beutner, G. L.; Young, I. S.; Davies, M. L.; Hickey, M. R.; Park, H.; Stevens, J. M.; Ye, Q. TCFH−NMI: Direct access to N-acyl imidazoliums for challenging amide bond formations. *Org. Lett.* **2018**, *20*, 4218−4222.

(30) Gilson, P. R.; Tan, C.; Jarman, K. E.; Lowes, K. N.; Curtis, J. M.; Nguyen, W.; Di Rago, A. E.; Bullen, H. E.; Prinz, B.; Duffy, S.; Baell, J. B.; Hutton, C. A.; Jousset Subroux, H.; Crabb, B. S.; Avery, V. M.; Cowman, A. F.; Sleebs, B. E. Optimization of 2-anilino 4-amino substituted qinazolines into potent antimalarial agents with oral *in vivo* activity. *J. Med. Chem.* **2017**, *60*, 1171−1188.

(31) Ding, X. C.; Ubben, D.; Wells, T. N. C. A framework for assessing the risk of resistance for anti-malarials in development. *Malar. J.* **2012**, *11*, No. 292.

(32) Jensen, A. M.; Sørensen, T. L.; Olesen, C.; Møller, J. V.; Nissen, P. Modulatory and catalytic modes of ATP binding by the calcium pump. *EMBO J.* **2006**, *25*, 2305−2314.

(33) Linares, M.; Viera, S.; Crespo, B.; Franco, V.; Gómez-Lorenzo, M. G.; Jiménez-Díaz, M. B.; Angulo-Barturen, Í.; Sanz, L. M.; Gamo, F.-J. Identifying rapidly parasiticidal anti-malarial drugs using a simple and reliable in vitro parasite viability fast assay. *Malar. J.* **2015**, *14*, No. 441.

(34) Dennis, A. S. M.; Lehane, A. M.; Ridgway, M. C.; Holleran, J. P.; Kirk, K. Cell swelling induced by the antimalarial KAE609 (Cipargamin) and other PfATP4-associated antimalarials. *Antimicrob. Agents Chemother.* **2018**, *62*, e00087−18.

(35) Ganesan, S. M.; Falla, A.; Goldfless, S. J.; Nasamu, A. S.; Niles, J. C. Synthetic RNA−protein modules integrated with native translation mechanisms to control gene expression in malaria parasites. *Nat. Commun.* **2016**, *7*, No. 10727.

(36) Saliba, K. J.; Kirk, K. pH regulation in the intracellular malaria parasite, *Plasmodium falciparum*. H(+) extrusion via a V-type H(+)-ATPase. *J. Biol. Chem.* **1999**, *274*, 33213−33219.

(37) van Schalkwyk, D. A.; Chan, X. W.; Misiano, P.; Gagliardi, S.; Farina, C.; Saliba, K. J. Inhibition of *Plasmodium falciparum* pH regulation by small molecule indole derivatives results in rapid parasite death. *Biochem. Pharmacol.* **2010**, *79*, 1291−1299.

(38) Schmitt, E. K.; Ndayisaba, G.; Yeka, A.; Asante, K. P.; Grobusch, M. P.; Karita, E.; Mugerwa, H.; Asiimwe, S.; Oduro, A.; Fofana, B.; Doumbia, S.; Su, G.; Csermak Renner, K.; Venishetty, V. K.; Sayyed, S.; Straimer, J.; Demin, I.; Barsainya, S.; Boulton, C.; Gandhi, P. Efficacy of cipargamin (KAE609) in a randomized, phase II dose-escalation study in adults in Sub-Saharan Africa with uncomplicated *Plasmodium falciparum* malaria. *Clin. Infect. Dis.* **2022**, *74*, 1831−1839.

(39) Delves, M. J.; Miguel-Blanco, C.; Matthews, H.; Molina, I.; Ruecker, A.; Yahiya, S.; Straschil, U.; Abraham, M.; León, M. L.; Fischer, O. J.; Rueda-Zubiaurre, A.; Brandt, J. R.; Cortés, Á.; Barnard, A.; Fuchter, M. J.; Calderón, F.; Winzeler, E. A.; Sinden, R. E.; Herreros, E.; Gamo, F. J.; Baum, J. A high throughput screen for next-generation leads targeting malaria parasite transmission. *Nat. Commun.* **2018**, *9*, No. 3805.

(40) Delves, M. J.; Straschil, U.; Ruecker, A.; Miguel-Blanco, C.; Marques, S.; Dufour, A. C.; Baum, J.; Sinden, R. E. Routine in vitro culture of *P. falciparum* gametocytes to evaluate novel transmission-blocking interventions. *Nat. Protoc.* **2016**, *11*, 1668−80.

(41) Franke-Fayard, B.; Trueman, H.; Ramesar, J.; Mendoza, J.; van der Keur, M.; van der Linden, R.; Sinden, R. E.; Waters, A. P.; Janse, C. J. A *Plasmodium berghei* reference line that constitutively expresses GFP at a high level throughout the complete life cycle. *Mol. Biochem. Parasitol.* **2004**, *137*, 23−33.

(42) Mohring, F.; van Schalkwyk, D. A.; Henrici, R. C.; Blasco, B.; Leroy, D.; Sutherland, C. J.; Moon, R. W. Cation ATPase (ATP4) orthologue replacement in the malaria parasite *Plasmodium knowlesi* reveals species-specific responses to ATP4-targeting drugs. *mBio* **2022**, *13*, No. e0117822.

(43) Gilson, P. R.; Nguyen, W.; Poole, W. A.; Teixeira, J. E.; Thompson, J. K.; Guo, K.; Stewart, R. J.; Ashton, T. D.; White, K. L.; Sanz, L. M.; Gamo, F. J.; Charman, S. A.; Wittlin, S.; Duffy, J.; Tonkin, C. J.; Tham, W. H.; Crabb, B. S.; Cooke, B. M.; Huston, C. D.; Cowman, A. F.; Sleebs, B. E. Evaluation of 4-amino 2-anilinoquinazolines against Plasmodium and other apicomplexan parasites in vitro and in a *P. falciparum* humanized NOD-scid IL2Rγ(null) mouse model of malaria. *Antimicrob. Agents Chemother.* **2019**, *63*, No. e01804-18.

(44) Makler, M. T.; Ries, J. M.; Williams, J. A.; Bancroft, J. E.; Piper, R. C.; Gibbins, B. L.; Hinrichs, D. J. Parasite lactate dehydrogenase as an assay for *Plasmodium falciparum* drug sensitivity. *Am. J. Trop. Med. Hyg.* **1993**, *48*, 739−741.

(45) Cingolani, P.; Platts, A.; Wang le, L.; Coon, M.; Nguyen, T.; Wang, L.; Land, S. J.; Lu, X.; Ruden, D. M. A program for annotating and predicting the effects of single nucleotide polymorphisms, SnpEff: SNPs in the genome of *Drosophila melanogaster* strain w1118; iso-2; iso-3. *Fly* **2012**, *6*, 80−92.

(46) Xi, R.; Hadjipanayis, A. G.; Luquette, L. J.; Kim, T. M.; Lee, E.; Zhang, J.; Johnson, M. D.; Muzny, D. M.; Wheeler, D. A.; Gibbs, R. A.; Kucherlapati, R.; Park, P. J. Copy number variation detection in whole-genome sequencing data using the Bayesian information criterion. *Proc. Natl. Acad. Sci. U.S.A.* **2011**, *108*, E1128−E1136.

(47) Richardson, L. W.; Ashton, T. D.; Dans, M. G.; Nguyen, N.; Favuzza, P.; Triglia, T.; Hodder, A. N.; Ngo, A.; Jarman, K. E.; Cowman, A. F.; Sleebs, B. E. Substrate peptidomimetic inhibitors of *P. falciparum* plasmepsin X with potent antimalarial activity. *ChemMedChem* **2022**, *17*, No. e202200306.

(48) Bailey, B. L.; Nguyen, W.; Ngo, A.; Goodman, C. D.; Gancheva, M. R.; Favuzza, P.; Sanz, L. M.; Gamo, F.-J.; Lowes, K. N.; McFadden, G. I.; Wilson, D. W.; Laleu, B.; Brand, S.; Jackson, P. F.; Cowman, A.

F.; Sleebs, B. E. Optimisation of 2-(N-phenyl carboxamide) triazolopyrimidine antimalarials with moderate to slow acting erythrocytic stage activity. *Bioorg. Chem.* **2021**, *115*, No. 105244.

(49) Favuzza, P.; de Lera Ruiz, M.; Thompson, J. K.; Triglia, T.; Ngo, A.; Steel, R. W. J.; Vavrek, M.; Christensen, J.; Healer, J.; Boyce, C.; Guo, Z.; Hu, M.; Khan, T.; Murgolo, N.; Zhao, L.; Penington, J. S.; Reaksudsan, K.; Jarman, K.; Dietrich, M. H.; Richardson, L.; Guo, K. Y.; Lopaticki, S.; Tham, W. H.; Rottmann, M.; Papenfuss, T.; Robbins, J. A.; Boddey, J. A.; Sleebs, B. E.; Sabroux, H. J.; McCauley, J. A.; Olsen, D. B.; Cowman, A. F. Dual plasmepsin-targeting antimalarial agents disrupt multiple stages of the malaria parasite life cycle. *Cell Host Microbe* **2020**, *27*, 642−658.e12.

(50) Usón, I.; Sheldrick, G. M. An introduction to experimental phasing of macromolecules illustrated by SHELX; new autotracing features. *Acta Crystallogr., Sect. D: Struct. Biol.* **2018**, *74*, 106−116.

(51) Dolomanov, O. V.; Bourhis, L. J.; Gildea, R. J.; Howard, J. A. K.; Puschmann, H. OLEX2: a complete structure solution, refinement and analysis program. *J. Appl. Crystallogr.* **2009**, *42*, 339−341.

(52) Bourhis, L. J.; Dolomanov, O. V.; Gildea, R. J.; Howard, J. A.; Puschmann, H. The anatomy of a comprehensive constrained, restrained refinement program for the modern computing environment - Olex2 dissected. *Acta Crystallogr., Sect. A: Found. Adv.* **2015**, *71*, 59−75.

📖 Recommended by ACS